

N 69 13 946

NASA CR 98571

NATIONAL AERONAUTICS AND SPACE ADMINISTRATION

CASE FILE

Technical Report **COPY** 32-1289

*Launch Dynamic Environment of the
Surveyor Spacecraft*

George L. Parker

**JET PROPULSION LABORATORY
CALIFORNIA INSTITUTE OF TECHNOLOGY
PASADENA, CALIFORNIA**

September 15, 1968

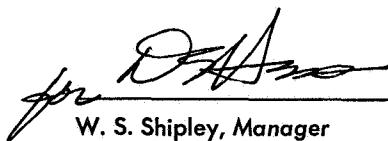
NATIONAL AERONAUTICS AND SPACE ADMINISTRATION

Technical Report 32-1289

*Launch Dynamic Environment of the
Surveyor Spacecraft*

George L. Parker

Approved by:

A handwritten signature in dark ink, appearing to read 'W. S. Shipley', is written over a horizontal line.

W. S. Shipley, Manager
Environmental Requirements Section

JET PROPULSION LABORATORY
CALIFORNIA INSTITUTE OF TECHNOLOGY
PASADENA, CALIFORNIA

September 15, 1968

TECHNICAL REPORT 32-1289

Copyright © 1968

**Jet Propulsion Laboratory
California Institute of Technology**

**Prepared Under Contract No. NAS 7-100
National Aeronautics & Space Administration**

Contents

I. Introduction	1
II. Data Acquisition and Reduction	5
A. Instrumentation	5
B. Data Analysis	8
1. Oscillogram analysis	9
2. Wideband average analysis	9
3. Sound pressure spectrum level analysis	9
4. Spectral density analysis	9
5. Shock spectrum analysis	9
6. Further analysis	9
III. Data Presentation	10
A. Oscillogram Presentation	10
B. Acoustic Environment	10
C. Random Vibration Environment	10
D. Transient Vibration or Shock Environment	11
IV. Conclusions and Recommendations	67

Tables

1. Transducer locations	5
2. Valid frequency ranges for ± 1 dB of constant frequency response	8
3. Transducer failures	8

Figures

1. Surveyor dynamic model	2
2. Surveyor spacecraft	3
3. Surveyor dynamic instrumentation	4
4. Installation of separation plane instrumentation, SD-1 and -2, SC-1 through -4	6
5. Installation of separation plane instrumentation, SC-5 through -7	6

Contents (contd)

Figures (contd)

6. Installation of spacecraft instrumentation, SD-1 and -2	7
7. Installation of spacecraft instrumentation, SD-1 and -2	7
8. Attenuation characteristics of accelerometer amplifier filter, SD-1 and -2, SC-1 through -4	7
9. Attenuation characteristics of telemetry channel filters, SD-1 and -2	8
10. Attenuation characteristics of discriminator output filter, SD-1 and -2, SC-1 through -7	8
11. Attenuation characteristics of accelerometer amplifier filters, SC-5 through -7	8
12. Oscillogram, SD-2, liftoff	12
13. Oscillogram, SD-2, liftoff	13
14. Oscillogram, SD-2, transonic	14
15. Oscillogram, SD-2, transonic	14
16. Oscillogram, SD-2, <i>Atlas</i> booster engine cutoff	15
17. Oscillogram, SD-2, <i>Atlas</i> booster engine cutoff	16
18. Oscillogram, SD-2, insulation panel jettison	17
19. Oscillogram, SD-2, insulation panel jettison	18
20. Oscillogram, SD-2, shroud separation	19
21. Oscillogram, SD-2, shroud separation	20
22. Oscillogram, SD-2, <i>Atlas</i> sustainer engine cutoff	21
23. Oscillogram, SD-2, <i>Atlas</i> sustainer engine cutoff	22
24. Oscillogram, SD-2, <i>Atlas/Centaur</i> separation	23
25. Oscillogram, SD-2, <i>Atlas/Centaur</i> separation	24
26. Oscillogram, SD-2, <i>Centaur</i> main engine ignition	25
27. Oscillogram, SD-2, <i>Centaur</i> main engine ignition	26
28. Oscillogram, SD-2, <i>Centaur</i> main engine cutoff	27
29. Oscillogram, SD-2, <i>Centaur</i> main engine cutoff	28
30. Oscillogram, SD-2, anomalies	29
31. Oscillogram, SC-1, landing gear extension	30
32. Oscillogram, SC-1, landing gear lock	31
33. Oscillogram, SC-1, omni antenna deploy	32
34. Sound pressure spectrum level, $\frac{1}{3}$ octave bands, CY 60Y, SD-1 and -2, liftoff	33

Contents (contd)

Figures (contd)

35. Sound pressure spectrum level, $\frac{1}{3}$ octave bands, CY 61Y, SD-1 and -2, liftoff	33
36. Acceleration spectral density, CY 490, SD-1 and -2, liftoff	33
37. Acceleration spectral density, CY 500, SD-1 and -2, liftoff	34
38. Acceleration spectral density, CY 510, SD-1 and -2, liftoff	34
39. Acceleration spectral density, maximum envelope and average for CY 520, 530, and 540; SD-1 and -2, and SC-1 through -4, liftoff	34
40. Acceleration spectral density, CY 520, 530, and 540; SD-1 and -2, and SC-1 through -4, liftoff	35
41. Acceleration spectral density, CA 7720, SC-5 through -7, liftoff	36
42. Acceleration spectral density, CA 7730, SC-5 through -7, liftoff	36
43. Acceleration spectral density, CY 490, SD-2, transonic	36
44. Acceleration spectral density, CY 500, SD-2, transonic	37
45. Acceleration spectral density, CY 510, SD-2, transonic	37
46. Acceleration spectral density, maximum envelope and average for CY 520, 530, and 540; SD-2 and SC-1 through -4, transonic	37
47. Acceleration spectral density, CY 520, 530, and 540; SD-2 and SC-1 through -4, transonic	38
48. Acceleration spectral density, CA 7720, SC-5 through -7, transonic	39
49. Acceleration spectral density, CA 7730, SC-5 through -7, transonic	39
50. Acceleration spectral density, CA 7720, SC-5 through -7, hydrogen boiloff valve operation	39
51. Acceleration spectral density, CA 7730, SC-5 through -7, hydrogen boiloff valve operation	39
52. Maximum envelope of the shock spectra for all transients, CY 490, SD-2	40
53. Maximum envelope of the shock spectra for all transients, CY 500, SD-2	40
54. Maximum envelope of the shock spectra for all transients, CY 510, SD-2	40
55. Maximum envelope of the shock spectra for all transients, torsion, SD-2	41
56. Maximum envelope of the shock spectra for all transients, X-axis, SD-2	41
57. Maximum envelope of the shock spectra for all transients, CY 520, 530, and 540, SD-2 and SC-1 through -4	41
58. Maximum envelope of the shock spectra for all transients, CA 7720, SC-5 through -7	42

Contents (contd)

Figures (contd)

59. Maximum envelope of the shock spectra for all transients, CA 7730, SC-5 through -7	42
60. Measured transient, CY 490, SD-2, insulation panel jettison	43
61. Shock spectrum, CY 490, SD-2, insulation panel jettison	43
62. Measured transient, CY 500, SD-2, insulation panel jettison	43
63. Shock spectrum, CY 500, SD-2, insulation panel jettison	43
64. Measured transient, CY 510, SD-2, insulation panel jettison	44
65. Shock spectrum, CY 510, SD-2, insulation panel jettison	44
66. Measured transient, torsion, SD-2, insulation panel jettison	44
67. Shock spectrum, torsion, SD-2, insulation panel jettison	44
68. Measured transient, X-axis, SD-2, insulation panel jettison	45
69. Shock spectrum, X-axis, SD-2, insulation panel jettison	45
70. Typical measured transient, CY 520, 530, and 540, SD-2 and SC-1 through -4, insulation panel jettison	45
71. Shock spectra, CY 520, 530, and 540, SD-2 and SC-1 through -4, insulation panel jettison	46
72. Typical measured transient, CA 7720, SC-5 through -7, insulation panel jettison	46
73. Shock spectra, CA 7720, SC-5 through -7, insulation panel jettison	46
74. Typical measured transient, CA 7730, SC-5 through -7, insulation panel jettison	47
75. Shock spectra, CA 7730, SC-5 through -7, insulation panel jettison	47
76. Typical measured transient, CY 520, 530, or 540, SD-2 and SC-1 through -4, shroud separation	47
77. Shock spectra, CY 520, 530, and 540, SD-2 and SC-1 through-4, shroud separation	48
78. Typical measured transient, CA 7720, SC-5 through -7, shroud separation	48
79. Shock spectra, CA 7720, SC-5 through -7, shroud separation	48
80. Typical measured transient, CA 7730, SC-5 through -7, shroud separation	49
81. Shock spectra, CA 7730, SC-5 through -7, shroud separation	49
82. Measured transient, CY 490, SD-2, <i>Atlas/Centaur</i> separation	49
83. Shock spectrum, CY 490, SD-2, <i>Atlas/Centaur</i> separation	50

Contents (contd)

Figures (contd)

84. Measured transient, CY 500, SD-2, <i>Atlas/Centaur</i> separation	50
85. Shock spectrum, CY 500, SD-2, <i>Atlas/Centaur</i> separation	50
86. Measured transient, CY 510, SD-2, <i>Atlas/Centaur</i> separation	50
87. Shock spectrum, CY 510, SD-2, <i>Atlas/Centaur</i> separation	51
88. Measured transient, torsion, SD-2, <i>Atlas/Centaur</i> separation	51
89. Shock spectrum, torsion, SD-2, <i>Atlas/Centaur</i> separation	51
90. Measured transient, X-axis, SD-2, <i>Atlas/Centaur</i> separation	51
91. Shock spectrum, X-axis, SD-2, <i>Atlas/Centaur</i> separation	52
92. Typical measured transient, CY 520, 530, or 540, SD-2 and SC-1 through -4, <i>Atlas/Centaur</i> separation	52
93. Shock spectra, CY 520, 530, and 540, SD-2 and SC-1 through -4, <i>Atlas/Centaur</i> separation	52
94. Typical measured transient, CA 7720, SC-5 through -7, <i>Atlas/Centaur</i> separation	52
95. Shock spectra, CA 7720, SC-5 through -7, <i>Atlas/Centaur</i> separation	53
96. Typical measured transient, CA 7730, SC-5 through -7, <i>Atlas/Centaur</i> separation	53
97. Shock spectra, CA 7730, SC-5 through -7, <i>Atlas/Centaur</i> separation	54
98. Typical measured transient, CA 7720, SC-5 through -7, <i>Centaur</i> main engine cutoff	54
99. Shock spectra, CA 7720, SC-5 through -7, <i>Centaur</i> main engine cutoff	55
100. Typical measured transient, CA 7720, SC-5 through -7, <i>Centaur</i> main engine cutoff 2	55
101. Shock spectra, CA 7720, SC-5 through -7, <i>Centaur</i> main engine cutoff 2	55
102. Typical measured transient, CY 520, 530, or 540, SC-1 through -4, landing gear extension	56
103. Shock spectra, CY 520, 530, and 540, SC-1 through -4, landing gear extension	56
104. Typical measured transient, CA 7720, SC-5 through -7, landing gear extension	56
105. Shock spectra, CA 7720, SC-5 through -7, landing gear extension	57
106. Typical measured transient, CA 7730, SC-5 through -7, landing gear extension	57
107. Shock spectra, CA 7730, SC-5 through -7, landing gear extension	58

Contents (contd)

Figures (contd)

108. Typical measured transient, CY 520, 530, or 540, SC-1 through -4, landing gear lock	58
109. Shock spectra, CY 520, 530, and 540, SC-1 through -4, landing gear lock	59
110. Typical measured transient, CA 7720, SC-5 through -7, landing gear lock	59
111. Shock spectra, CA 7720, SC-5 through -7, landing gear lock	60
112. Typical measured transient, CA 7730, SC-5 through -7, landing gear lock	60
113. Shock spectra, CA 7730, SC-5 through -7, landing gear lock	61
114. Typical measured transient, CY 520, 530, or 540, SC-1 through -4, omni antenna deploy	61
115. Shock spectra, CY 520, 530, and 540, SC-1 through -4, omni antenna deploy	61
116. Typical measured transient, CA 7720, SC-5 through -7, omni antenna deploy	62
117. Shock spectra, CA 7720, SC-5 through -7, omni antenna deploy	62
118. Typical measured transient, CA 7730, SC-5 through 7-, omni antenna deploy	63
119. Shock spectra, CA 7730, SC-5 through -7, omni antenna deploy	63
120. Typical measured transient, CY 520, 530, or 540, SD-2 and SC-1 through -4, anomaly	64
121. Shock spectra, CY 520, 530, and 540, SD-2 and SC-1 through -4, anomaly	64
122. Typical measured transient, CA 7720, SC-5 through -7, anomaly	65
123. Shock spectra, CA 7720, SC-5 through -7, anomaly	65
124. Typical measured transient, CA 7730, SC-5 through -7, anomaly	66
125. Shock spectra, CA 7730, SC-5 through -7, anomaly	66

Abstract

The dynamic environment of the *Surveyor* dynamic models and operational spacecraft during the boost phase of flight is defined. The data acquisition systems and analysis techniques are discussed. Summary flight data from each of nine spacecraft launches for all measured periods of high acoustic energy and random vibration are included. Also included are the transient responses to various pyrotechnic, staging, and jettison events of the boost phase.

Launch Dynamic Environment of the *Surveyor* Spacecraft

I. Introduction

During the boost phase of flight, the *Surveyor* spacecraft was subjected to a variable vibration environment by the *Atlas/Centaur* launch vehicle consisting of acoustically induced random vibration and the transient response to discrete flight events. All spacecraft were instrumented with microphones and/or accelerometers in order to obtain data on the acoustic and vibratory environments. This report is a summary of the reduced data measured predominantly at the *Centaur/Surveyor* separation plane from all *Surveyor* flights.

Two different spacecraft configurations were launched on the *Atlas/Centaur* vehicle, and three different instrumentation plans were employed. The first two *Surveyor* spacecraft to be launched, designated SD-1 and -2, were dynamic models (see Fig. 1) of the operational spacecraft. Each consisted of an operational-type spaceframe with dummy components simulating the mass properties of those items they represented. These spacecraft were the same overall physical size as the operational spacecraft, being approximately 86 in. across at the widest point (landing legs folded) and approximately 100 in.

tall. The SD-1 spacecraft weighed approximately 1600 lb, and the SD-2 weighed approximately 2200 lb, which was the weight of the operational spacecraft. All weight changes on the dynamic models were made by adding or removing ballast from the retro motor simulator. The attachment of the dynamic models to the *Centaur* payload adapter with three separation latches located 120 deg apart on the upper ring of the adapter was the same as for the operational spacecraft. These two spacecraft had the most complete instrumentation, which included microphones for acoustic measurements as well as accelerometers. All data were continuously telemetered throughout the boost phase of the flight.

The seven operational *Surveyor* spacecraft (see Fig. 2) launches that succeeded the dynamic model flights had less complete instrumentation. The first four (SC-1 through -4) had more instrumentation than the last three (SC-5 through -7), but all data on these four flights were telemetered on two channels with one channel of continuous data and one channel of commutated data. The last three spacecraft had two channels of continuous data. The instrumentation plans are discussed in detail in Section II.

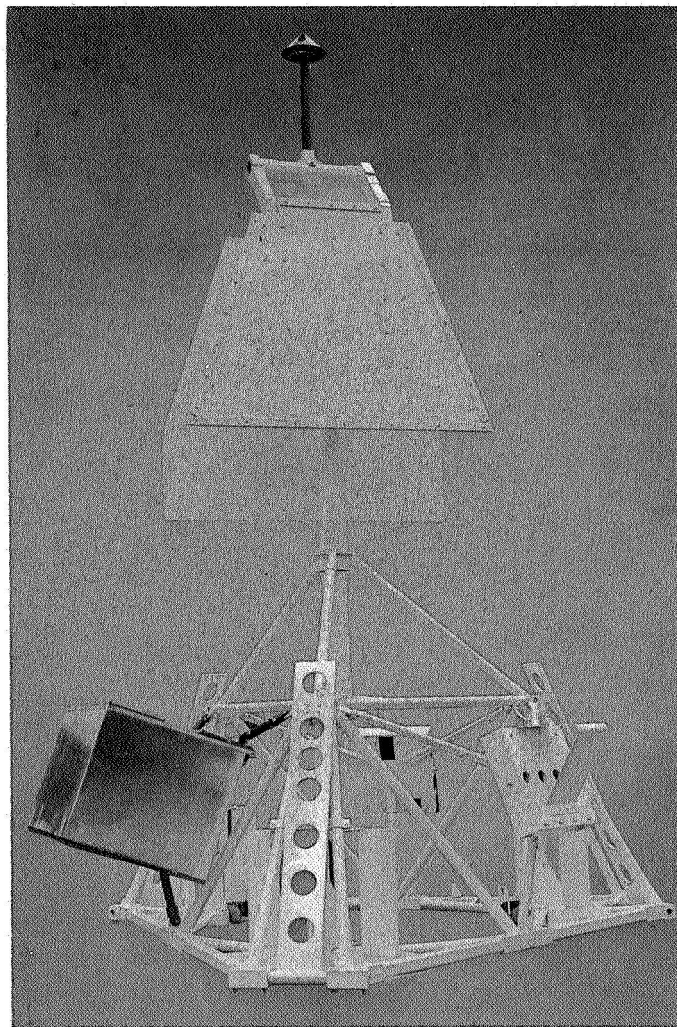


Fig. 1. Surveyor dynamic model

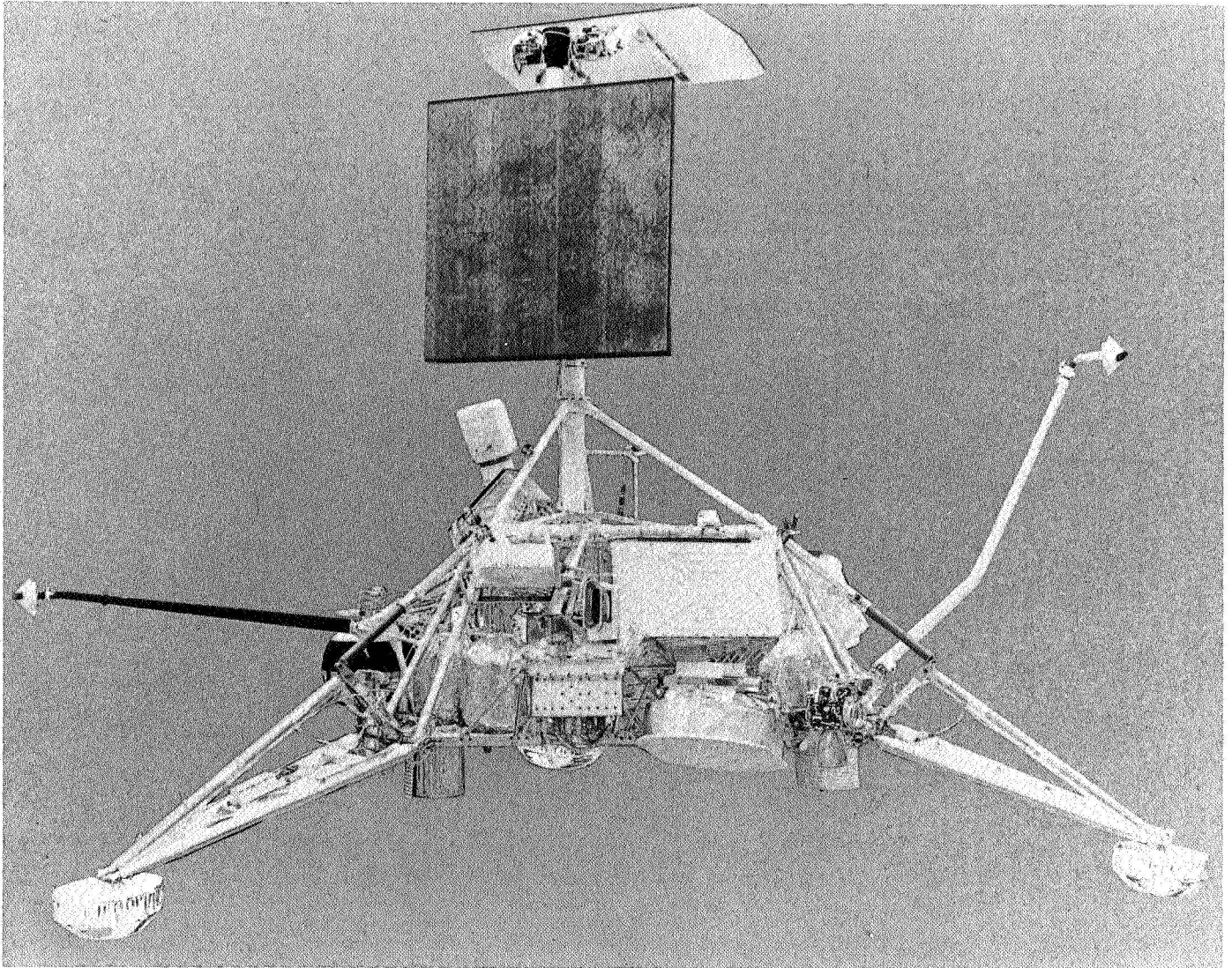


Fig. 2. Surveyor spacecraft

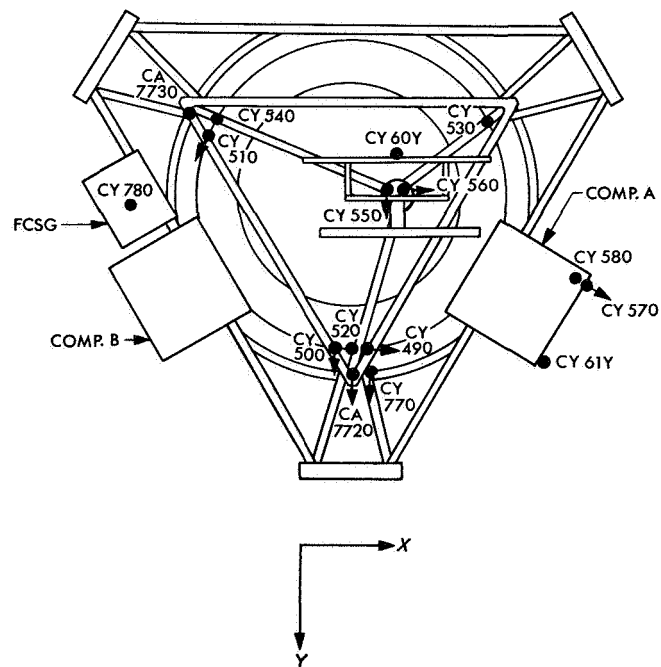
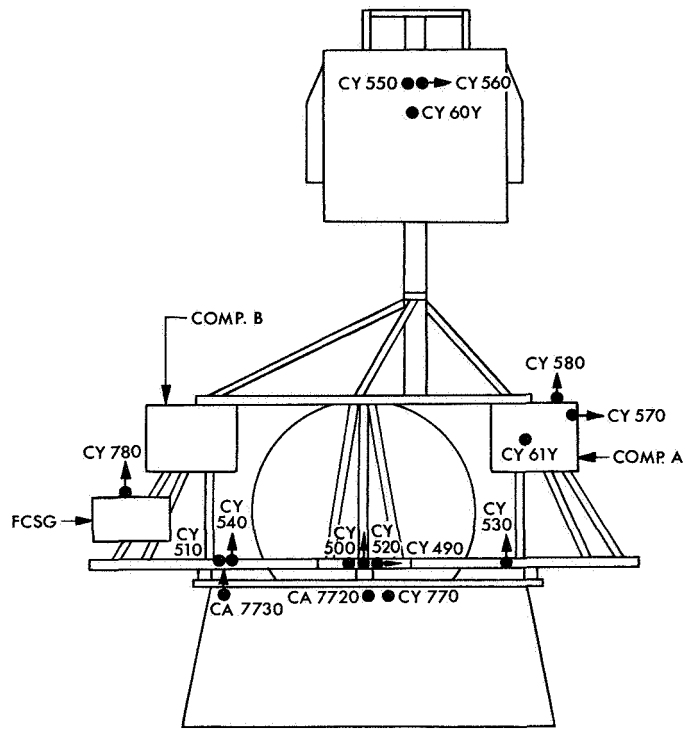


Fig. 3. Surveyor dynamic instrumentation

Table 1. Transducer locations

Channel	Transducer	Location	Range	Commuation rate	Spacecraft	Comments
9	CY 560	Top of mast, X	$\pm 10 g$	—	SD-1 and -2	See note ^e
10	CY 550	Top of mast, Y	$\pm 10 g$	—	SD-1 and -2	See note ^e
11	CY 580	Compartment A, Z	$\pm 10 g$	—	SD-1 and -2	See note ^e
12	CY 490	Attach point, X	$\pm 10 g$	—	SD-1 and -2	First instrumentation plan (SD-1 and -2)
13	CY 500	Attach point, Y	$\pm 10 g$	—	SD-1 and -2	
14	CY 510	Attach point, tangential	$\pm 10 g$	—	SD-1 and -2	
15	CY 570	Compartment A, outboard	$\pm 10 g$	—	SD-1 and -2	
C	CY 60Y	Solar panel	160 dB	—	SD-1 and -2	
E	CY 61Y	Compartment A, outboard	160 dB	—	SD-1 and -2	Second instrumenta- tion plan (SC-1 through -4)
16, 17 ^a	CY 520	Attach point, Z	$\pm 10 g$	—	SD-1 and -2, SC-1 through -4	
17, 14 ^b	CY 530	Attach point, Z	$\pm 10 g$	0.533 s every 2.7 s ^d	SD-1 and -2, SC-1 through -4	
18, 14 ^c	CY 540	Attach point, Z	$\pm 10 g$	0.533 s every 2.7 s ^d	SD-1 and -2, SC-1 through -4	
14	CY 770	Adapter, radial	$\pm 10 g$	0.533 s every 2.7 s	SC-1 through -4	See note ^e
14	CY 780	Flight control sensor group, Z	$\pm 10 g$	0.533 s every 2.7 s	SC-1 through -4	See note ^e
14	CA 7720	Adapter, radial	$\pm 10 g$	—	SC-5 through -7	Third instrumentation plan (SC-5 through -7)
17	CA 7730	Adapter, Z	$\pm 10 g$	—	SC-5 through -7	

^aTelemetered on channel 16 for SD-1 and -2 and on channel 17 for SC-1 through -4.

^bTelemetered on channel 17 for SD-1 and -2 and on channel 14 for SC-1 through -4.

^cTelemetered on channel 18 for SD-1 and -2 and on channel 14 for SC-1 through -4.

^dFor SC-1 through -4 only.

^eData from these accelerometers is not included in this report.

The reduced data contained in Section II describes the dynamic environment of the spacecraft as represented by all measured periods of random vibration, high-level acoustic energy, and various occurrences of transient response. Except for the acoustic measurements, all reduced data in Section II were measured at the *Centaur/Surveyor* separation plane. Data are available from other locations on the spacecraft, but the intent of this report is to define the spacecraft system environment at the *Centaur/Surveyor* separation plane. Figure 3 and Table 1 show all transducer locations for all flights; the accelerometers which provided data not included in this report are indicated. The reduced data have been separated according to instrumentation location and the presentation format allows comparison of related measurements between flights.

II. Data Acquisition and Reduction

A. Instrumentation

The instrumentation system which was utilized to measure the *Surveyor* flight dynamic environment consisted of (1) transducers located at the *Centaur/Surveyor* separation plane and at various locations on the spacecraft, (2) the signal conditioning and telemetry equipment located in the *Centaur*, and (3) the receiving facilities of the Eastern Test Range. Magnetic tape copies of the original recorded data were received at JPL approximately one week after each flight.

All accelerometers and microphones utilized were of the piezoelectric type. The data from these transducers were telemetered in FM/FM multiplex on standard

IRIG (Inter-Range Instrumentation Group) subcarrier bands. All accelerometer and microphone locations for all flights are shown in Fig. 3. Shown in Table 1 are the IRIG channel assignment and commutation rates for commutated channels, transducer identification numbers (General Dynamics/Convair nomenclature), transducer orientations, nominal ranges, and the spacecraft applicability for each transducer location. The three different instrumentation plans are identified in Table 1 by spacecraft grouping, i.e., SD-1 and -2 SC-1 through -4, and SC-5 through -7 each had different overall instrumentation locations. Some transducer locations, however, were the same for most flights (also shown in Table 1), allowing both flight-to-flight comparisons of the environment and statistical manipulation.

Typical installations for the separation plane transducers for the three instrumentation plans are shown in Fig. 4 for the SD-1 and -2 and SC-1 through -4 plans, and in Fig. 5 for the SC-5 through -7 plan. The details of the SC-1 through -4 installations are slightly different from those shown in Fig. 4. However, no pictures were taken of the actual SC-1 through -4 installations because

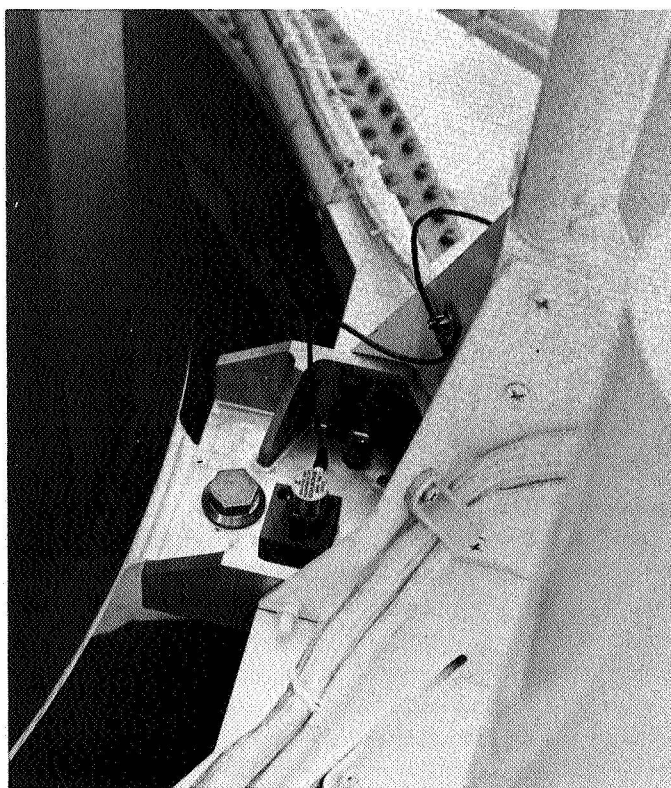


Fig. 4. Installation of separation plane instrumentation, SD-1 and -2, SC-1 through -4

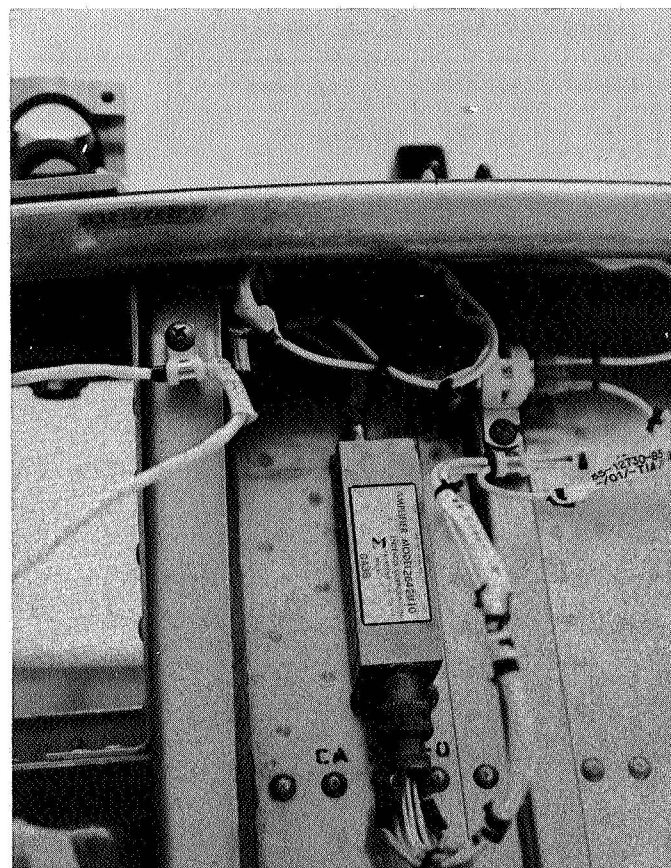


Fig. 5. Installation of separation plane instrumentation, SC-5 through -7

of the difficulty in gaining access to the accelerometer locations. As shown, these accelerometers were mounted either on the spacecraft "column base" next to the spacecraft/adaptor attach points or below the upper ring of the *Centaur* payload adapter next to the attach points. Figures 6 and 7 show the microphone installations on SD-1 and -2, which were the only flights for acoustic measurements. Figure 7 also shows the installation of two accelerometers on the simulated compartments of SD-1 and -2.

Instrumentation frequency response is dependent on transducer frequency response, signal conditioning and telemetry characteristics, and demultiplexing effects. The most significant effect is probably the low-pass filters in the instrumentation systems and the low-pass filter used in the output of the discriminator during data playback. For SD-1 and -2, each accelerometer channel had two low-pass filters, the first of which was an accelerometer amplifier filter that had the attenuation characteristics as shown in Fig. 8. The second low-pass filter in the

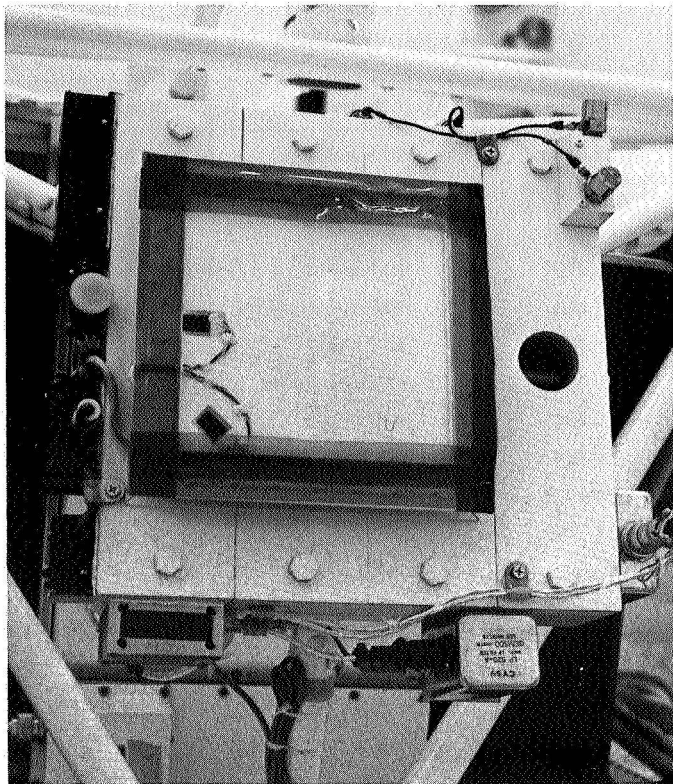


Fig. 6. Installation of spacecraft instrumentation, SD-1 and -2

system for each channel was an IRIG bandwidth filter that provided the attenuation characteristics as shown in Fig. 9 for the channels of interest. For data reduction, the discriminator output filters were set at three times the IRIG recommended values, at the expense of signal-to-noise ratio, providing attenuation as shown in the normalized curve of Fig. 10. For SC-1 through -4 the accelerometer amplifier filters and the discriminator output filters were used providing attenuation as shown in Figs. 8 and 10. Since no end-to-end calibration was performed on the instrumentation systems of SD-1 and -2 or SC-1 through -4, the frequency response of the system is assumed to be represented by the combined characteristics of the various filters. Table 2 contains the assumed valid frequency range for these flights based on the filter characteristics.

For SC-5 through -7 the accelerometer amplifier filters had the characteristics as shown in Fig. 11 for the IRIG channels 14 and 17 accelerometers, respectively. For data reduction, the discriminator output filters were set at three times the IRIG recommended values as shown in Fig. 10. Additionally, the two SC-5 accelerometer/telemetry systems were subjected to a partial end-to-end

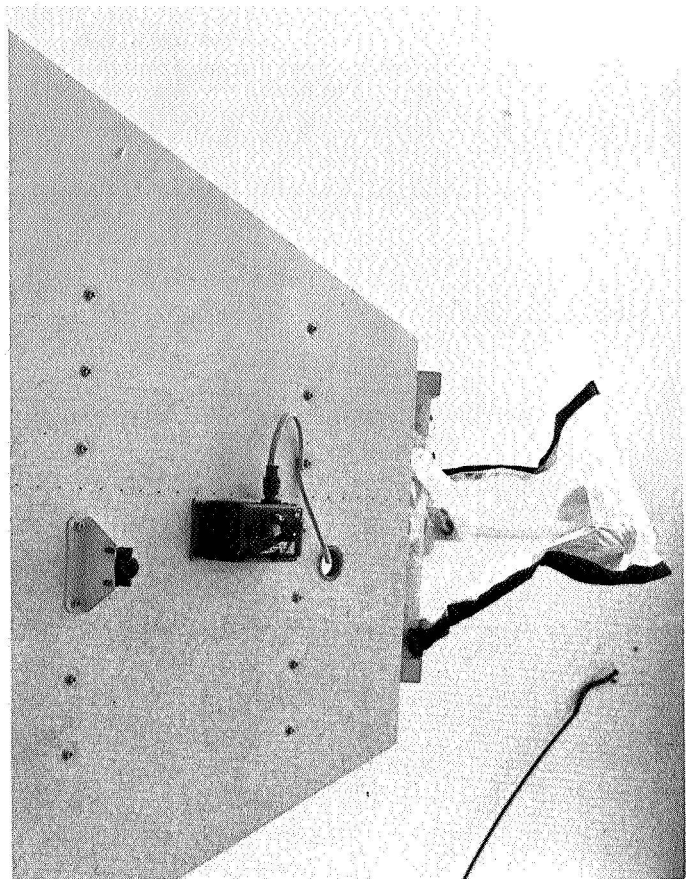


Fig. 7. Installation of spacecraft instrumentation, SD-1 and -2

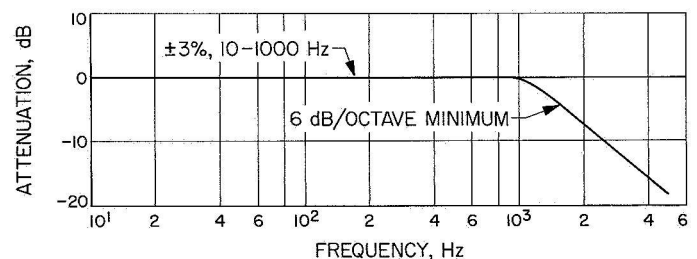


Fig. 8. Attenuation characteristics of accelerometer amplifier filter, SD-1 and -2, SC-1 through -4

calibration consisting of a voltage insertion at the amplifier input and the recording and playback of the telemetry signal. This calibration revealed a $\pm 3\%$ error for accelerometer CA 7730 and a $\pm 5\%$ error for accelerometer CA 7720. These values can be assumed to be typical system error ranges for SC-5 through -7. The valid frequency ranges for the measurements on these flights are given in Table 2.

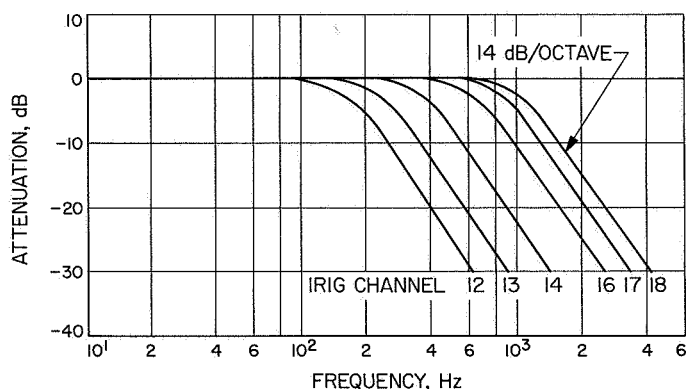


Fig. 9. Attenuation characteristics of telemetry channel filters, SD-1 and -2

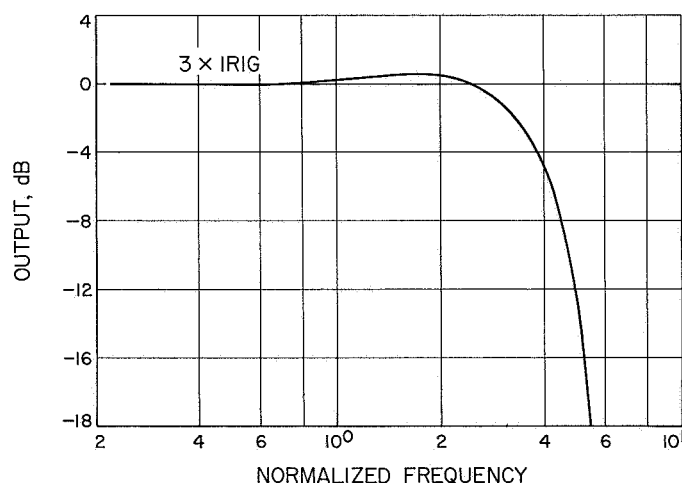


Fig. 10. Attenuation characteristics of discriminator output filter, SD-1 and -2, SC-1 through -7

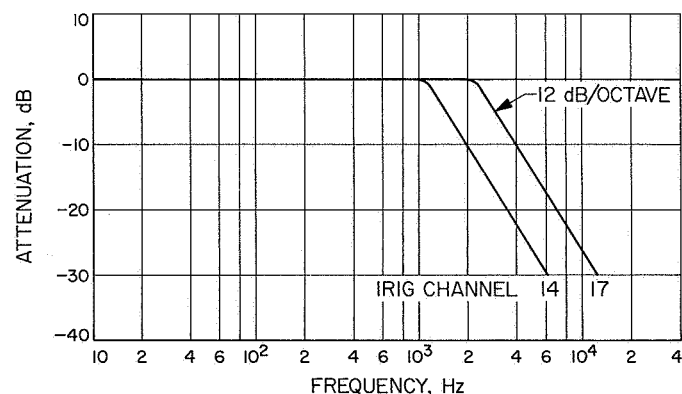


Fig. 11. Attenuation characteristics of accelerometer amplifier filters, SC-5 through -7

Table 2. Valid frequency ranges for ± 1 dB of constant frequency response

Transducer	Spacecraft	Frequency range, Hz
CY 490	SD-1 and -2	2-125
CY 500	SD-1 and -2	2-200
CY 510	SD-1 and -2	2-300
CY 520	SD-1 and -2	2-500
CY 520	SC-1 through -4	2-1150
CY 530	SD-1 and -2	2-700
CY 530	SC-1 through -4	2-970
CY 540	SD-1 and -2	2-800
CY 540	SC-1 through -4	2-970
CA 7720	SC-5 through -7	2-2300
CA 7730	SC-5 through -7	2-970
Torsion	SD-1 and -2	2-100
Translation	SD-1 and -2	2-100

Table 3. Transducer failures

Transducer	Spacecraft	Comments
All	SD-1	Booster failed at liftoff
CY 580	SC-1	Failed after 3 min 20 s of flight
CY 520	SC-2	Attributed to loose connectors
CY 530	SC-2	Attributed to loose connectors
CY 770	SC-2	Attributed to loose connectors
CY 530	SC-3	Disconnected prior to liftoff

There were several instrumentation failures during the series of flights. In addition, the launch vehicle for the SD-1 spacecraft failed shortly after liftoff. All transducer failures are given in Table 3 so that an accounting can be made for data missing from the data presentation portion of this report.

B. Data Analysis

The raw flight data were subjected to several types of analyses in order to better characterize the environment. These analyses included:

- (1) Oscillogram analysis (instantaneous g level vs time).
- (2) Wideband average analysis (rms g level vs time).
- (3) Sound pressure spectrum level analysis (sound pressure vs frequency).
- (4) Acceleration spectral density analysis (g^2/Hz vs frequency).

- (5) Shock spectrum analysis (peak g response vs oscillator natural frequency).

Each type of analysis provided detail knowledge of some characteristic of the flight environment as indicated by the description of the various analyses in the following paragraphs.

1. Oscillogram analysis. For each flight, all data channels plus a time code and, for some flights, a signal strength indication were recorded on an oscillogram for visual presentation. Galvanometer frequency responses were compatible with the accelerometer system frequency responses and paper speed was 6.4 in./s. Oscillogram presentations provide a continuous record of the dynamic environment of each flight from which anomalous dynamic events can be identified and the dynamic severity of the flight evaluated for "quick look" reports. For further data reduction, these records serve to establish a time reference and, through time increments, a frequency reference. Also, the appropriate type of further analysis is indicated by the type of data, i.e., random vibration or transient. Invalid data resulting from instrumentation or telemetry and receiving problems are often easily detected from the oscillogram presentation.

2. Wideband average analysis. For some flights, the wideband average (or rms) was presented as a function of time. This type of presentation is used for selecting the time portions of the data to be subjected to more detailed analysis. After the SC-1 flight, this type of analysis was discontinued because all analysis to that time was basically identical. No samples of this type of presentation are included in this report.

3. Sound pressure spectrum level analysis. The sound pressure spectrum level analysis presented in this report was accomplished using the same digital spectrum analysis technique used for power spectral density computation which results in a 1.0-Hz constant bandwidth presentation of an effective 10-Hz constant bandwidth analysis. This constant bandwidth analysis is then converted into a $\frac{1}{3}$ octave band analysis by means of a conversion program.

4. Spectral density analysis. All spectral density analysis presented in this report was derived using a digital technique of power (acceleration) spectral density computation. Analysis parameters ranged as follows:

Resolution: 2.5 and/or 15 or 19 Hz.

Sample Length: 0.533 to 4.0 s, predominantly 2.0 s.

The computational portion of the analysis is performed on an IBM 7094 digital computer. Analysis output consists of plots of the autocorrelation function and the spectral density function. The spectrum values for each plot are stored on cards for later manipulation.

5. Shock spectrum analysis. The analysis of transient vibration or shock was accomplished by the use of shock spectrum analysis. The shock spectrum presents the peak response to the transient (applied as a base excitation) of a single-degree-of-freedom system of spring, mass, and damper as a function of system natural frequency and damping. All spectra presented in this report were made with $Q = 20$ ($Q = 1/2\zeta$, where ζ = fraction of critical damping). Additional analysis for $Q = \infty$ and $Q = 10$ was performed but is not included in this report.

The computation of the shock spectrum is performed on an IBM 7094 computer after the analog-to-digital conversion of the data signal. The computed spectrum is presented in plotted form, and is also stored on cards for later manipulation. The frequency range of the analysis is selected to be compatible with the data acquisition system frequency range and with a visual estimate of the frequency content of the transient being analyzed. Sample rates for the analog-to-digital conversion were typically selected to be at least 10 to 20 times the highest frequency content.

6. Further analysis. In order to better evaluate the large amounts of reduced data resulting from the above data analysis techniques, a capability for manipulating sets of data was developed. The data manipulation is accomplished on a digital computer using the spectral data stored on cards. The following manipulations can be performed.

- (1) Maximum and/or minimum envelope.
- (2) Average levels.
- (3) Percentile level estimation.
- (4) Ratio between spectra.
- (5) Product of a spectrum and a spectra ratio.
- (6) One-third octave conversion.
- (7) Plot overlay.

Several of the capabilities mentioned earlier have been applied to the *Surveyor* reduced data and are included in this report.

III. Data Presentation

The complete flight dynamic environment has been subdivided into four areas of interest. These are (1) the combined environment as represented by the oscillogram presentation, (2) the acoustic environment, (3) the random vibration environment, and (4) the transient vibration or shock environment.

For the random vibration and the transient or shock environments the data are presented in three groups. The three groups represent the separation plane dynamic environments as separated into the following three sets of flights with like and/or unique measurements based on the instrumentation plans (see Table 1): (1) SD-1 and -2, (2) SD-1 and -2 and SC-1 through -4, and (3) SC-5 through -7. Acoustic measurements were like and unique on SD-1 and -2 only and, therefore, this subdivision has only one group of data. The presentation of the data in sets of like and/or unique measurements allows a direct flight-to-flight comparison of data. The comparison is enhanced by the fact that the reduced data from like measurements are plotted on one graph.

Samples of raw data for the reduced acoustic and random vibration data are shown in the oscillogram presentation. Samples of raw data for the reduced transient or shock data are shown with each combined shock spectrum plot and also in the oscillogram presentation. Each of the four subdivisions of data is discussed further below.

A. Oscillogram Presentation

Oscillograms of typical dynamic data for each flight event have been taken from the SD-2 and SC-1 flights and are given in Figs. 12-33. The SD-2 data is presented because of the comprehensive instrumentation. Those events not measured on the SD-2 flight are shown with SC-1 data.

B. Acoustic Environment

Acoustic measurements were made only on SD-1 and -2. The liftoff sound pressure spectrum levels are given

in Figs. 34 and 35. Acoustic levels at times other than the two shown were below the measuring capability of the instrumentation. The overall sound pressure level (SPL) of the transducer system noise averaged 118.3 dB for the two microphones. Agreement between the two flights is good as it should be since all important parameters were virtually identical for the two flights.

C. Random Vibration Environment

As expected, the flight times for high-level random vibration are the liftoff and transonic regions. Power spectral density (PSD) analysis was performed on the data from all flights at these times. The results of the PSD analysis on all separation plane transducers are given in Figs. 36-51.

For all flights, each transducer system noise level was analyzed from data recorded before booster engine ignition. The PSDs of the liftoff random vibration data were generally 15 to 20 dB above the system noise PSDs, and the PSDs of the transonic random vibration data were generally 8 to 10 dB above the system noise PSDs.

As discussed above, there are three groups of data for flights with like measurements, and within each group the reduced data from like measurements are plotted on one graph to ease flight-to-flight comparisons. In cases where the composite plot is made up of a large number of individual measurements, a composite maximum envelope and average are given in a separate graph for clarity. Also, where both 2.5-Hz and 15- or 19-Hz PSD analysis was performed on the data from any one accelerometer, the plots were combined such that the resolution of the combined plot is 2.5 Hz up to 500 Hz and 15 or 19 Hz from 500 Hz on. These combined plots are easily recognized in the presentation of the data due to the finely resolved spectrum below 500 Hz.

The first grouping in this subdivision represents the only complete lateral axis set of transducers to be included in the instrumentation plans. Unfortunately, these transducers had rather low frequency response limits because of the IRIG bandwidth filtering in each system and are of limited usefulness in determining the high-frequency lateral axis random vibration environment. The plots do show, however, that as the frequency response limit increases, the measured random vibration level increases and approaches the longitudinal axis value shown in the second grouping.

The second grouping includes data from like measurements on SD-1 and -2, and SC-1 through -4 and represents the longitudinal axis random vibration as measured on the spacecraft side of the separation plane. SD-1 and -2 were dynamic models with both overall and detail differences from the flight spacecraft. In the region of the separation plane accelerometers, though, the structural details were quite similar to those of the flight spacecraft. Also, the PSD (and shock spectrum) analysis revealed similar results for the two types of spacecraft. For these reasons the data have been grouped. Measurements of CY 520, 530, and 540 are considered like measurements for any one flight and are so included in the flight-to-flight grouping. The PSD plots of the commutated measurements CY 530 and 540 for SC-1 through -4 are the average of the PSDs for two sequential commutations during the times of maximum random vibration, the result being a similar sample for the analysis of the commutated and uncommutated measurements. However, the PSDs of the data from the uncommutated channels are still statistically more accurate.

The third grouping presents the longitudinal and lateral axis random vibration environment as measured on the payload adapter side of the separation plane. Since the measurements were made at only one point, how well they represent the environments of their respective axes is unknown, especially for the lateral axis. The structure on which the transducers were mounted was considerably different from the structure on which the spacecraft separation plane transducers were mounted as the spacecraft separation plane transducers were mounted on rela-

tively rigid and heavy structures when compared to that of the payload adapter separation plane transducers.

In reviewing the data, it is seen that the grouped measurements are in close agreement with one another except at the higher frequencies. This is due to the different frequency response characteristics of the various channels, and, therefore, the frequency response limits of Table 2 must be referred to when reviewing the data.

D. Transient Vibration or Shock Environment

The separation plane transient vibration or shock environment is presented in the form of maximum envelopes, for each transducer grouping, of the composite shock spectra for the transient events in Figs. 52-59. Additionally typical time history traces and all associated shock spectra for the various flight transients or shocks are given in Figs. 60-125. The shock spectra of some transients recorded during flight are not included in the report because the transients either had magnitudes only slightly greater than the magnitude of the system noise or exhibited peculiar characteristics not associated with dynamic events (e.g., the *Centaur* main engine cutoff transient). The shock spectra of these types of transients would be subject to questionable interpretation. Grouping is as indicated above and the discussions of grouping and frequency response in the random vibration section apply here also. The transients labeled "anomaly" were actually caused by straining or stress relief of stresses from thermal and dynamic loading of the launch vehicle as concluded during a study of the transients. (See Ref. 1.)

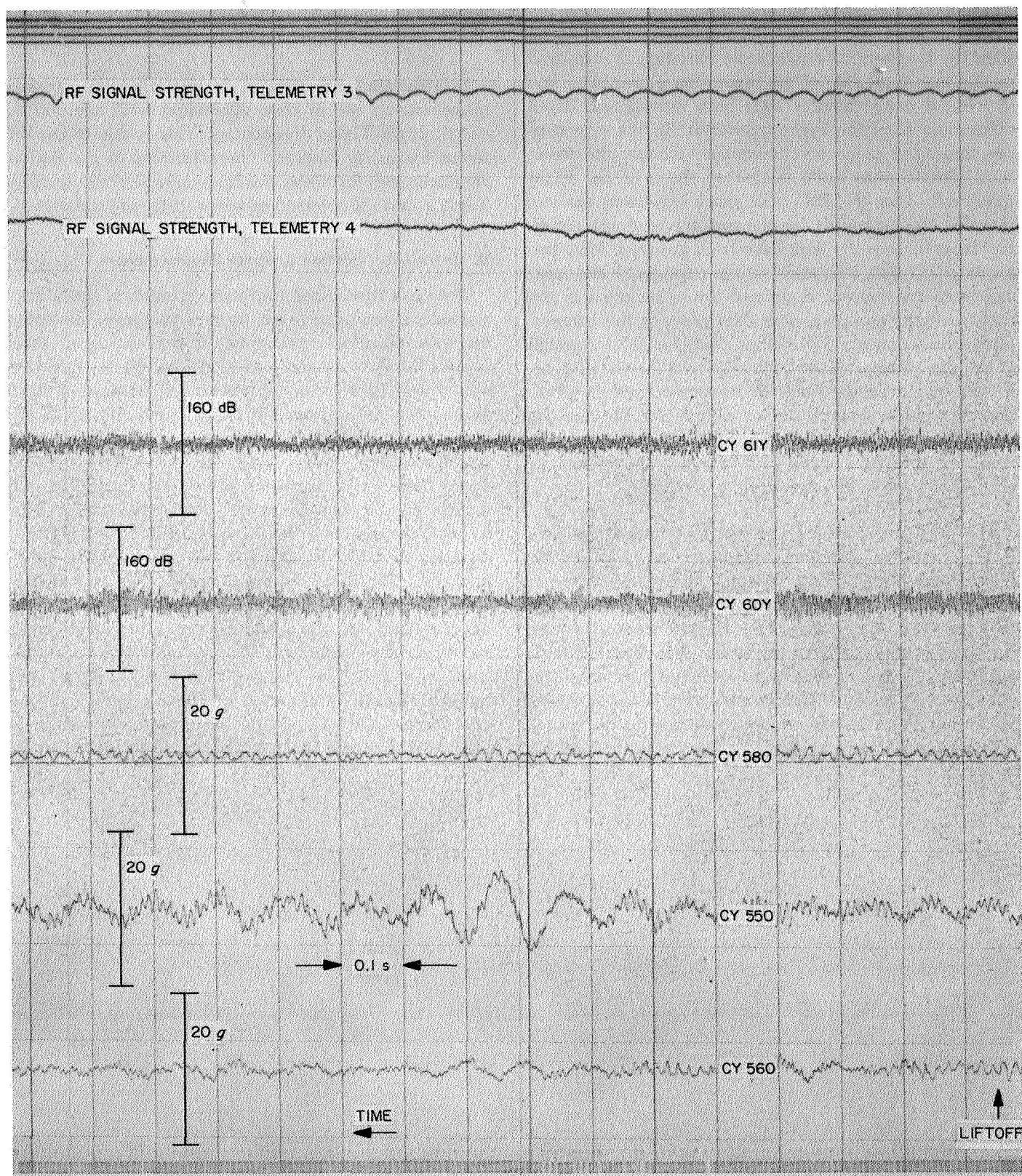


Fig. 12. Oscillogram, SD-2, liftoff

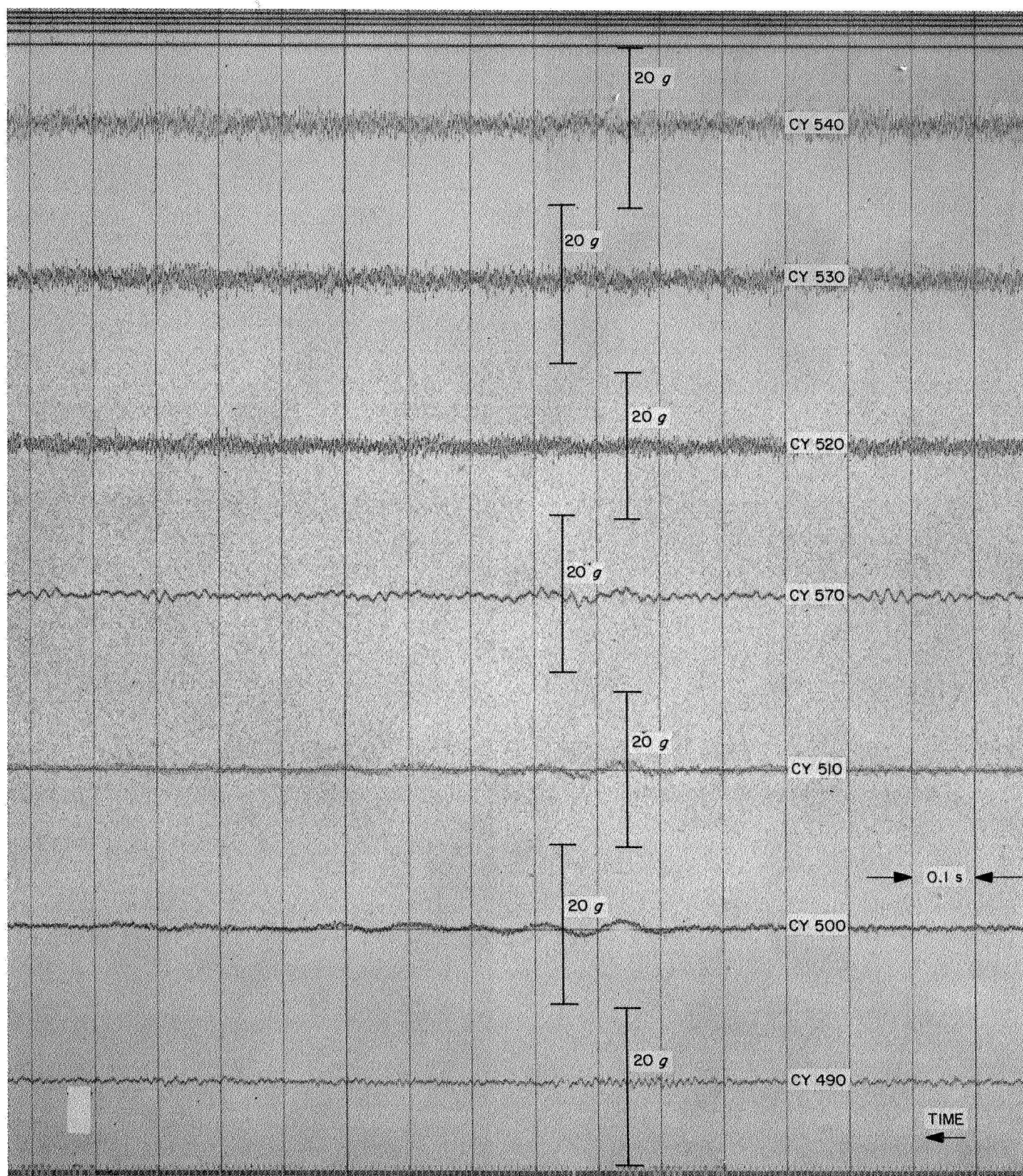


Fig. 13. Oscillogram, SD-2, liftoff

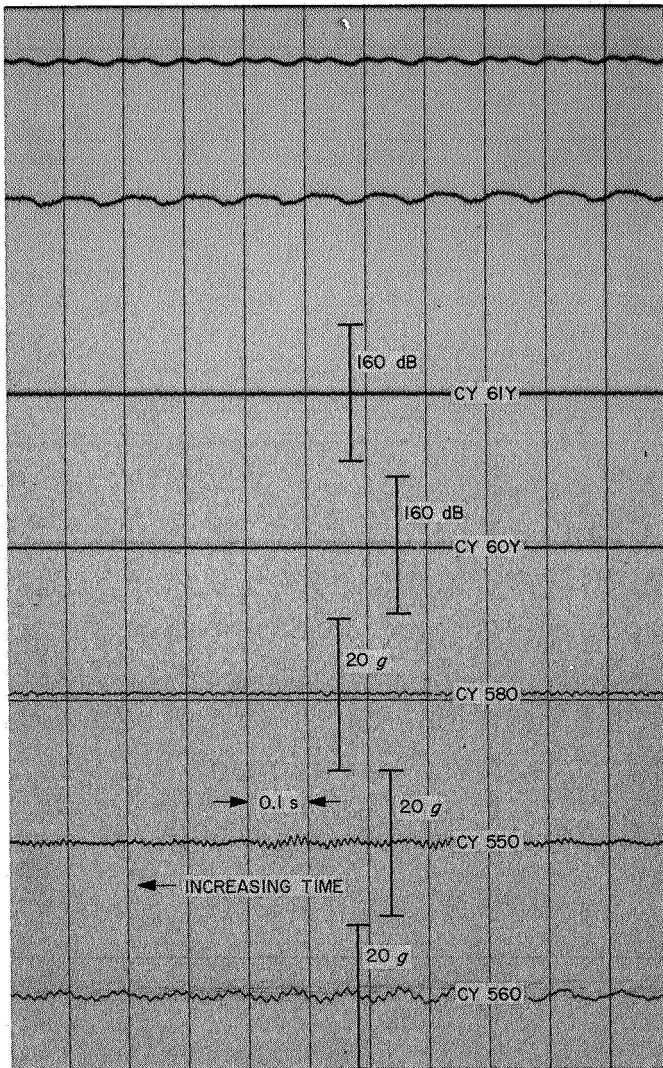


Fig. 14. Oscillogram, SD-2, transonic

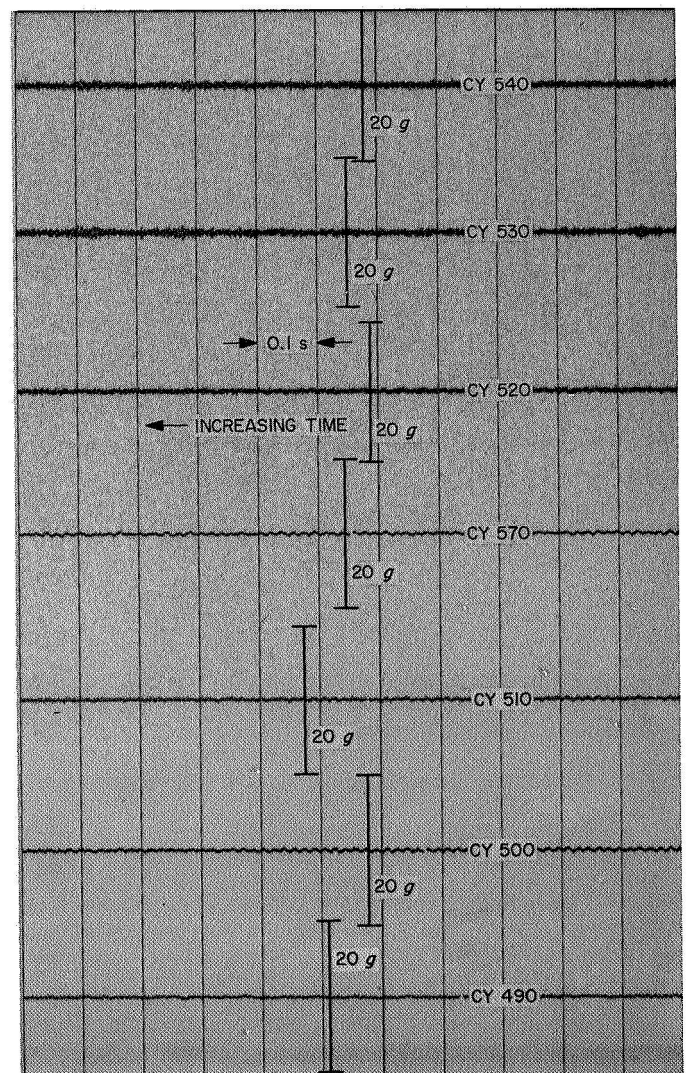


Fig. 15. Oscillogram, SD-2, transonic

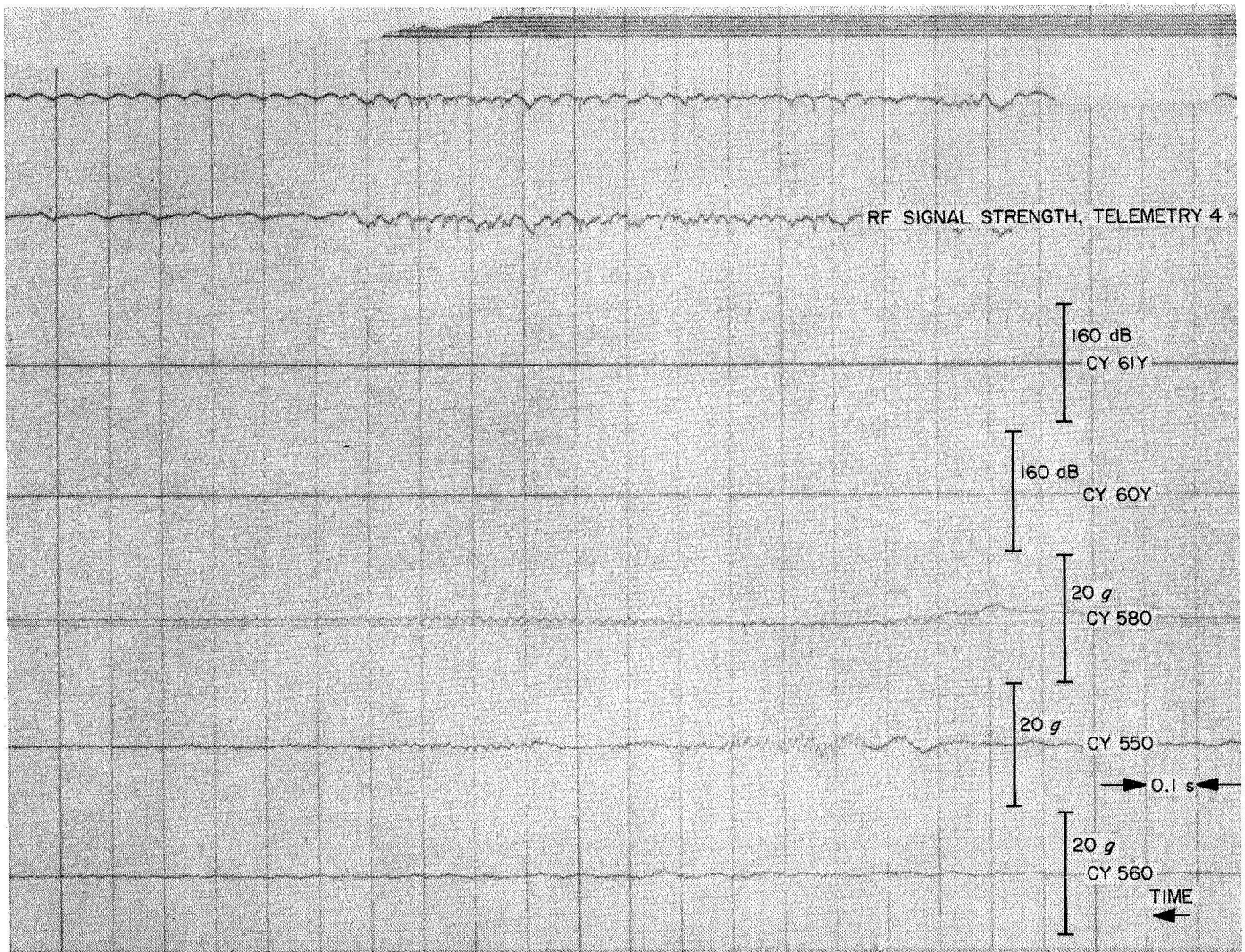


Fig. 16. Oscillogram, SD-2, Atlas booster engine cutoff

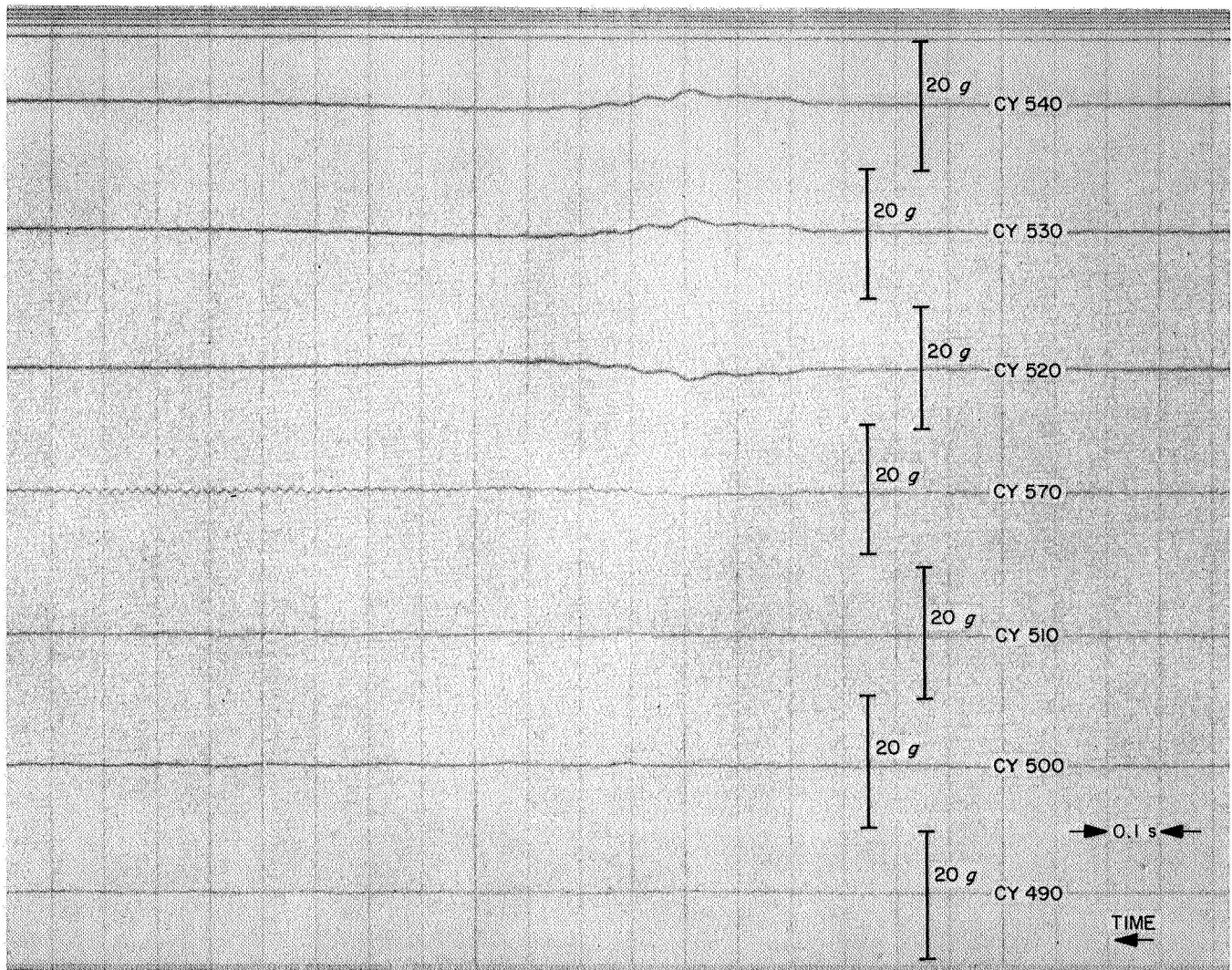


Fig. 17. Oscillogram, SD-2, Atlas booster engine cutoff

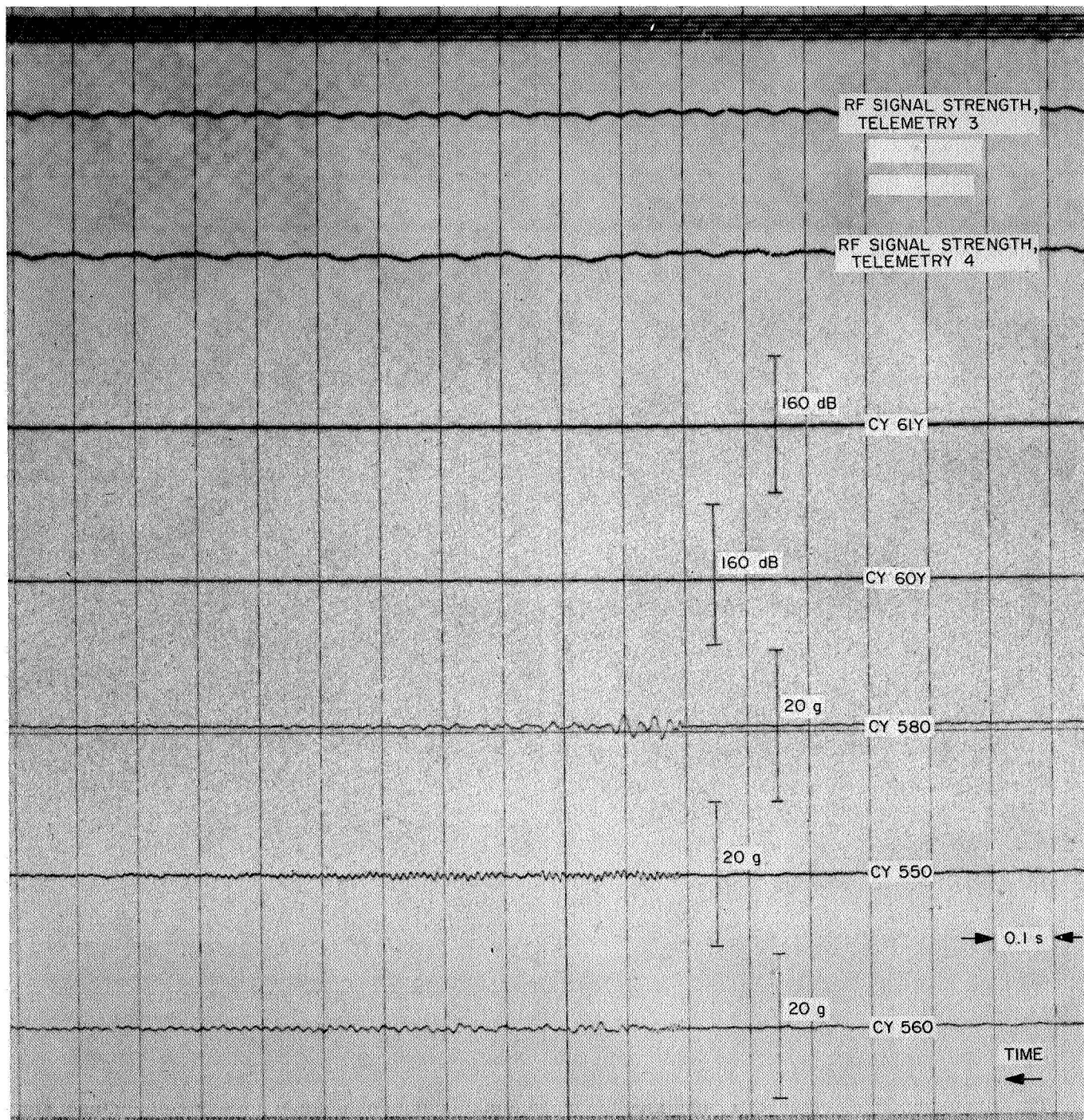


Fig. 18. Oscillogram, SD-2, insulation panel jettison

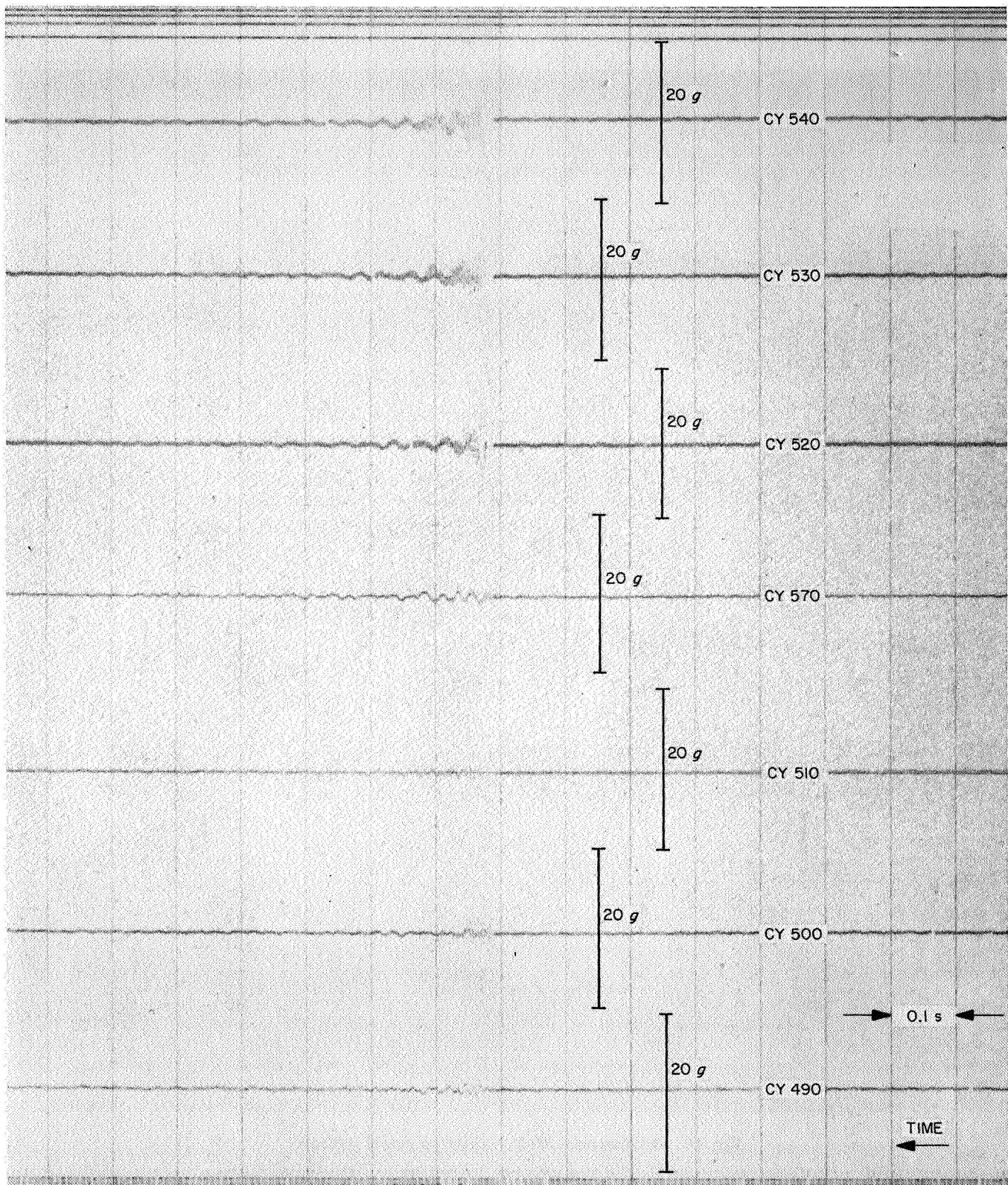


Fig. 19. Oscillogram, SD-2, insulation panel jettison

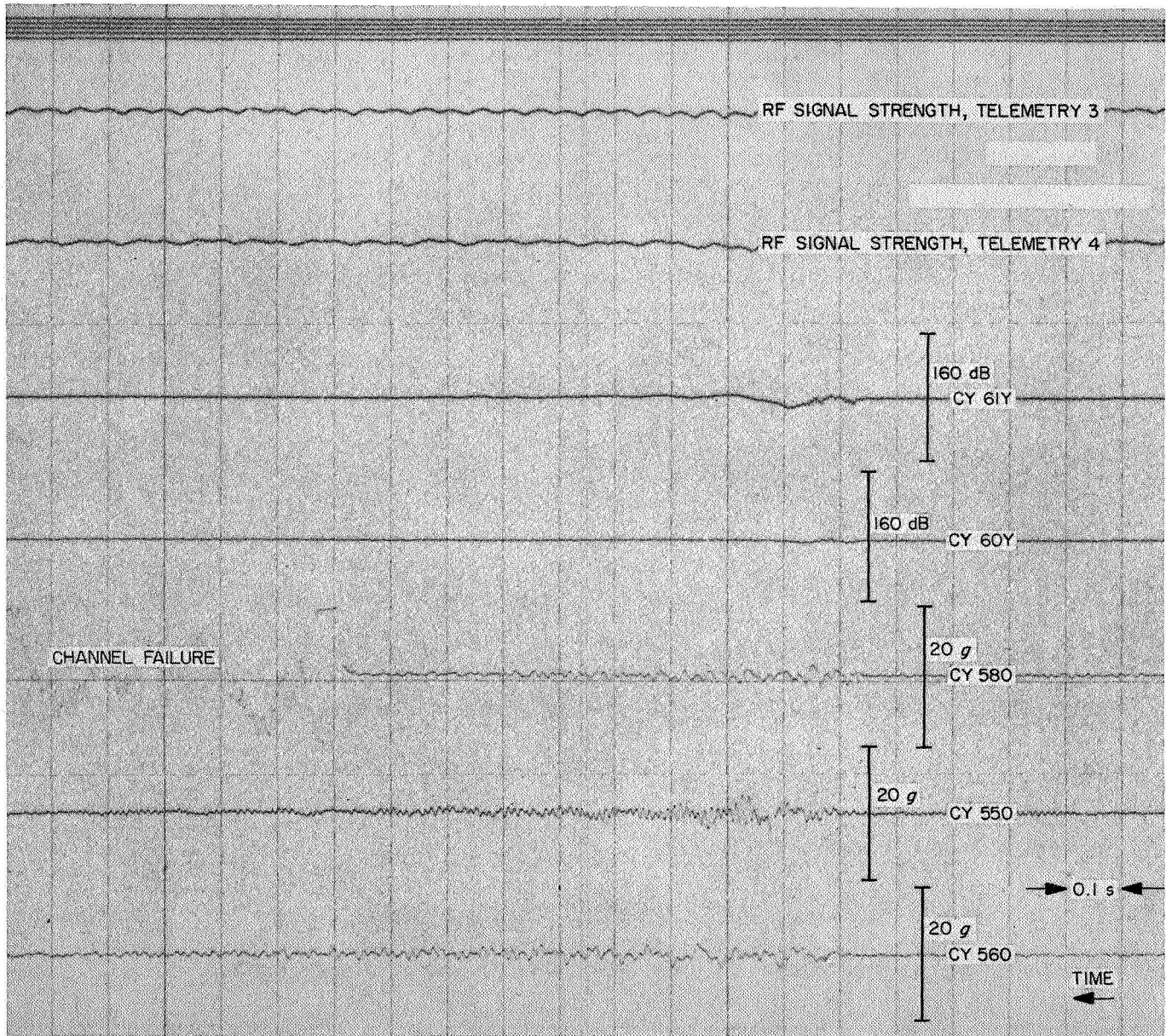


Fig. 20. Oscillogram, SD-2, shroud separation

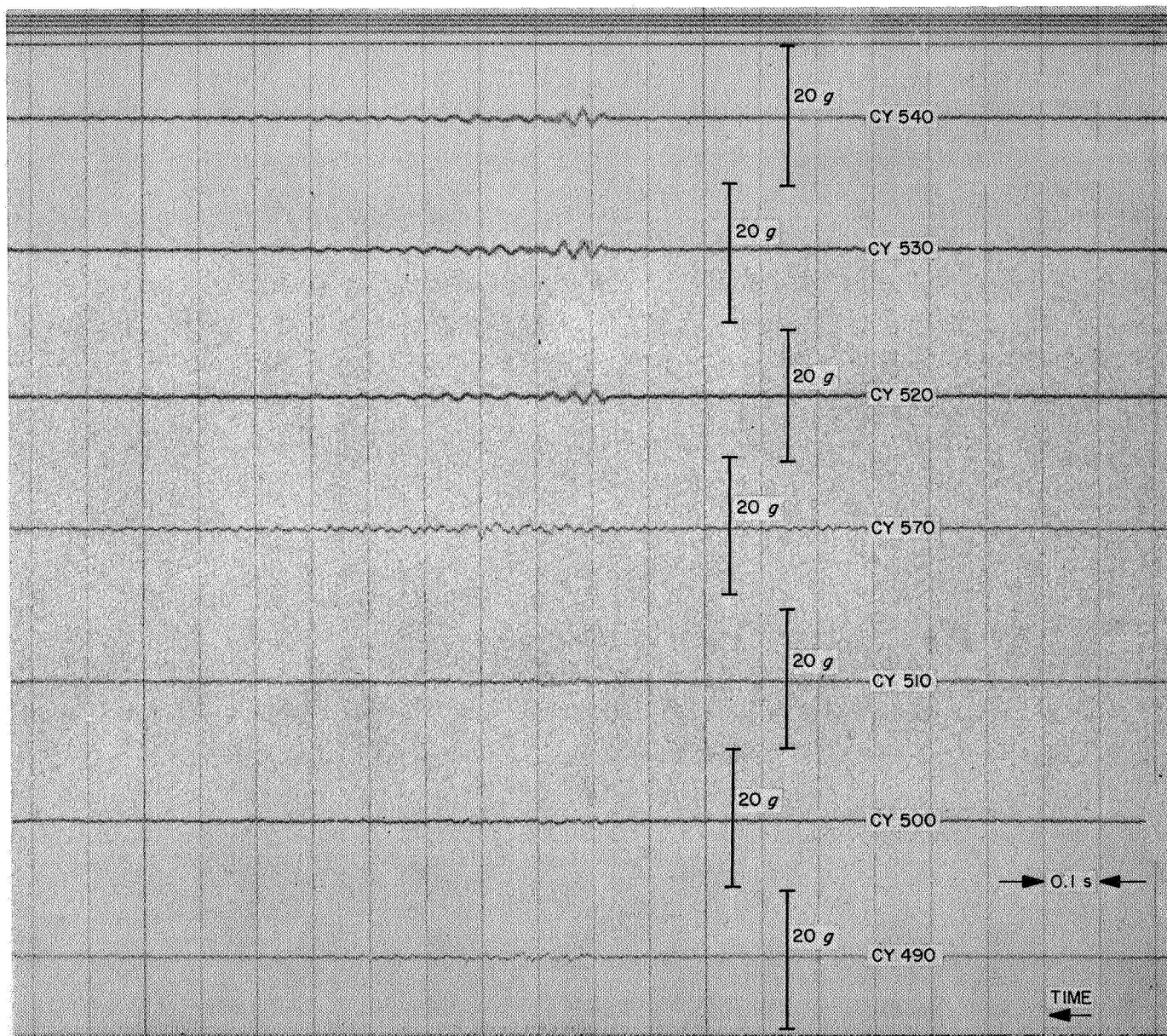


Fig. 21. Oscillogram, SD-2, shroud separation

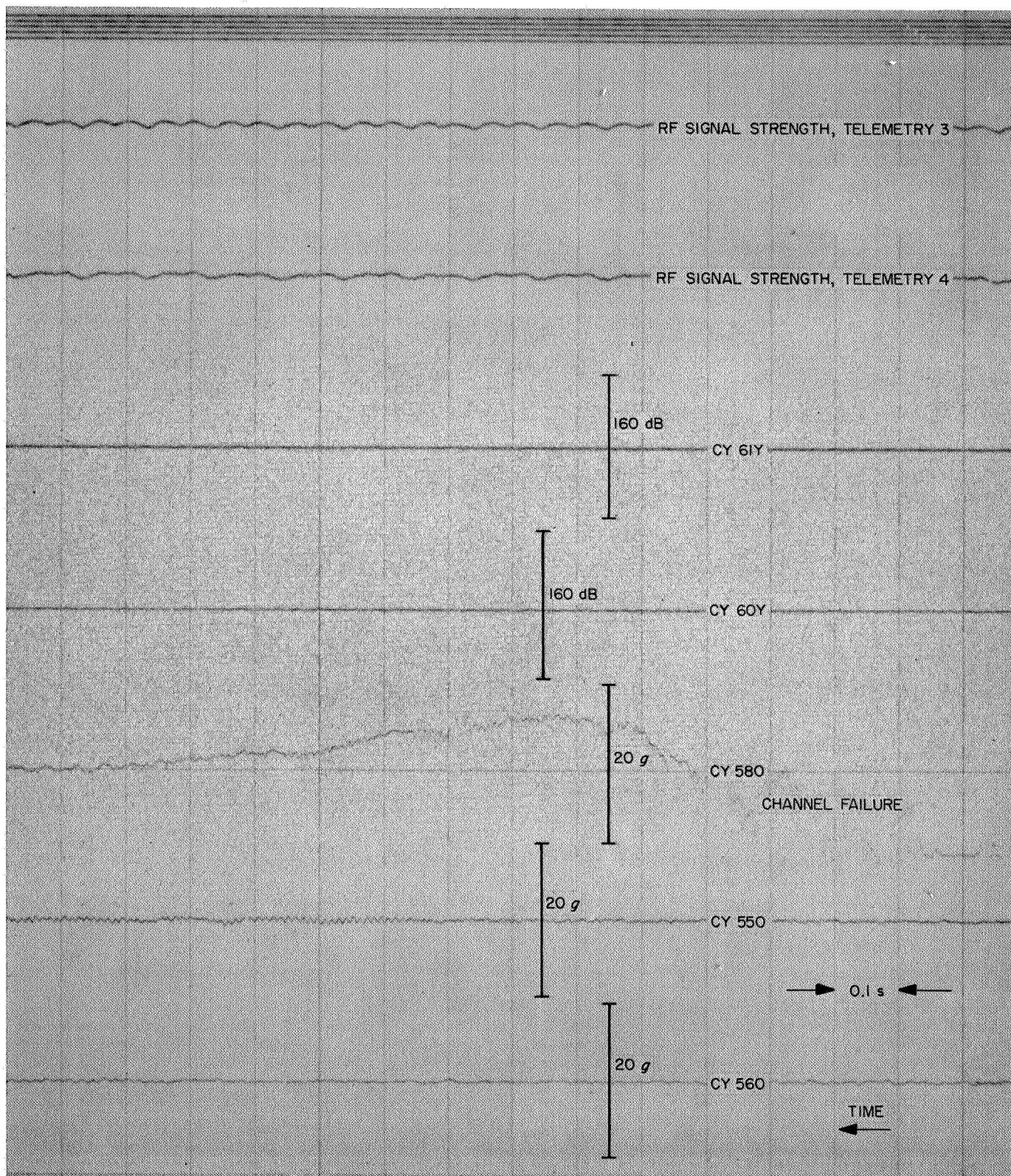


Fig. 22. Oscillogram, SD-2, Atlas sustainer engine cutoff

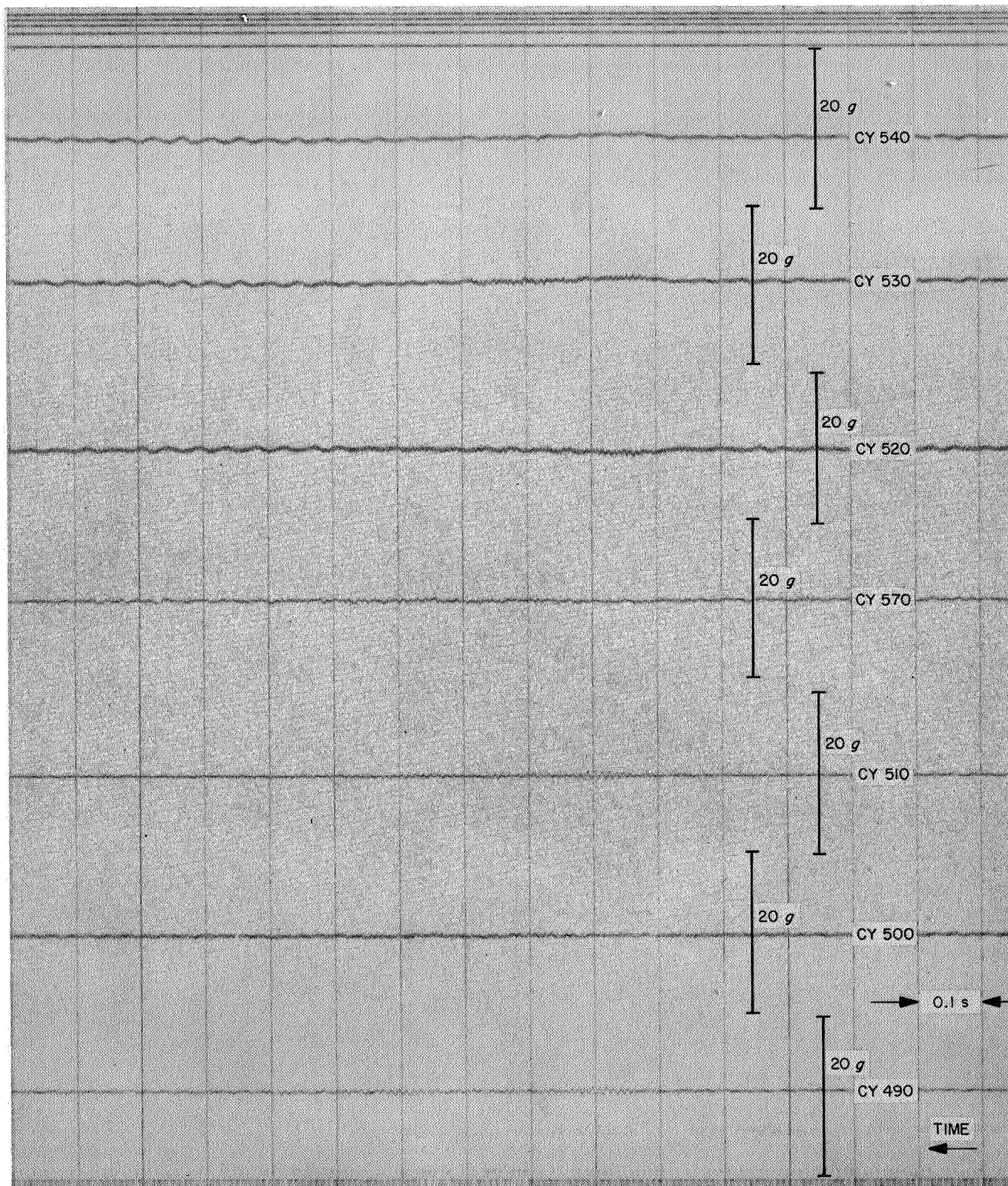


Fig. 23. Oscillogram, SD-2, *Atlas* sustainer engine cutoff

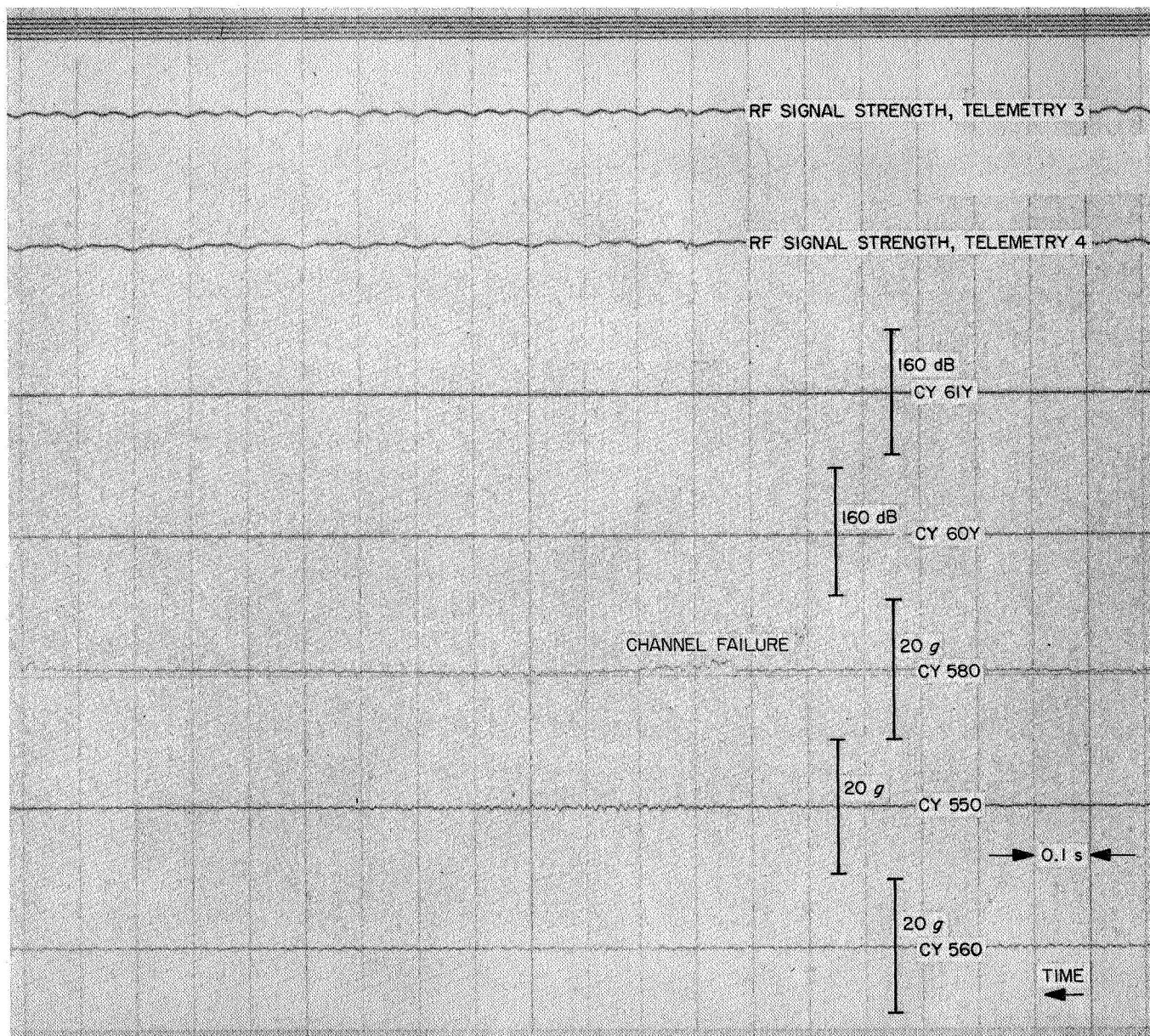


Fig 24. Oscillogram, SD-2, Atlas/Centaur separation

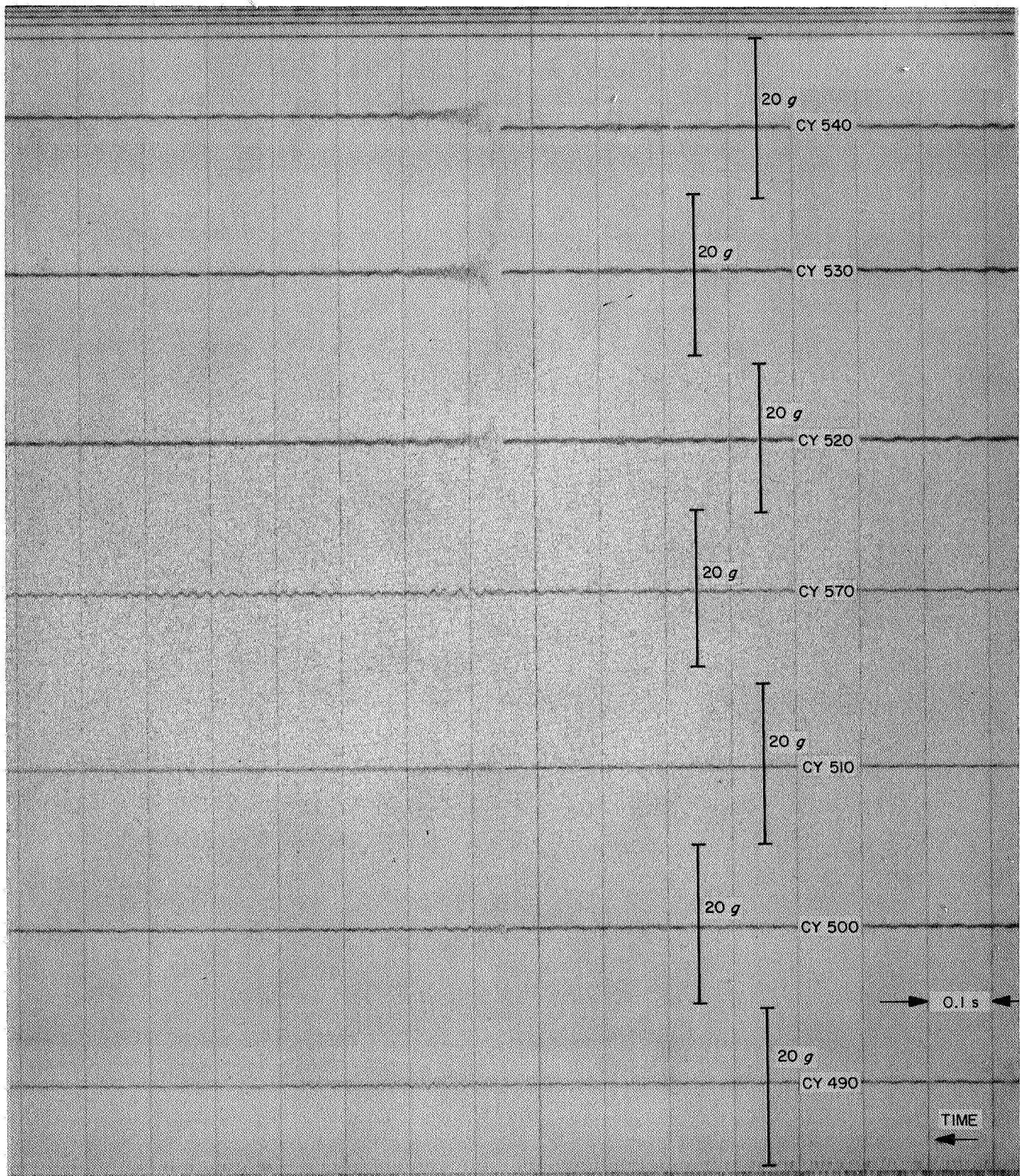


Fig. 25. Oscillogram, SD-2, Atlas/Centaur separation

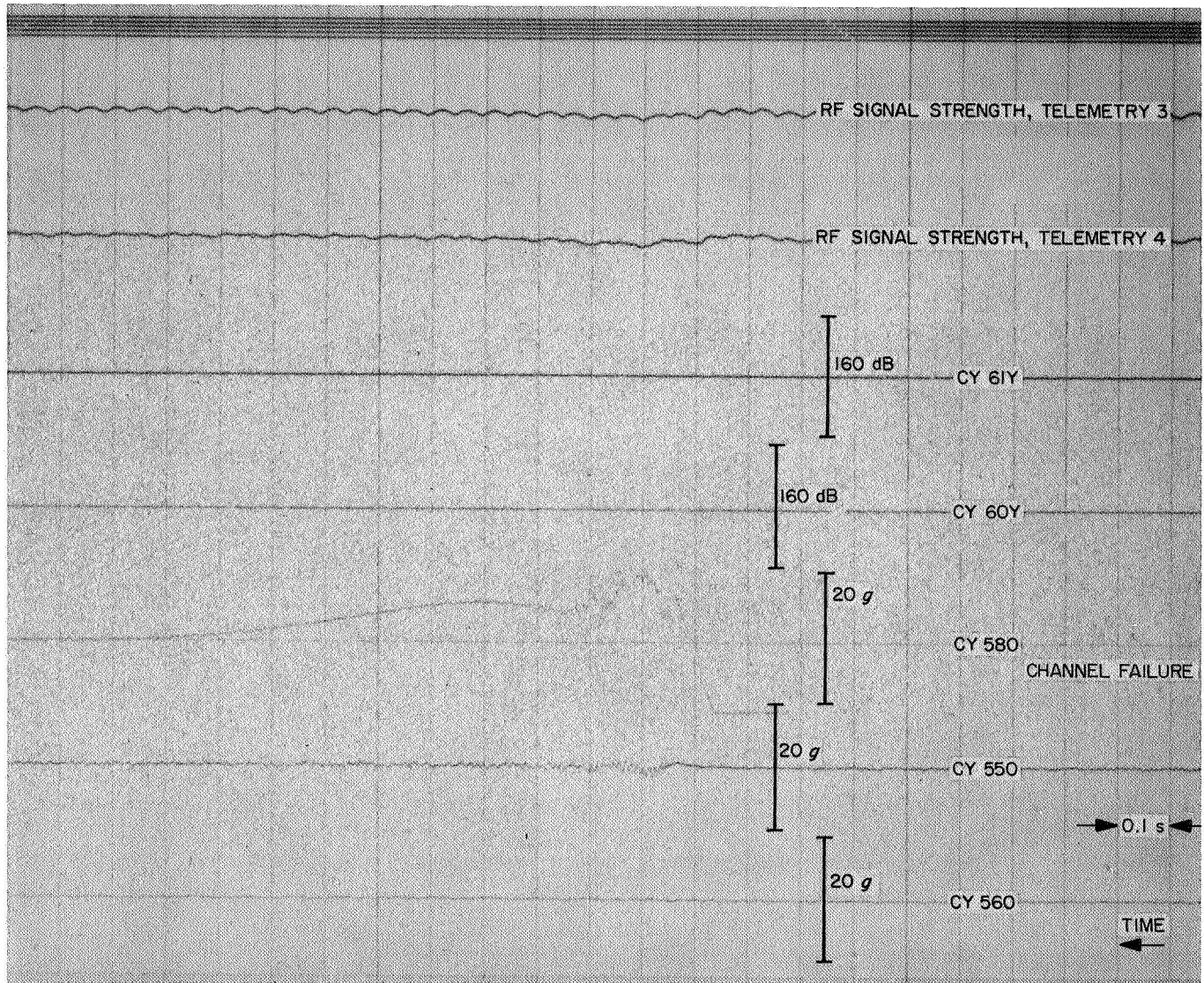


Fig. 26. Oscillogram, SD-2, Centaur main engine ignition

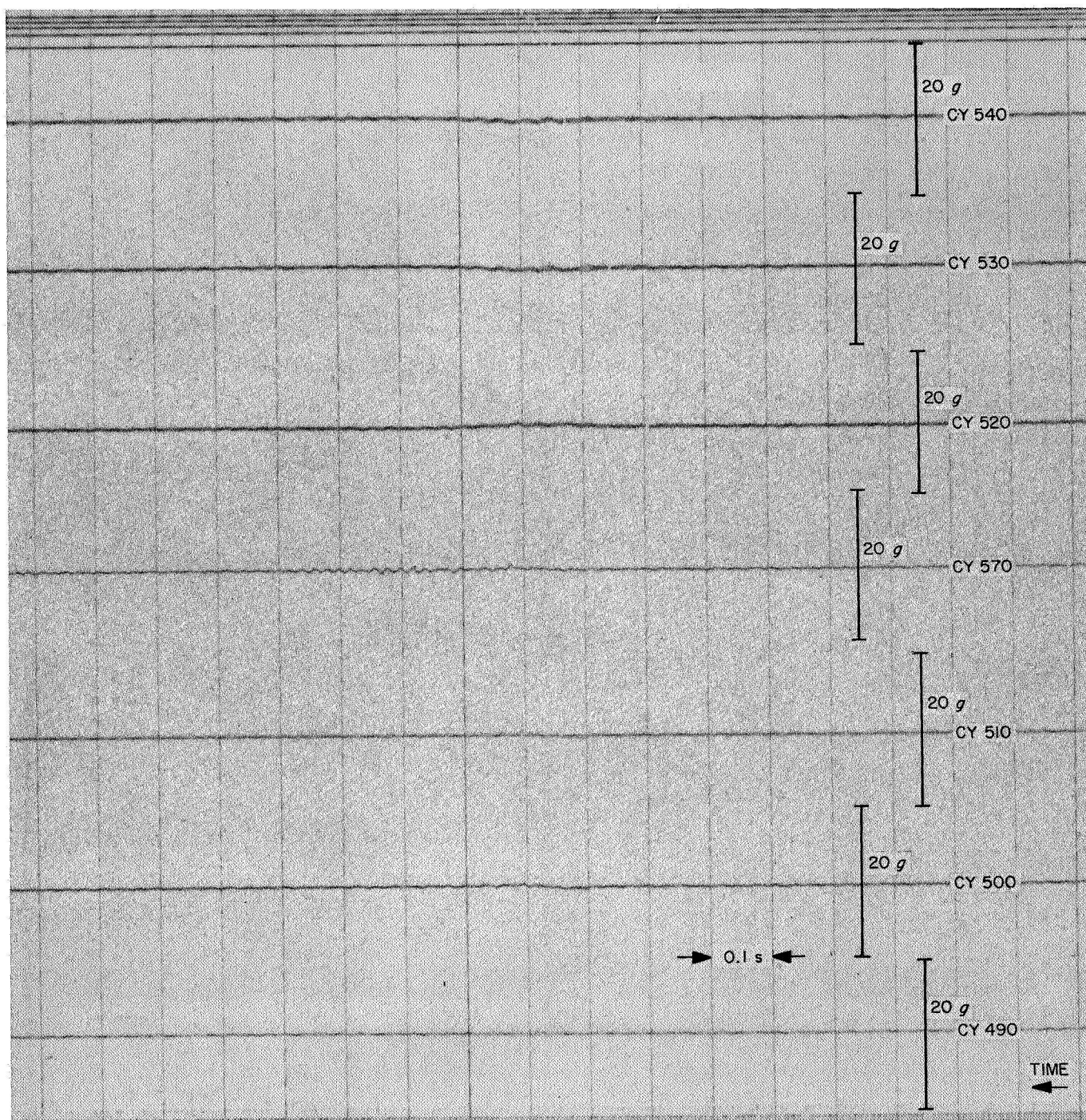


Fig. 27. Oscillogram, SD-2, Centaur main engine ignition

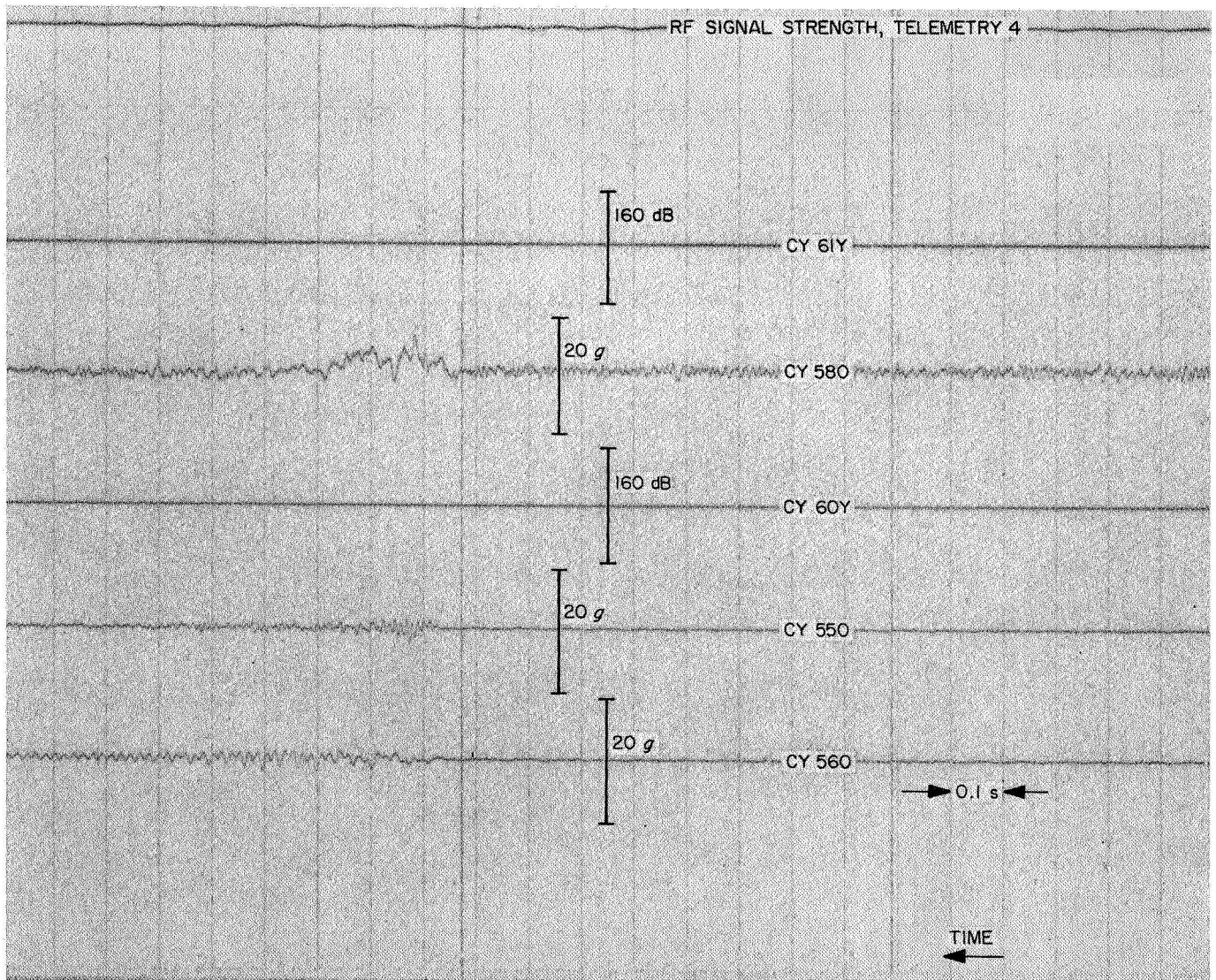


Fig. 28. Oscillogram, SD-2, Centaur main engine cutoff

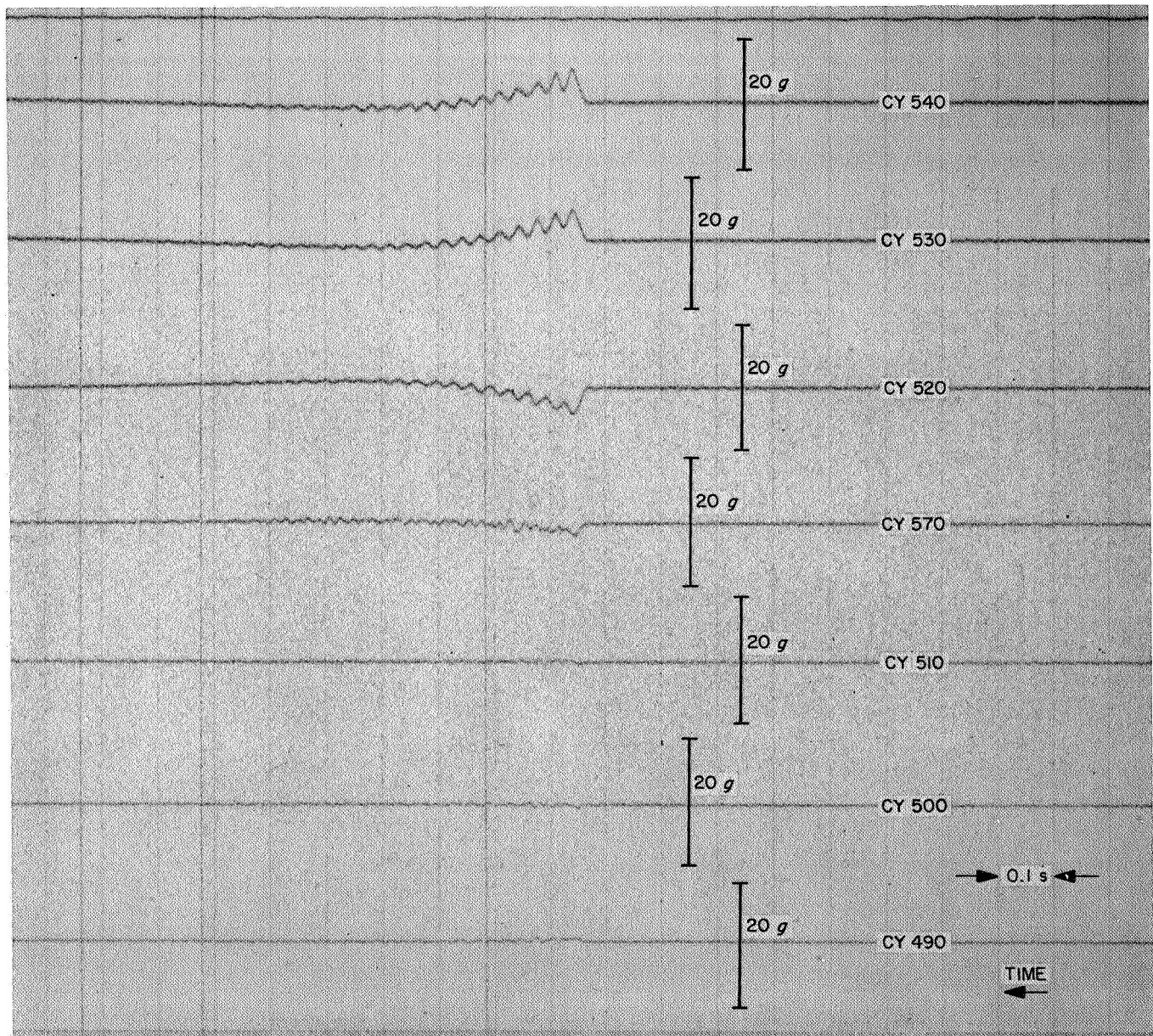


Fig. 29. Oscillogram, SD-2, Centaur main engine cutoff

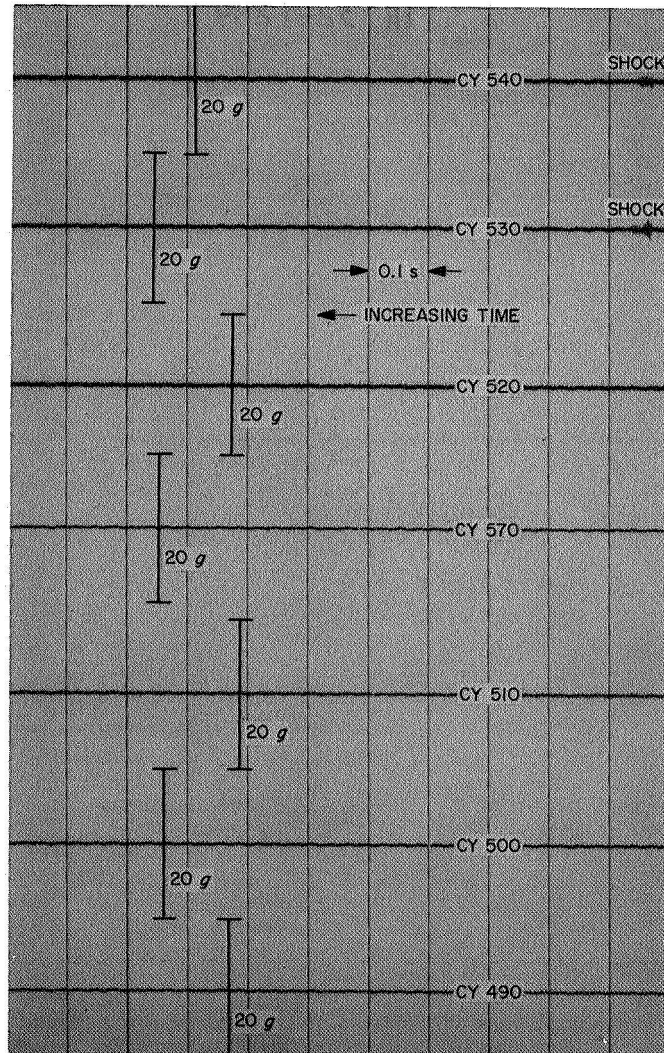


Fig. 30. Oscillogram, SD-2, anomalies

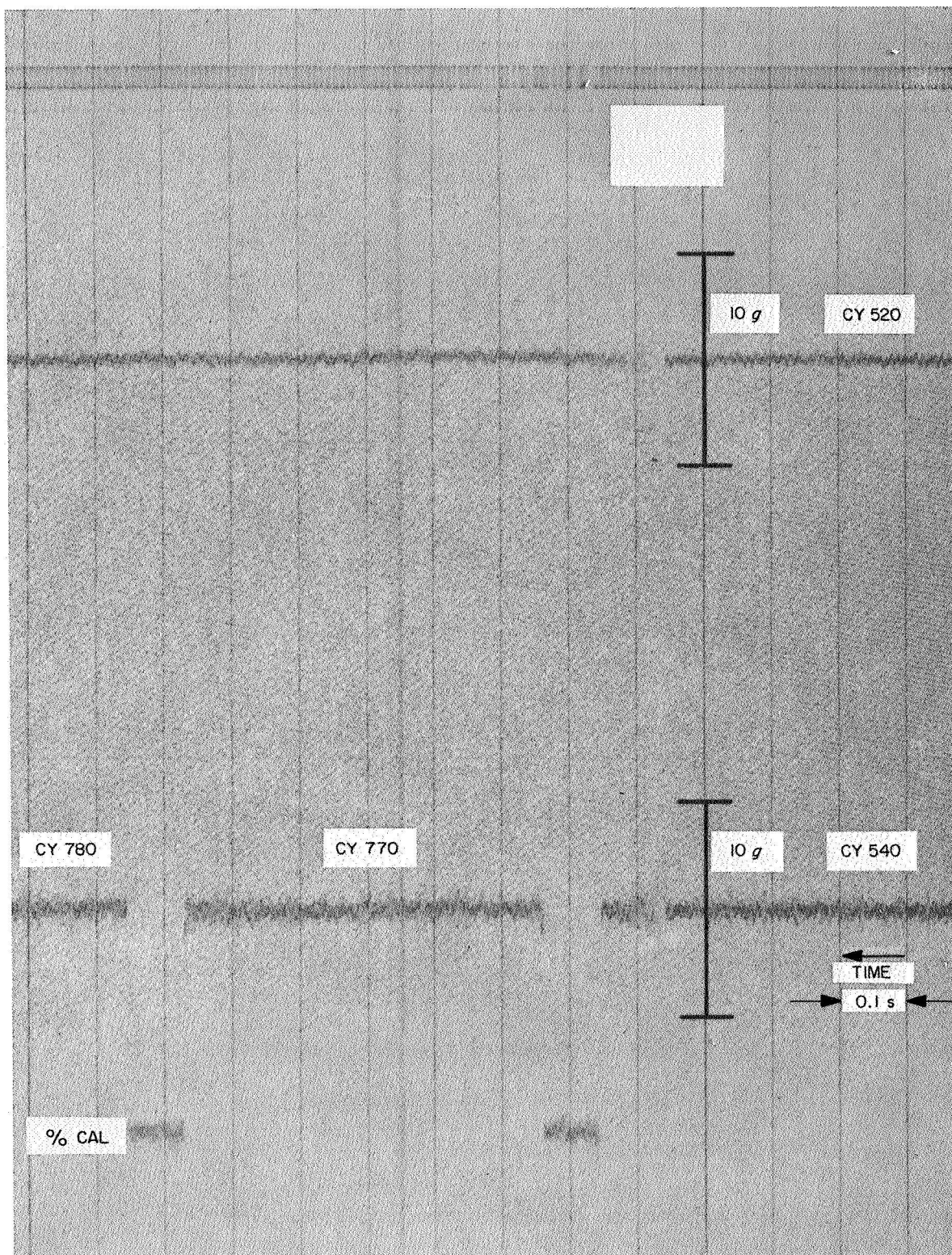


Fig. 31. Oscillogram, SC-1, landing gear extension

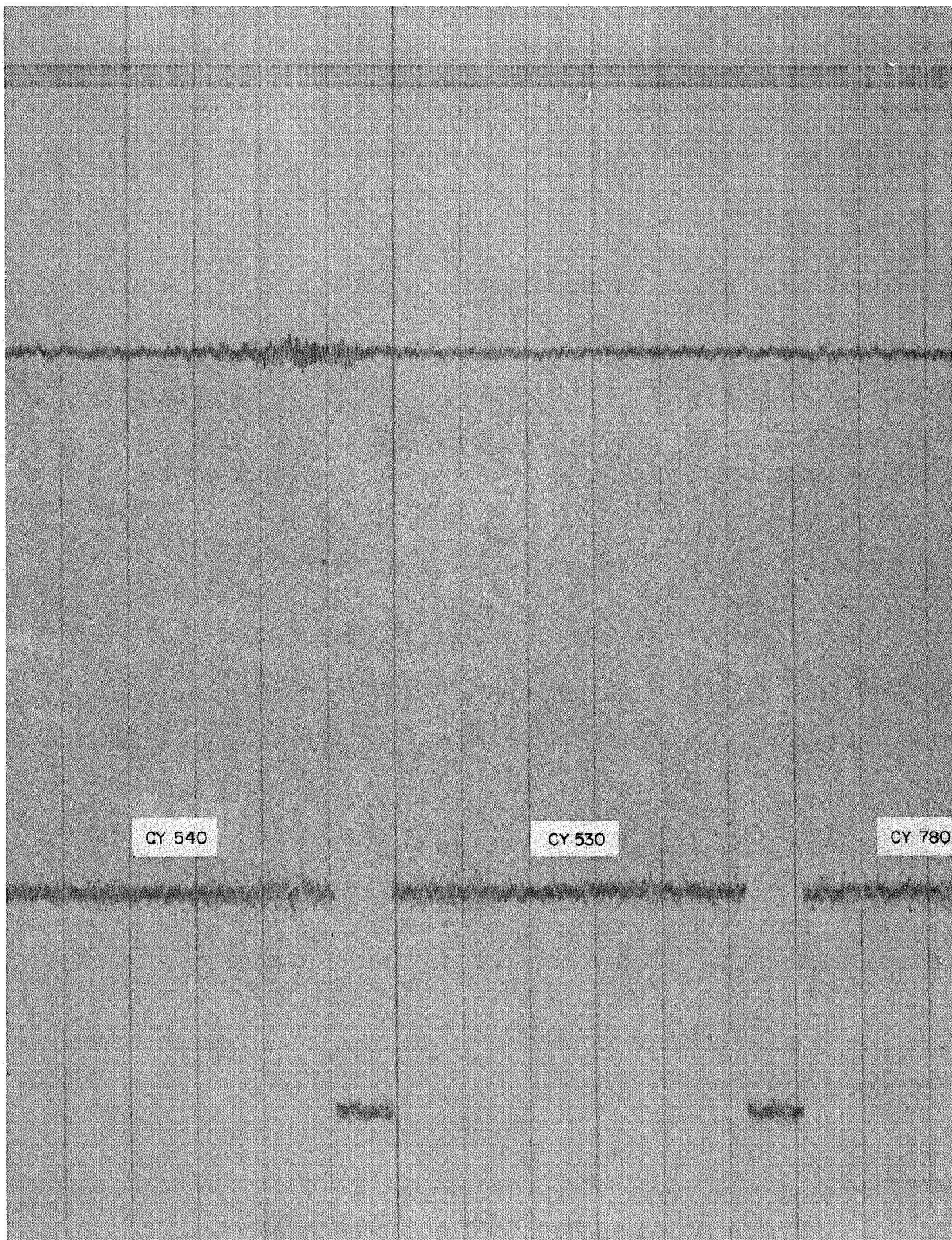


Fig. 32. Oscillogram, SC-1, landing gear lock

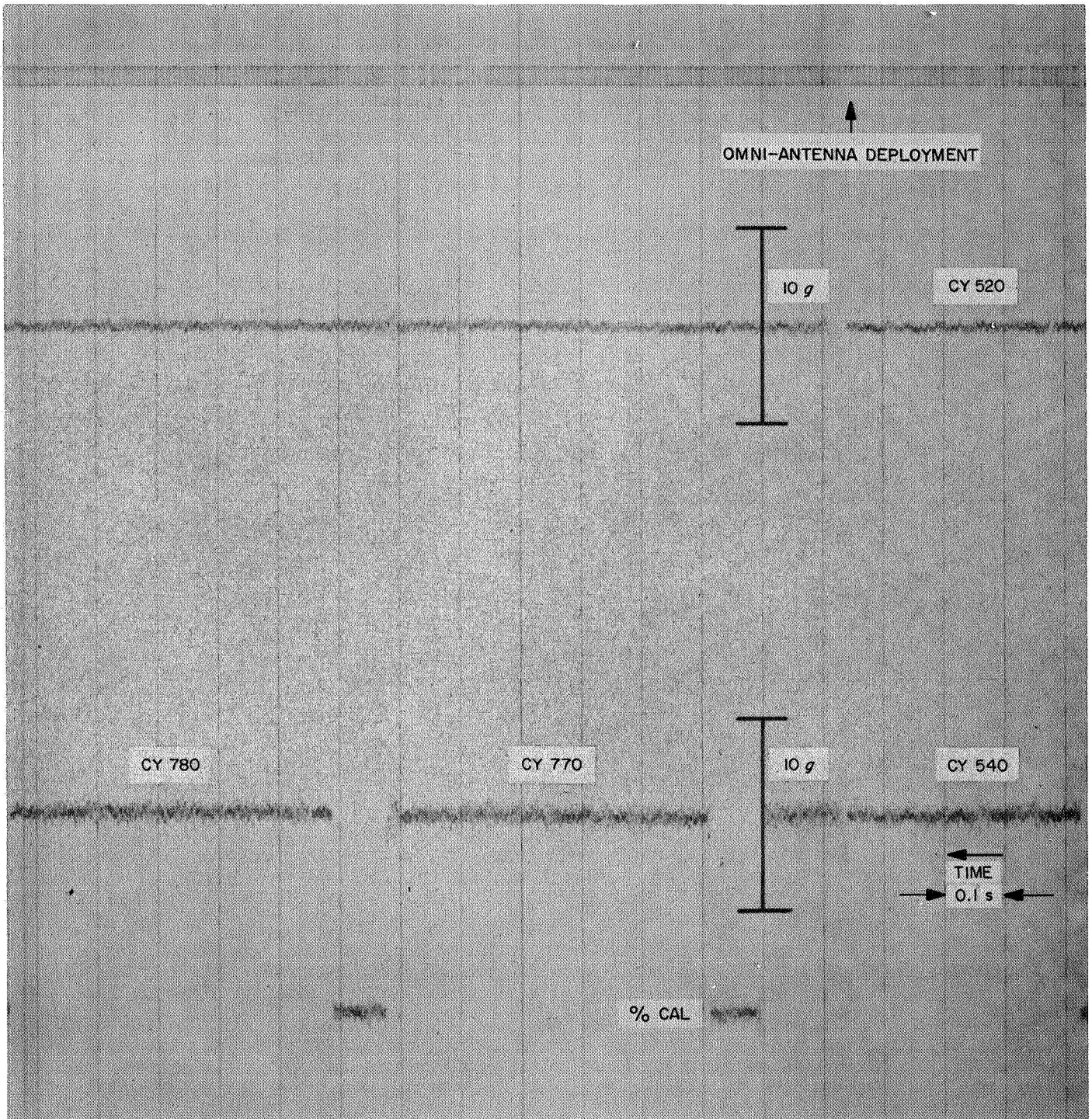


Fig. 33. Oscillogram, SC-1, omni antenna deploy

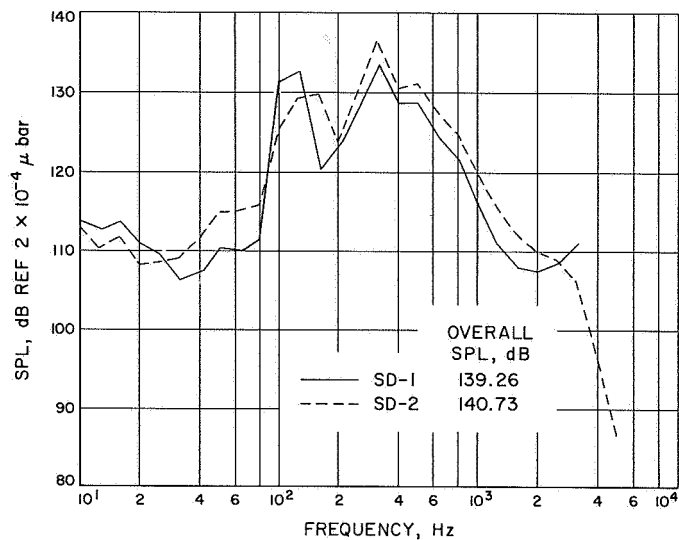


Fig. 34. Sound pressure spectrum level, $\frac{1}{3}$ octave bands, CY 60Y, SD-1 and -2, liftoff

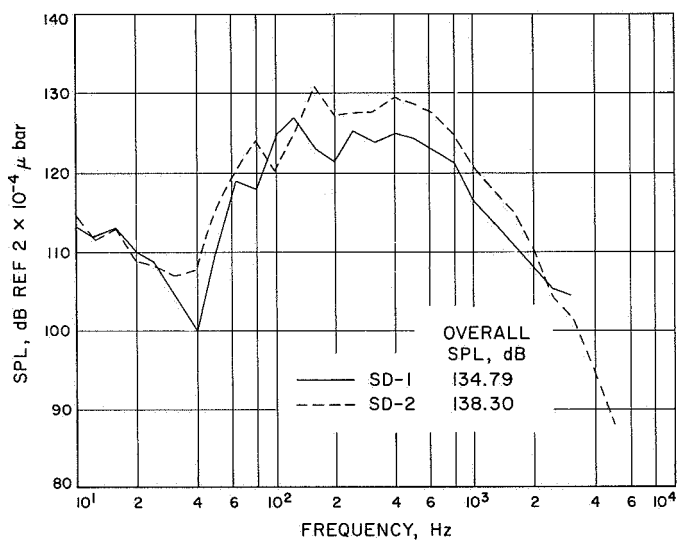


Fig. 35. Sound pressure spectrum level, $\frac{1}{3}$ octave bands, CY 61Y, SD-1 and -2, liftoff

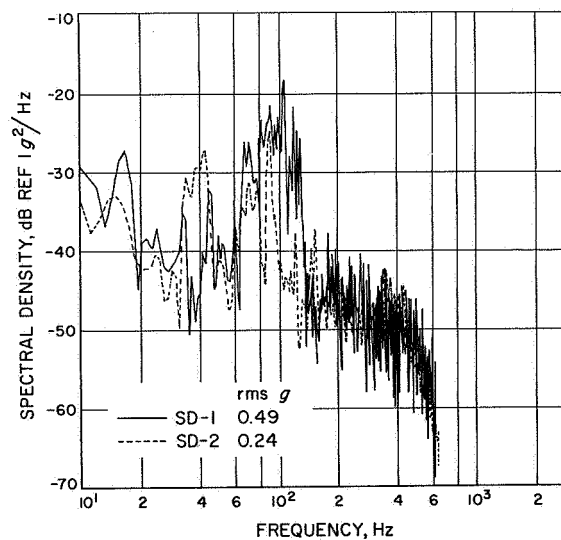


Fig. 36. Acceleration spectral density, CY 490, SD-1 and -2, liftoff

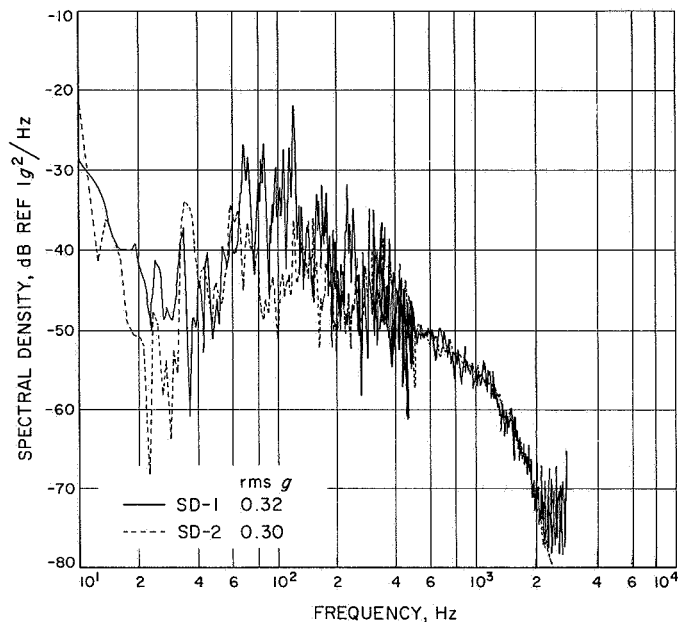


Fig. 37. Acceleration spectral density, CY 500, SD-1 and -2, liftoff

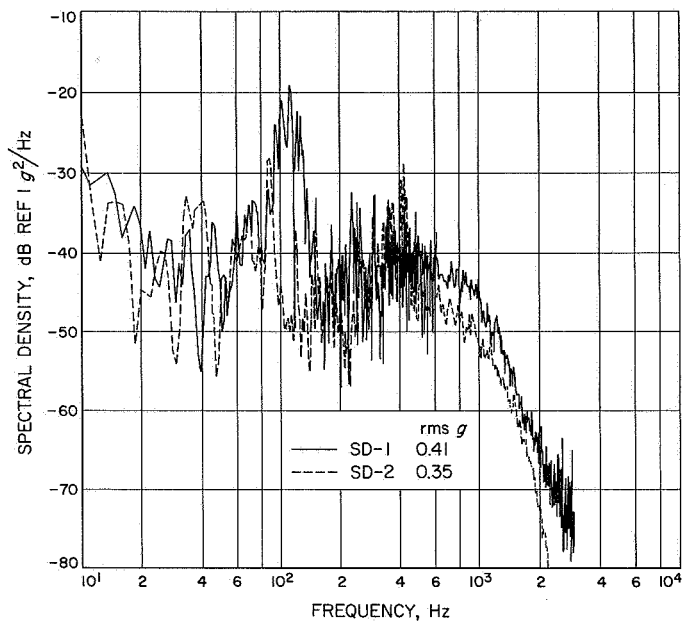


Fig. 38. Acceleration spectral density, CY 510, SD-1 and -2, liftoff

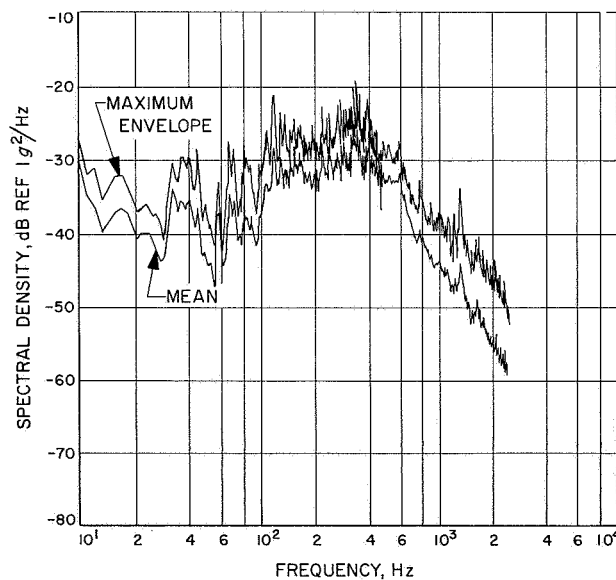


Fig. 39. Acceleration spectral density, maximum envelope and average for CY 520, 530 and 540; SD-1 and -2 and SC-1 through -4, liftoff

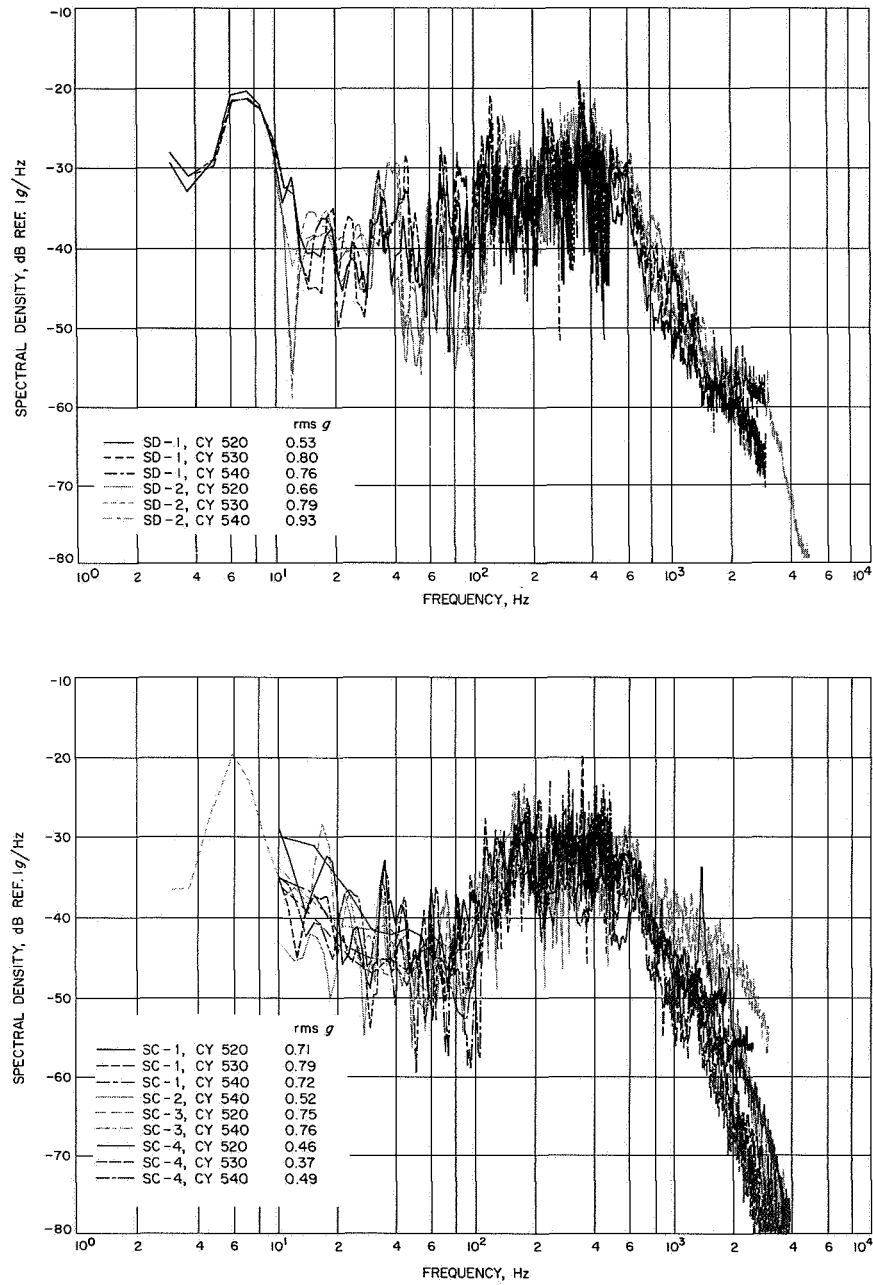


Fig. 40. Acceleration spectral density, CY 520, 530, and 540; SD-1 and -2, and SC-1 through -4, liftoff

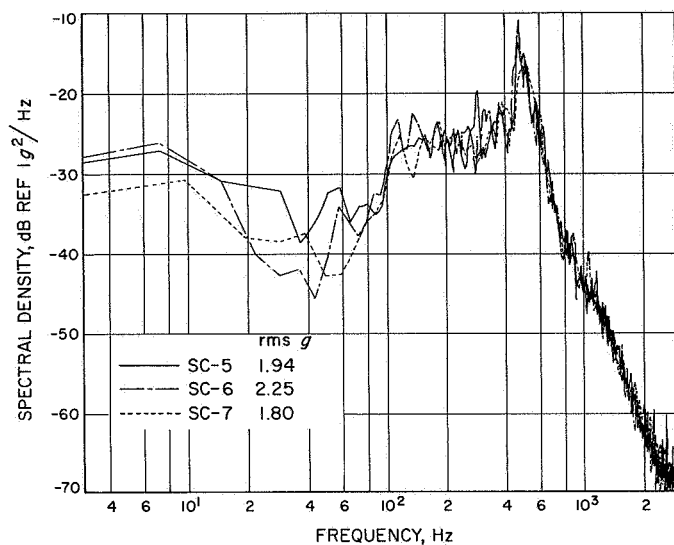


Fig. 41. Acceleration spectral density, CA 7720, SC-5 through -7, liftoff

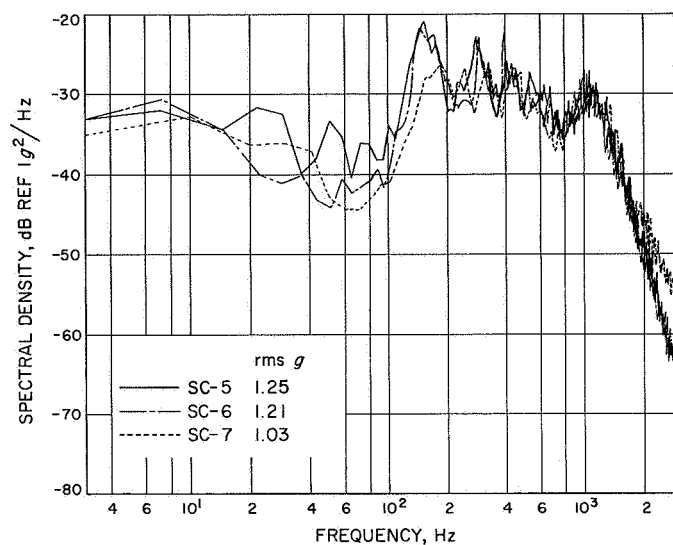


Fig. 42. Acceleration spectral density, CA 7730, SC-5 through -7, liftoff

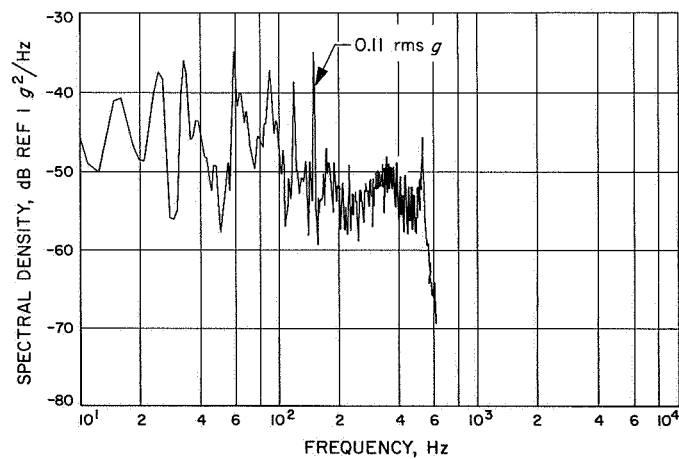


Fig. 43. Acceleration spectral density, CY 490, SD-2, transonic

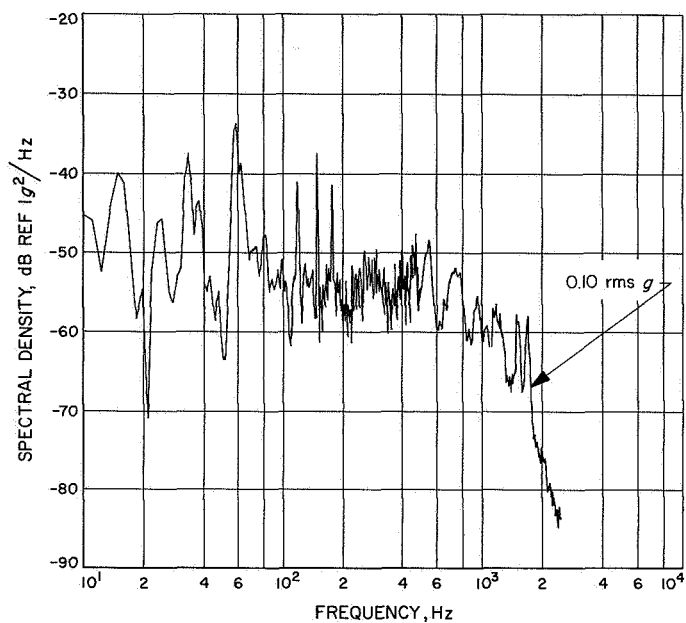


Fig. 44. Acceleration spectral density, CY 500, SD-2, transonic

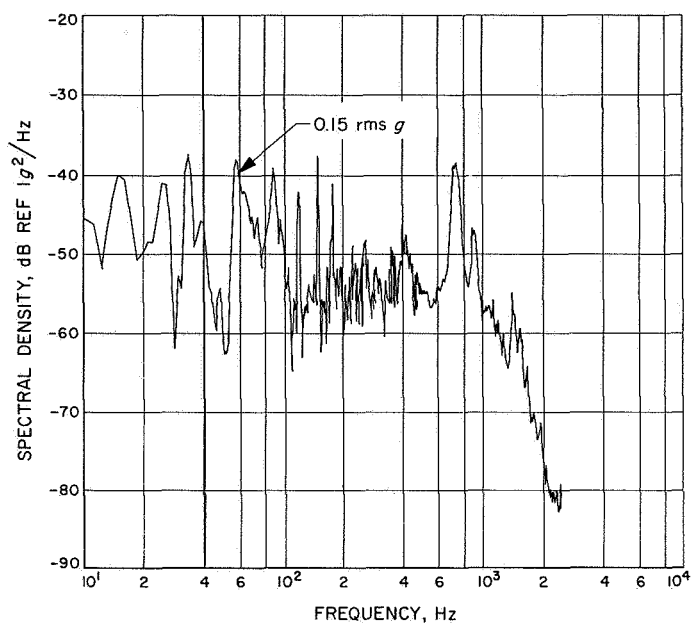


Fig. 45. Acceleration spectral density, CY 510, SD-2, transonic

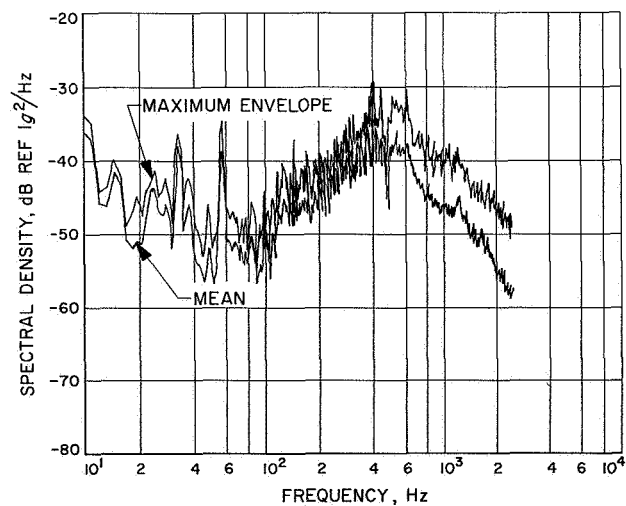


Fig. 46. Acceleration spectral density, maximum envelope and average for CY 520, 530, and 540, SD-2 and SC-1 through -4, transonic

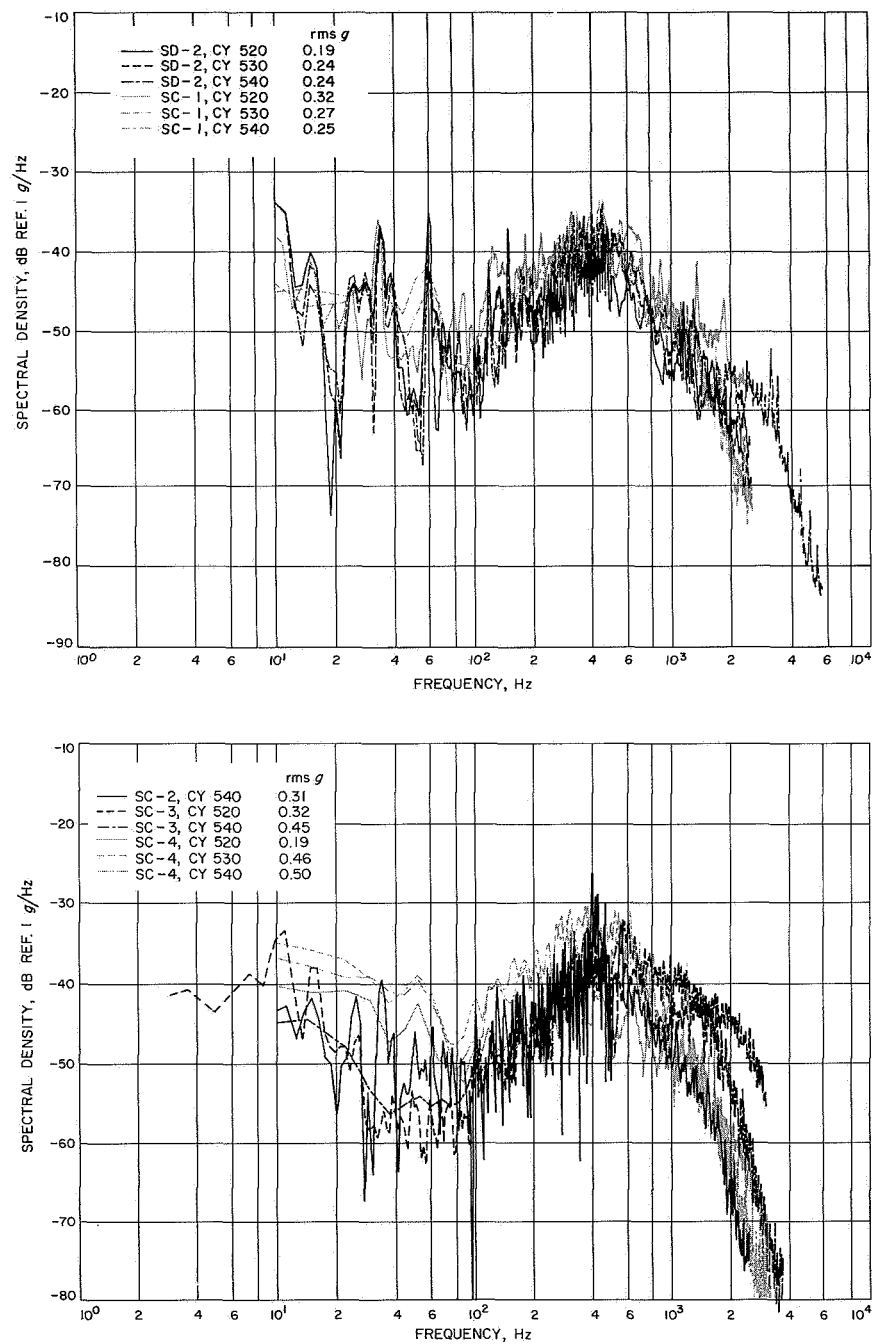


Fig. 47. Acceleration spectral density, CY 520, 530, and 540, SD-2, and SC-1 through -4, transonic

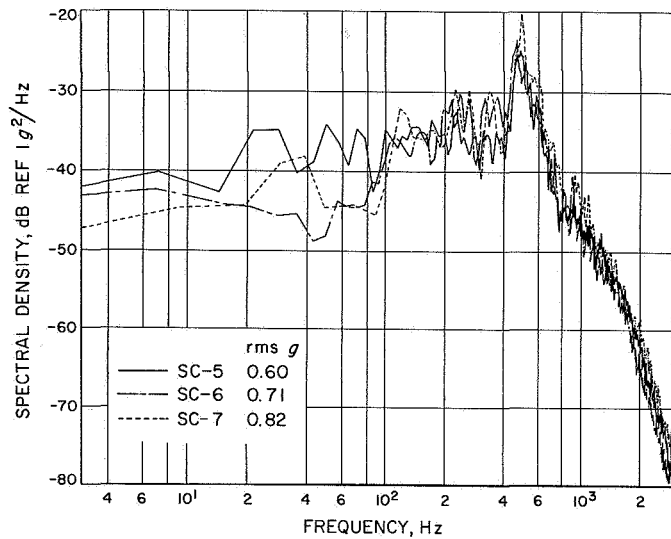


Fig. 48. Acceleration spectral density, CA 7720, SC-5 through -7, transonic

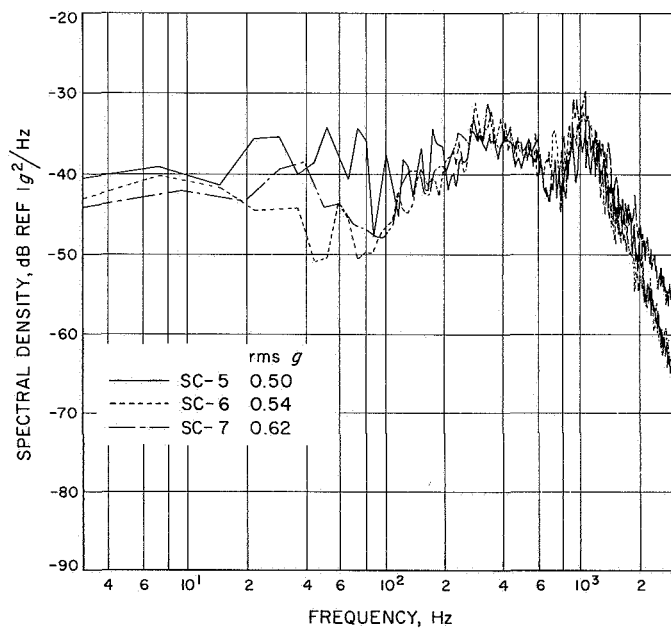


Fig. 49. Acceleration spectral density, CA 7730, SC-5 through -7, transonic

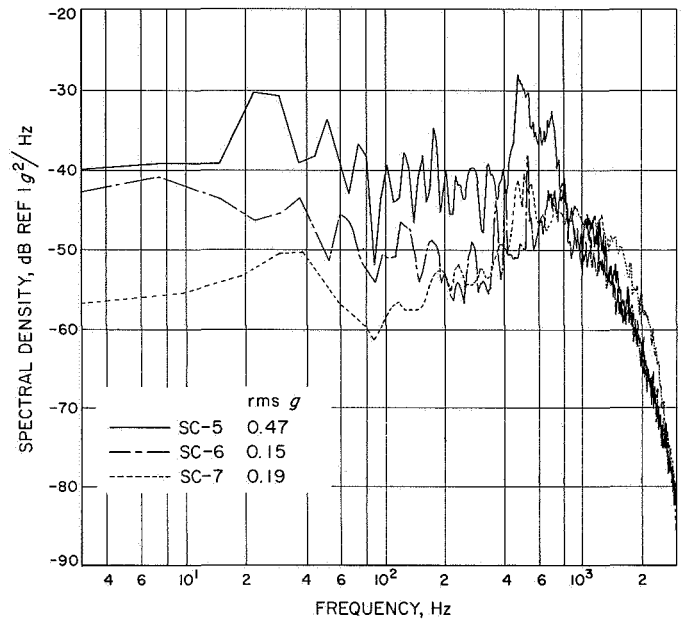


Fig. 50. Acceleration spectral density, CA 7720, SC-5 through -7, hydrogen boiloff valve operation

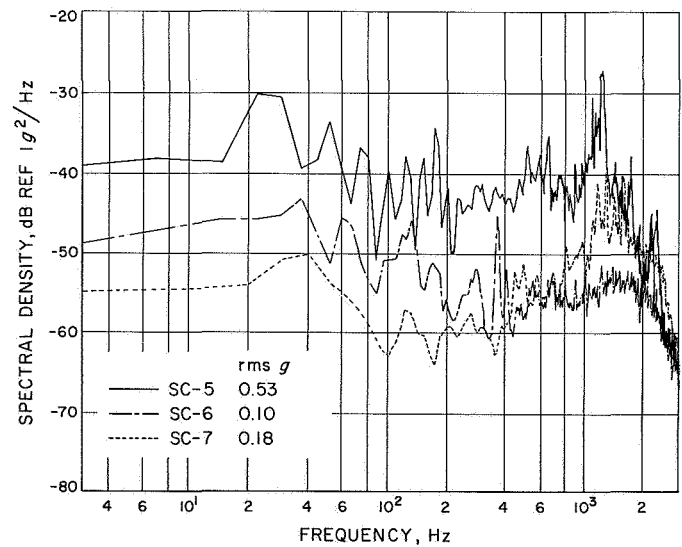


Fig. 51. Acceleration spectral density, CA 7730, SC-5 through -7, hydrogen boiloff valve operation

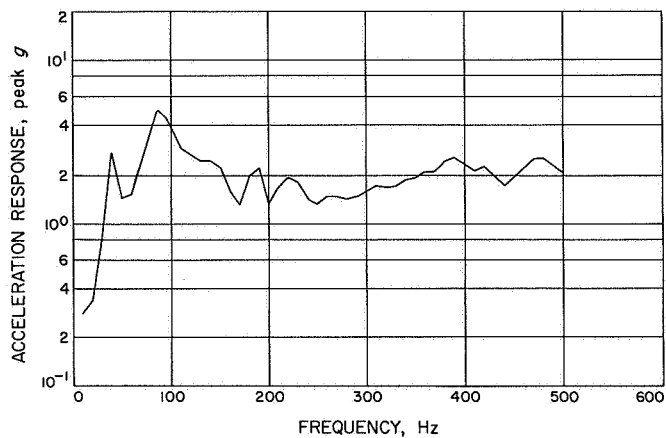


Fig. 52. Maximum envelope of the shock spectra for all transients, CY 490, SD-2

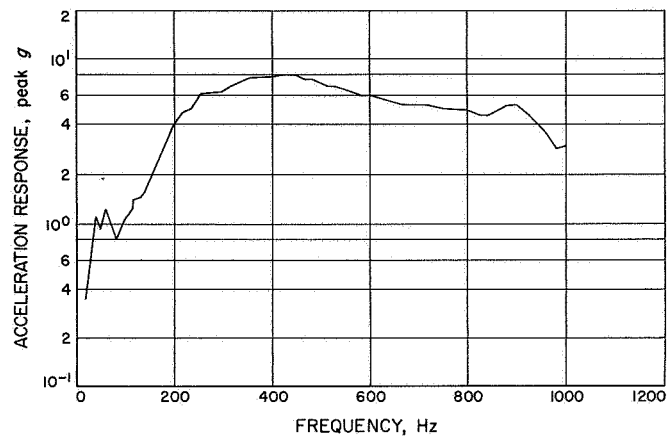


Fig. 53. Maximum envelope of the shock spectra for all transients, CY 500, SD-2

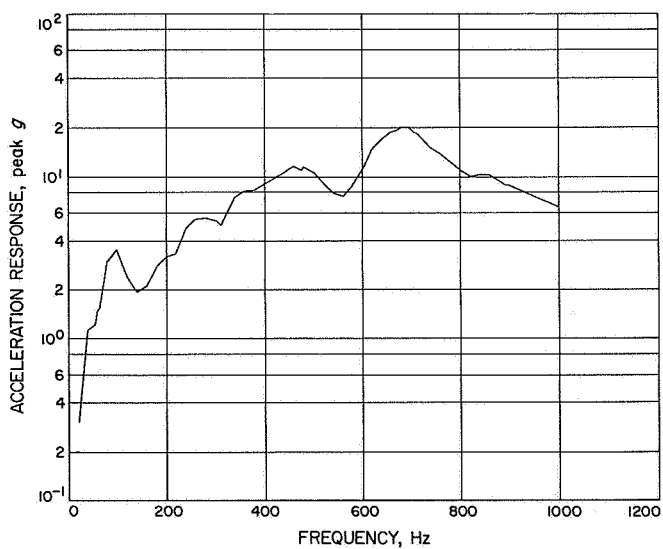


Fig. 54. Maximum envelope of the shock spectra for all transients, CY 510, SD-2

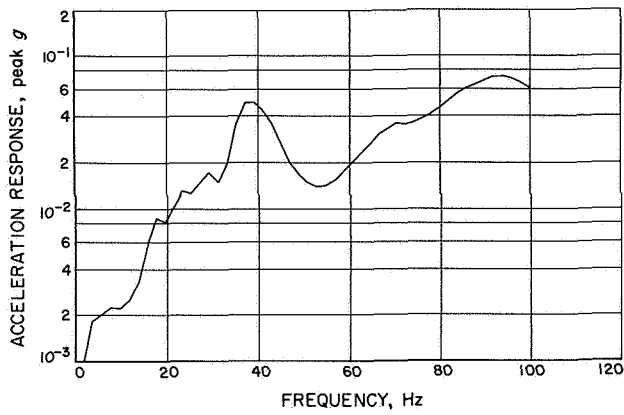


Fig. 55. Maximum envelope of the shock spectra for all transients, torsion, SD-2

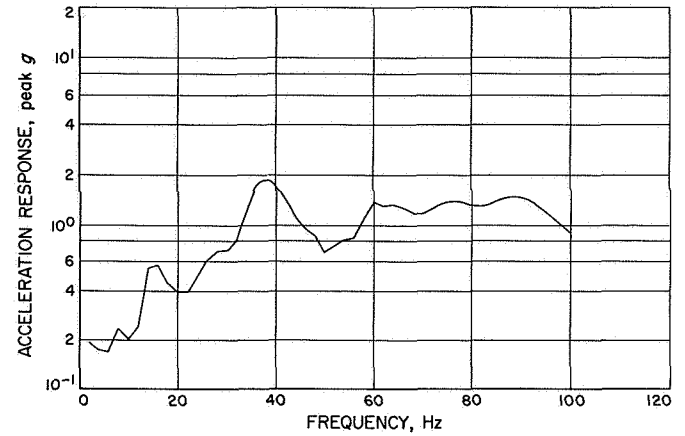


Fig. 56. Maximum envelope of the shock spectra for all transients, X-axis, SD-2

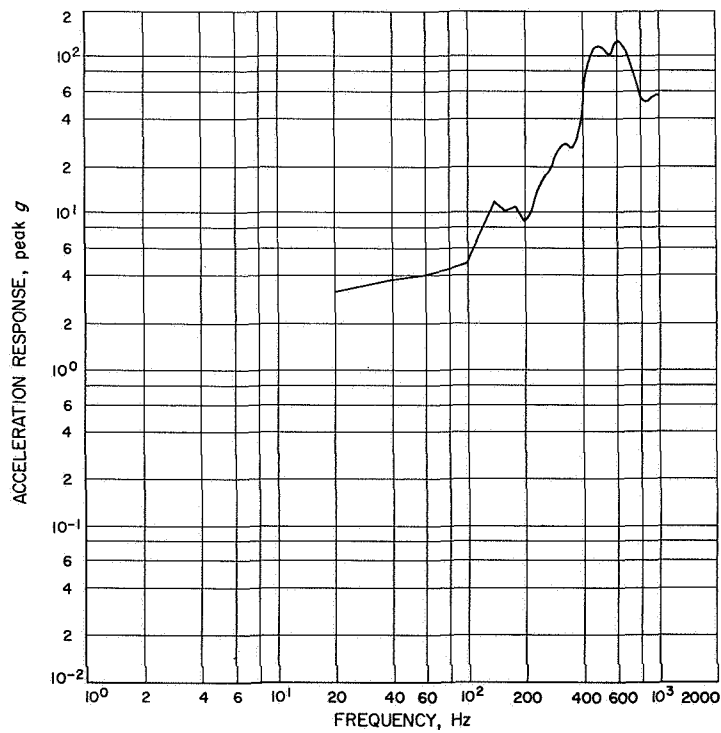


Fig. 57. Maximum envelope of the shock spectra for all transients, CY 520, 530, and 540, SD-2 and SC-1 through -4

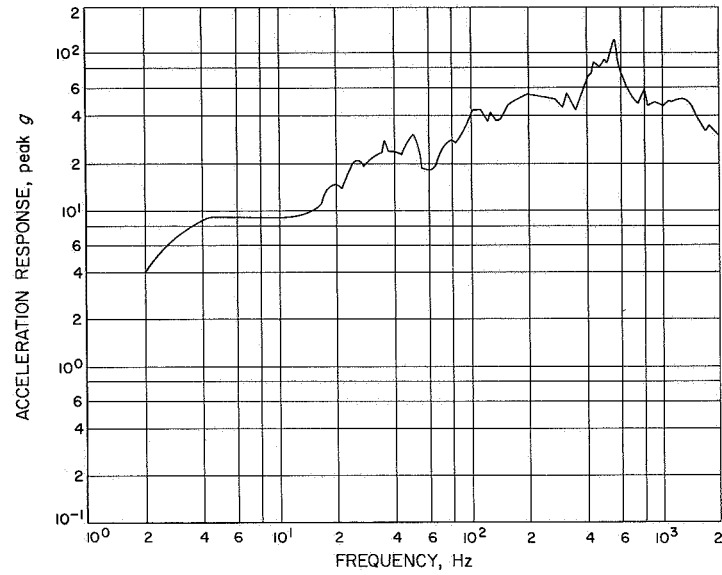


Fig. 58. Maximum envelope of the shock spectra for all transients, CA 7720, SC-5 through -7

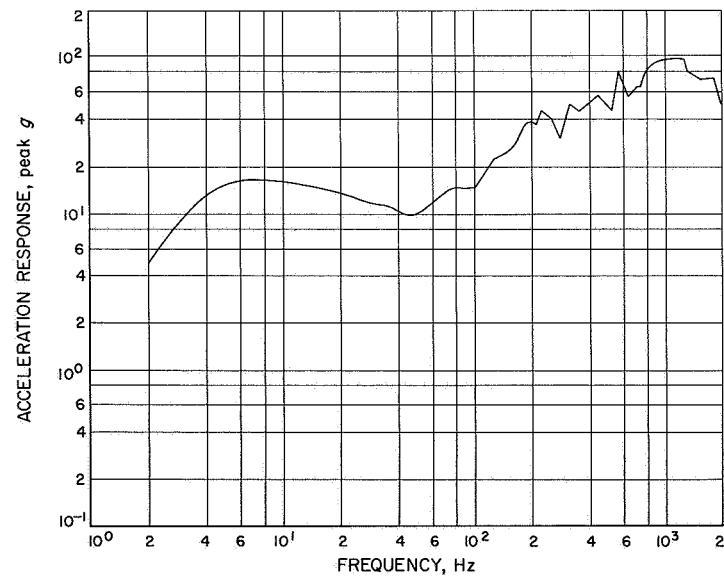


Fig. 59. Maximum envelope of the shock spectra for all transients, CA 7730, SC-5 through -7

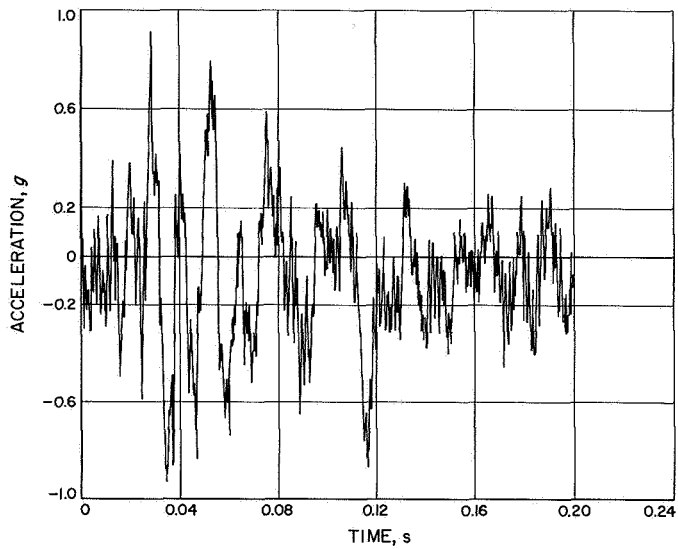


Fig. 60. Measured transient, CY 490, SD-2, insulation panel jettison

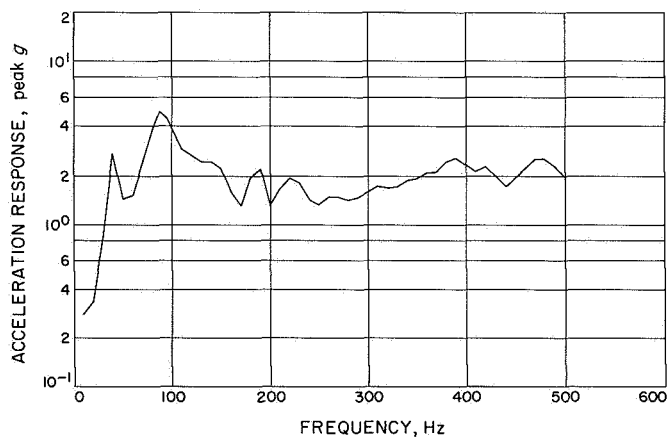


Fig. 61. Shock spectrum, CY 490, SD-2, insulation panel jettison

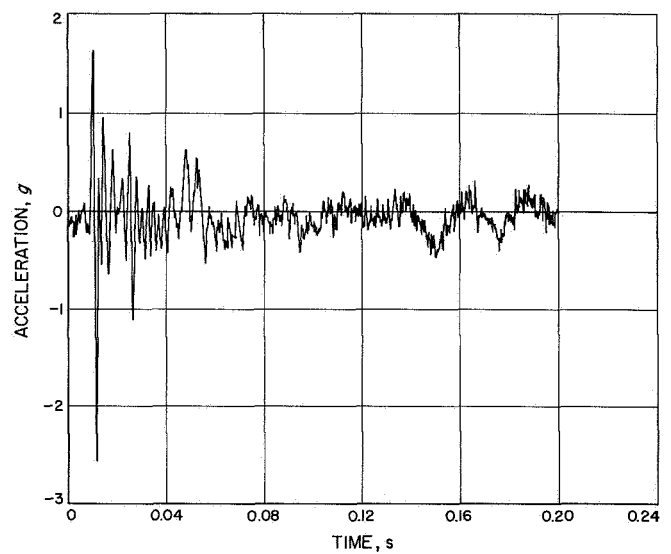


Fig. 62. Measured transient, CY 500, SD-2, insulation panel jettison

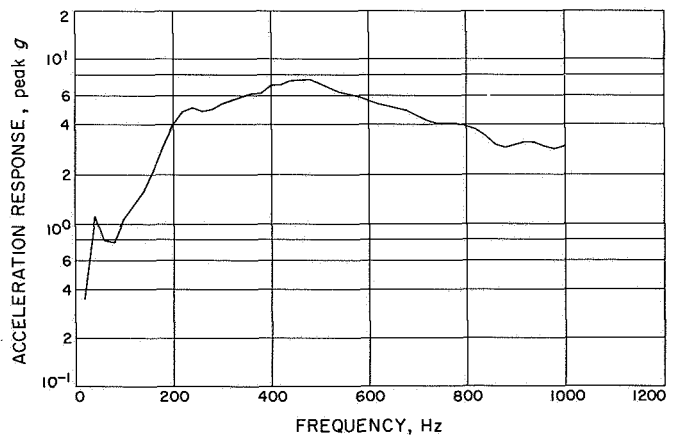


Fig. 63. Shock spectrum, CY 500, SD-2, insulation panel jettison

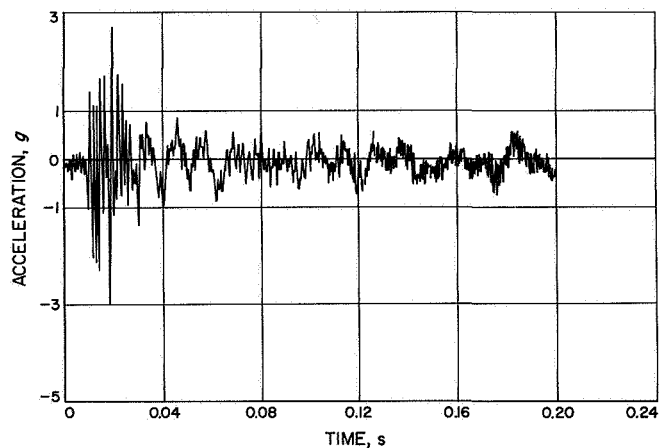


Fig. 64. Measured transient, CY 510, SD-2, insulation panel jettison

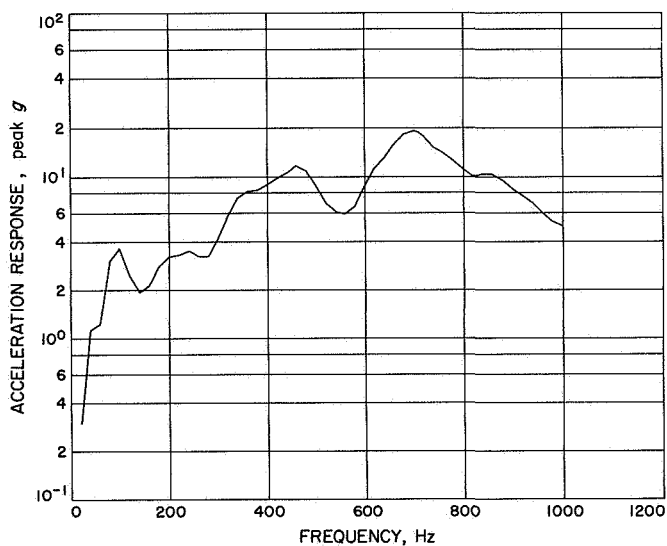


Fig. 65. Shock spectrum, CY 510, SD-2, insulation panel jettison

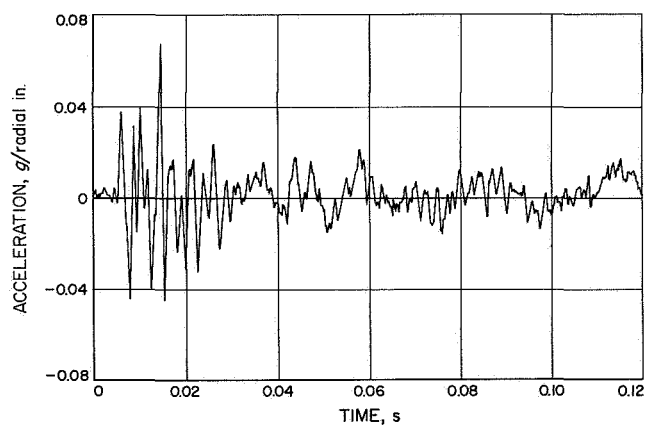


Fig. 66. Measured transient, torsion, SD-2, insulation panel jettison

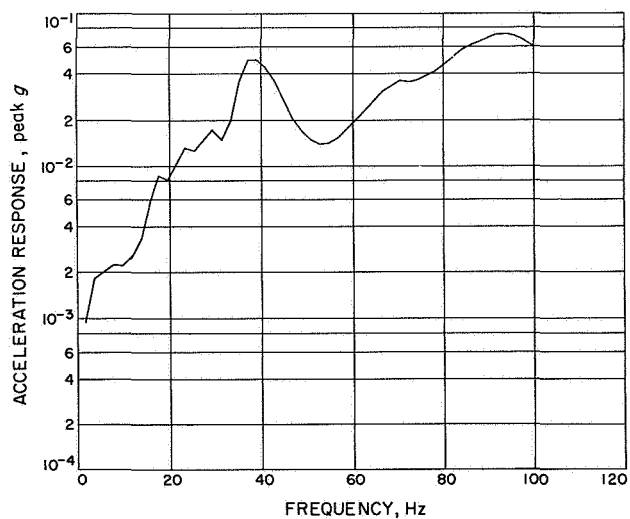
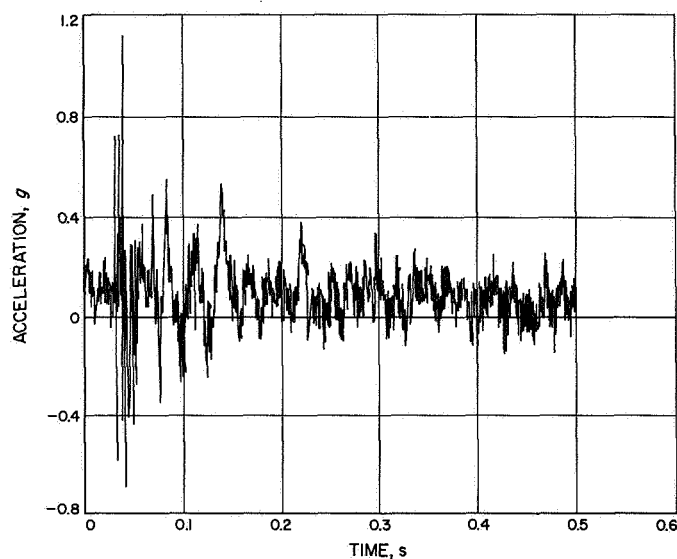
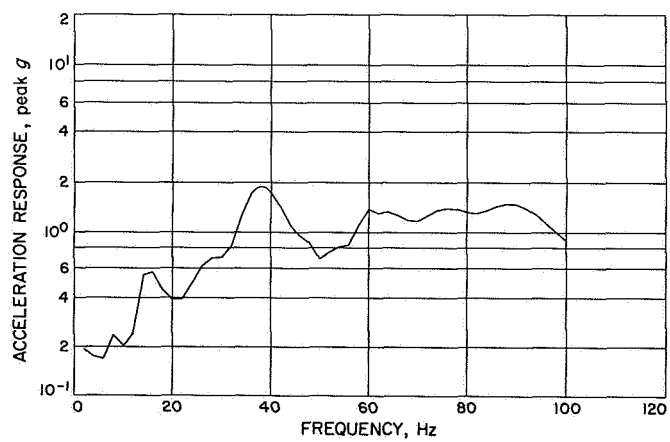


Fig. 67. Shock spectrum, torsion, SD-2, insulation panel jettison



**Fig. 68. Measured transient, X-axis, SD-2,
insulation panel jettison**



**Fig. 69. Shock spectrum, X-axis, SD-2,
insulation panel jettison**

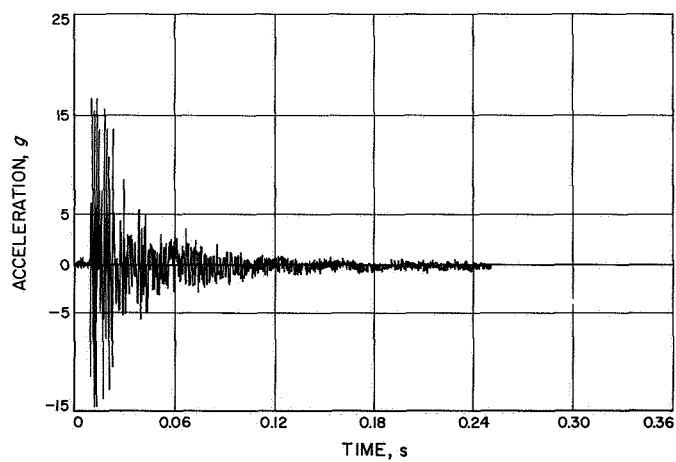


**Fig. 70. Typical measured transient, CY 520, 530, or
540, SD-2 and SC-1 through -4, insulation panel jettison**

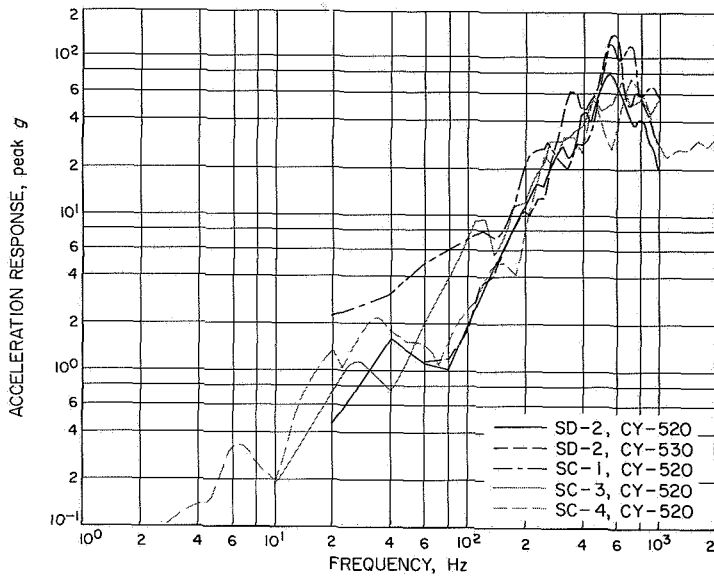


Fig. 71. Shock spectra, CY 520, 530, and 540, SD-2 and SC-1 through -4, insulation panel jettison

Fig. 72. Typical measured transient, CA 7720, SC-5 through -7, insulation panel jettison

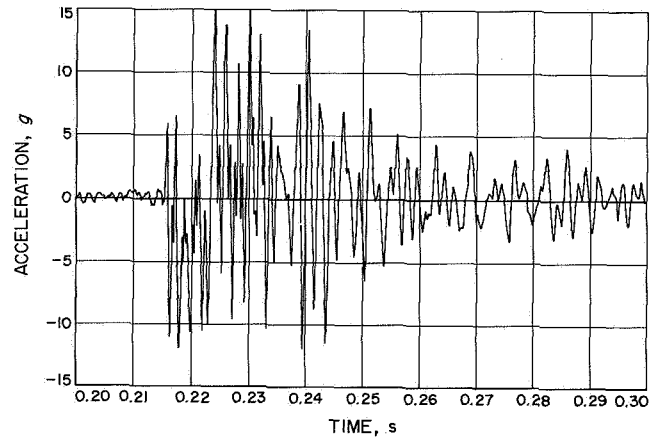
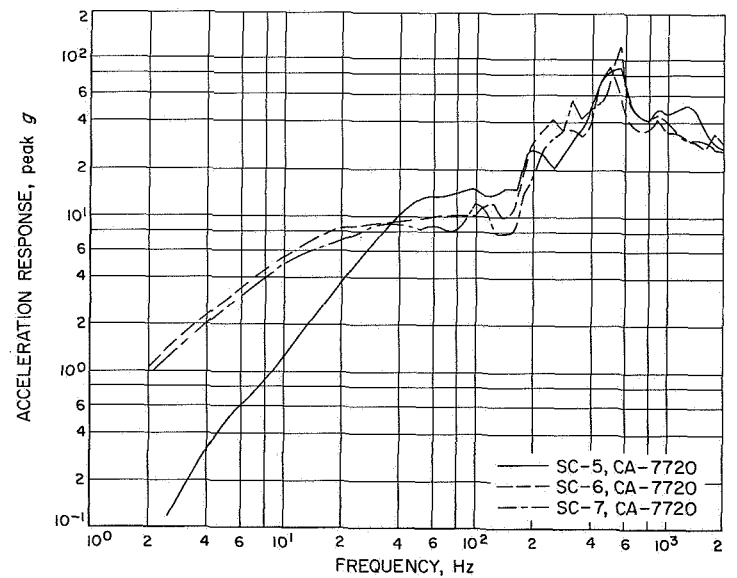


Fig. 73. Shock spectra, CA 7720, SC-5 through -7, insulation panel jettison



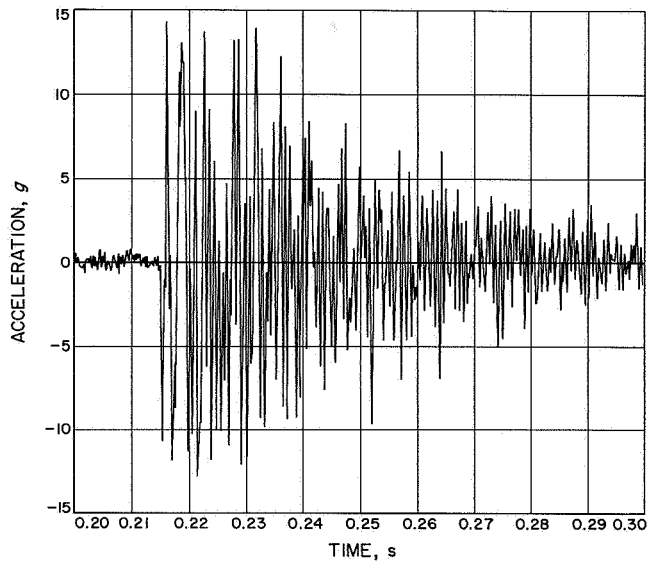


Fig. 74. Typical measured transient, CA 7730, SC-5 through -7, insulation panel jettison

Fig. 75. Shock spectra, CA 7730, SC-5 through -7, insulation panel jettison

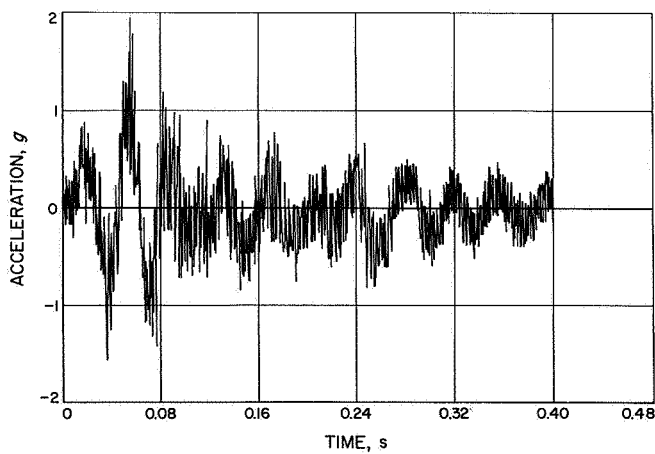
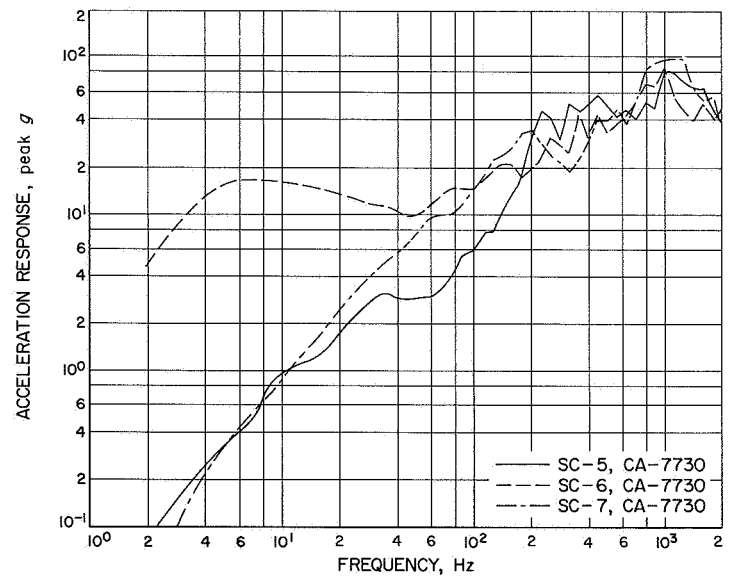


Fig. 76. Typical measured transient, CY 520, 530, or 540, SD-2 and SC-1 through -4, shroud separation

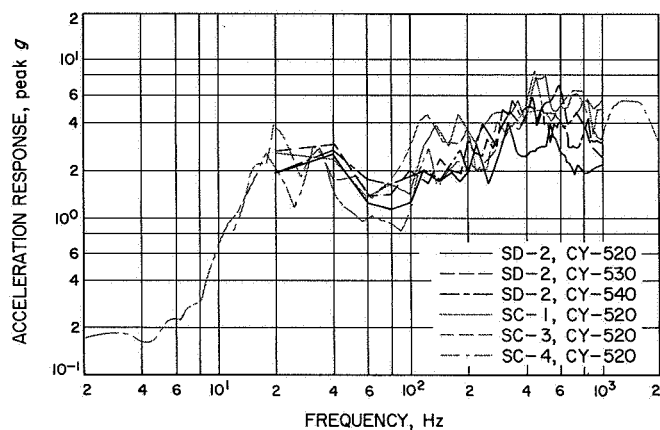


Fig. 77. Shock spectra, CY 520, 530, and 540, SD-2 and SC-1 through -4, shroud separation

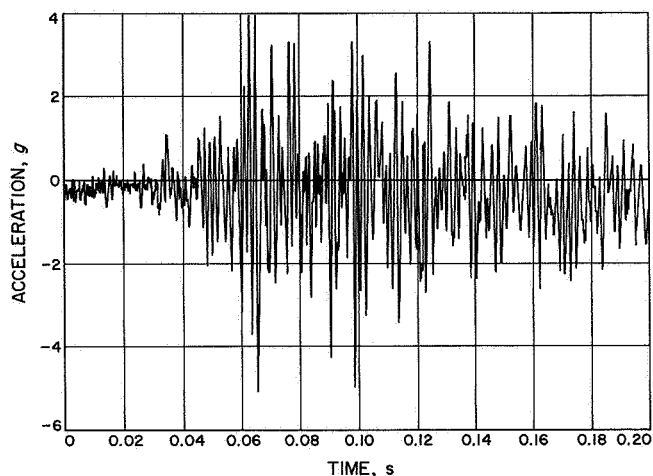


Fig. 78. Typical measured transient, CA 7720, SC-5 through -7, shroud separation

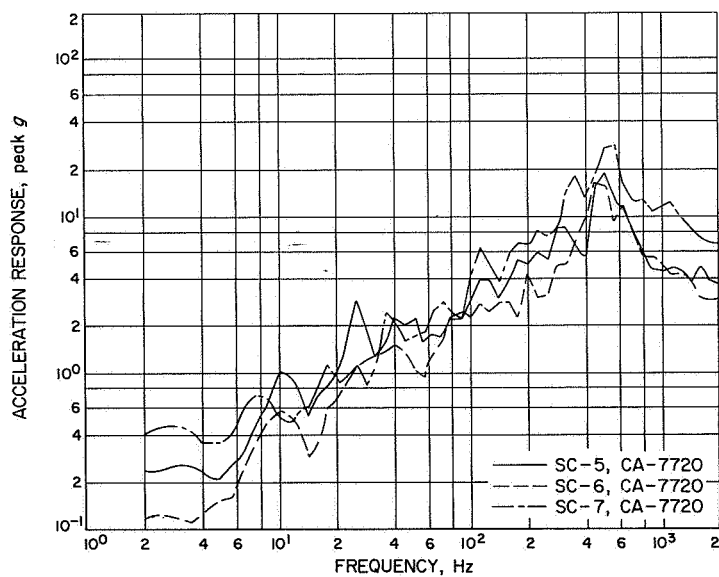
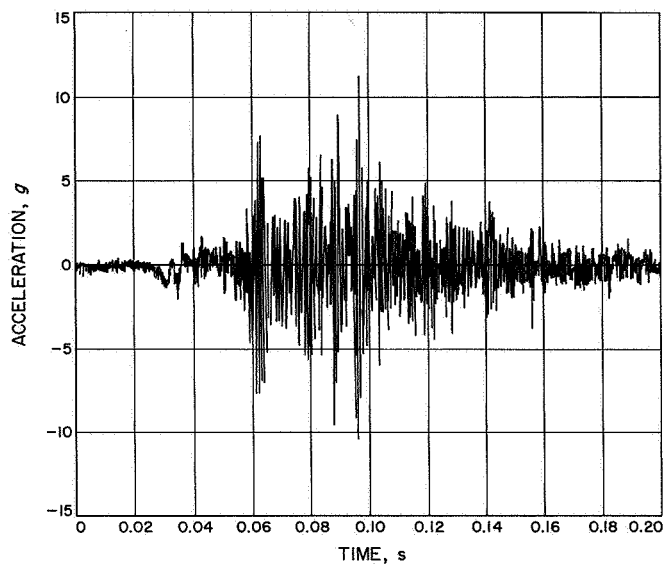
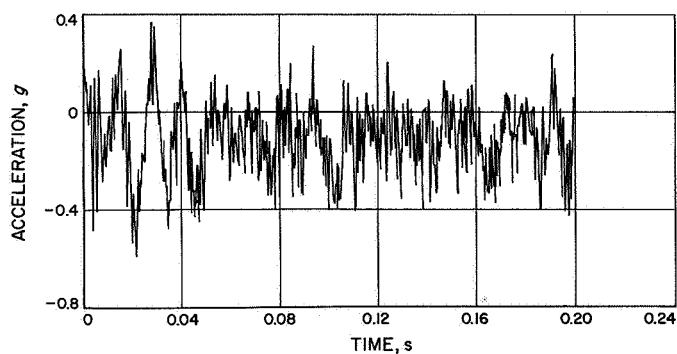
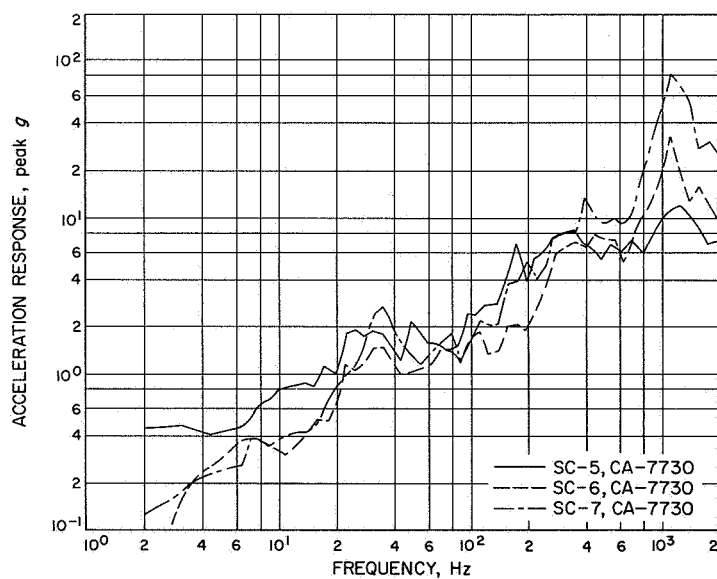


Fig. 79. Shock spectra, CA 7720, SC-5 through -7, shroud separation



**Fig. 80. Typical measured transient, CA 7730,
SC-5 through -7, shroud separation**

**Fig. 81. Shock spectra, CA 7730, SC-5 through -7,
shroud separation**



**Fig. 82. Measured transient, CY 490, SD-2,
Atlas/Centaur separation**

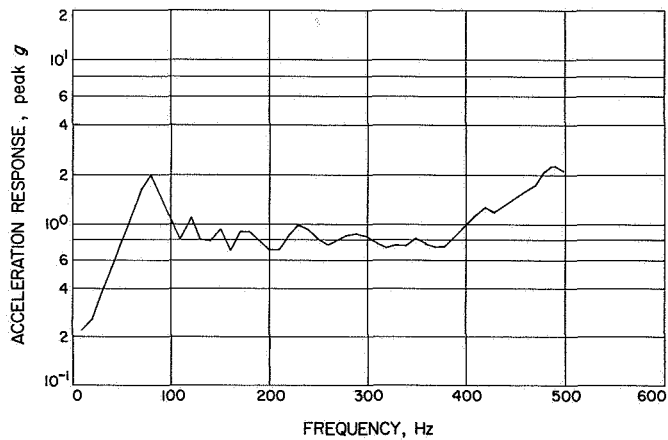


**Fig. 83. Shock spectrum, CY 490, SD-2,
Atlas/Centaur separation**

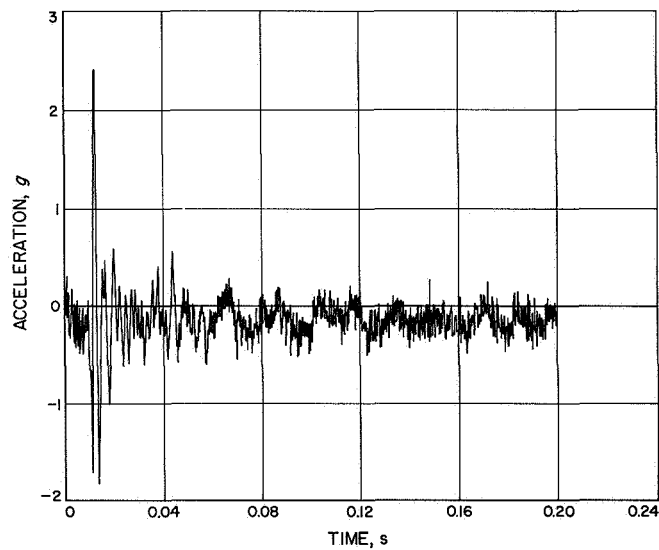


**Fig. 84. Measured transient, CY 500, SD-2,
Atlas/Centaur separation**

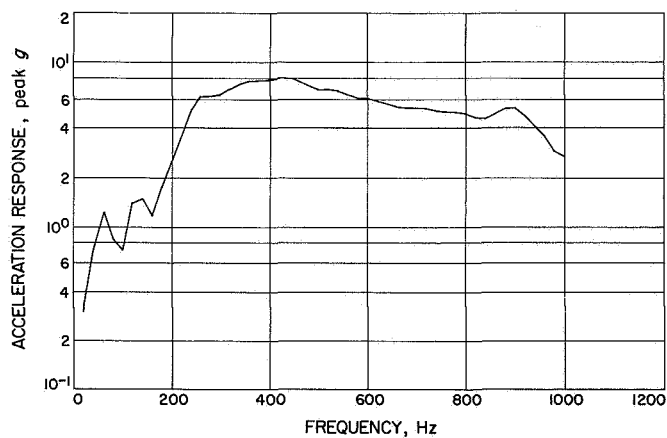


**Fig. 85. Shock spectrum, CY 500, SD-2,
Atlas/Centaur separation**

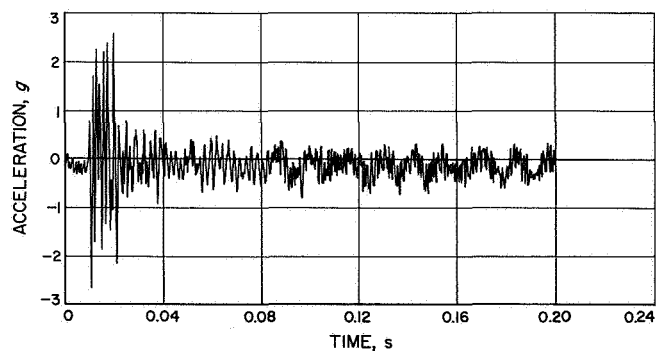


**Fig. 86. Measured transient, CY 510, SD-2,
Atlas/Centaur separation**

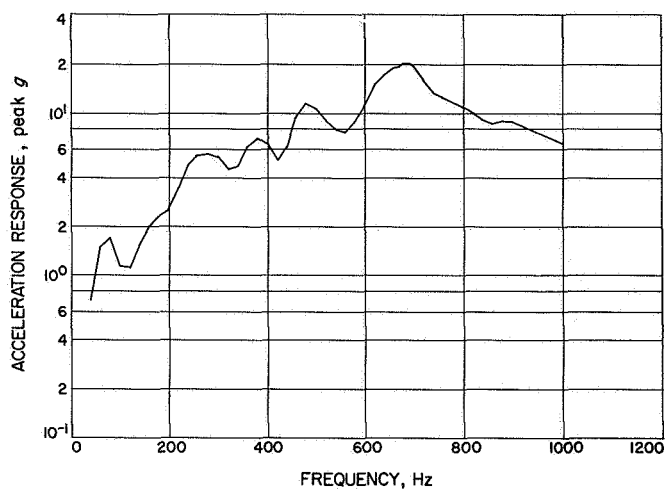


**Fig. 87. Shock spectrum, CY 510, SD-2,
Atlas/Centaur separation**

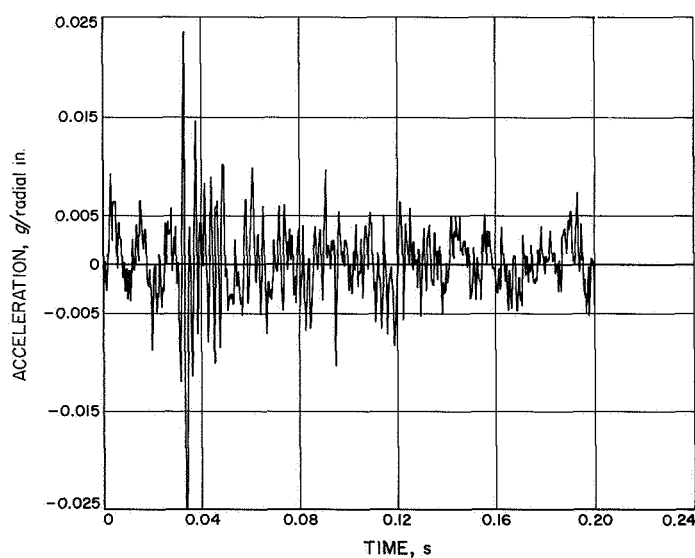


**Fig. 88. Measured transient, torsion, SD-2,
Atlas/Centaur separation**

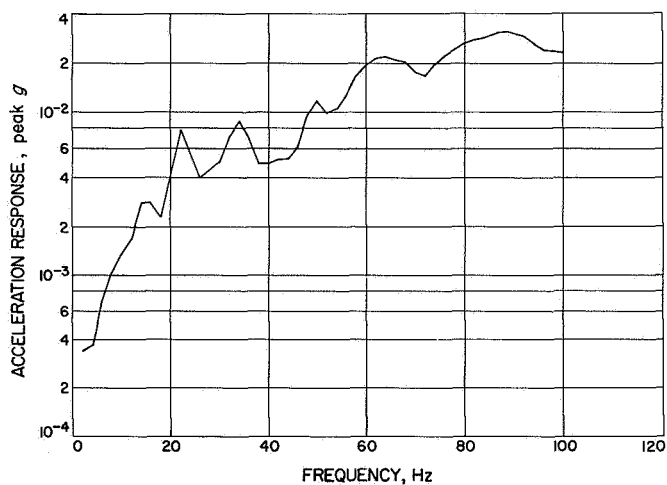


**Fig. 89. Shock spectrum, torsion, SD-2,
Atlas/Centaur separation**

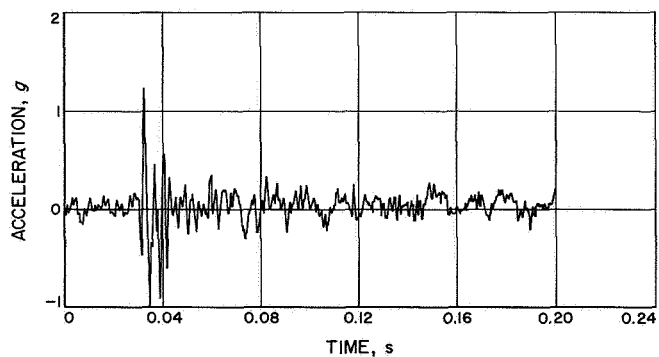


**Fig. 90. Measured transient, X-axis, SD-2,
Atlas/Centaur separation**

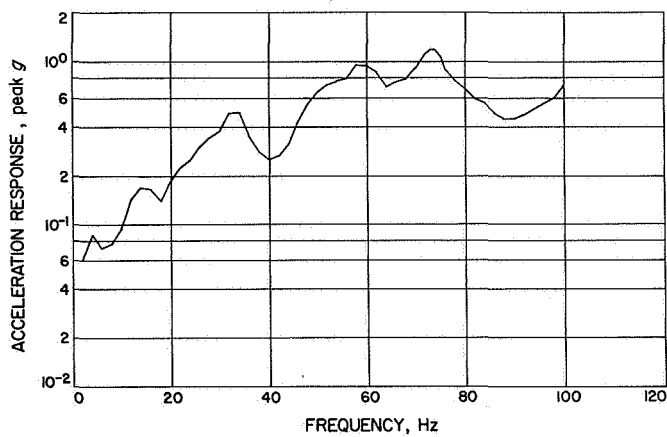


Fig. 91. Shock spectrum, X-axis, SD-2, Atlas/Centaur separation

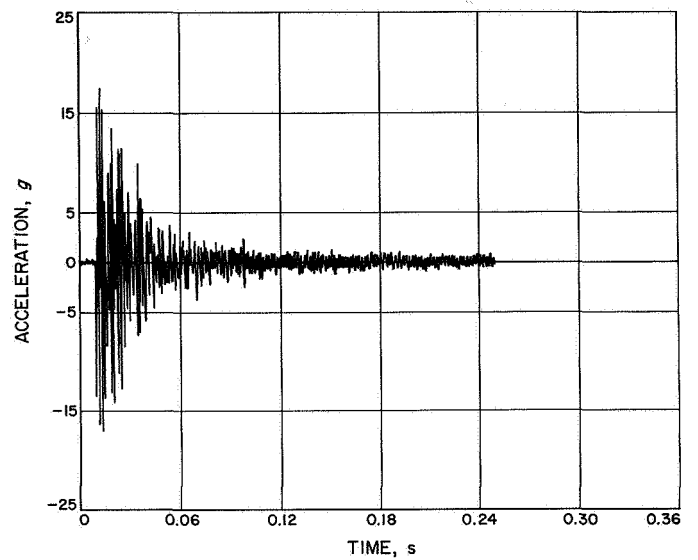


Fig. 92. Typical measured transient, CY 520, 530, or 540, SD-2 and SC-1 through -4, Atlas/Centaur separation

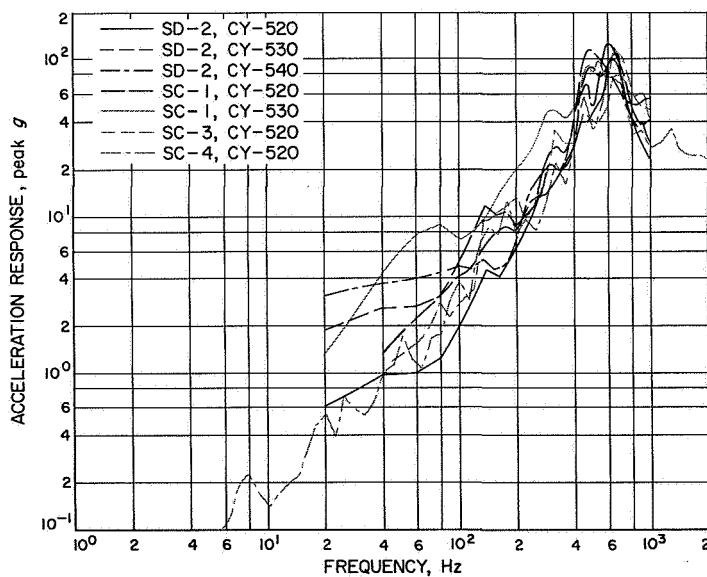


Fig. 93. Shock spectra, CY 520, 530, and 540, SD-2 and SC-1 through -4, Atlas/Centaur separation

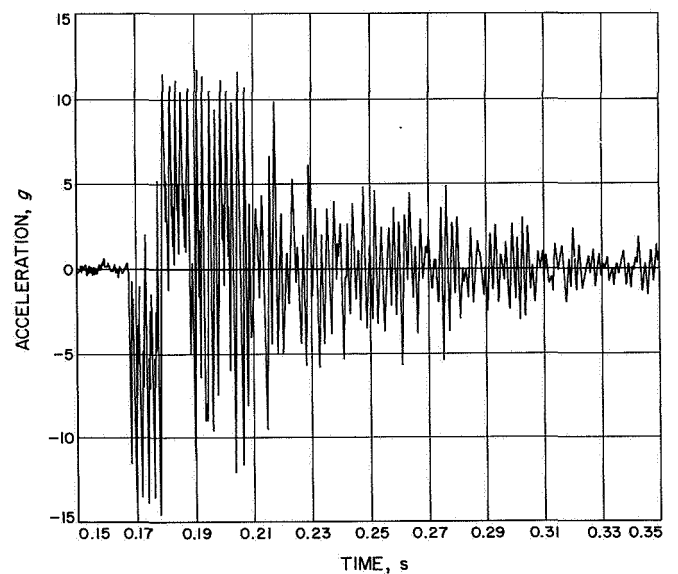


Fig. 94. Typical measured transient, CA 7720, SC-5 through -7, Atlas/Centaur separation

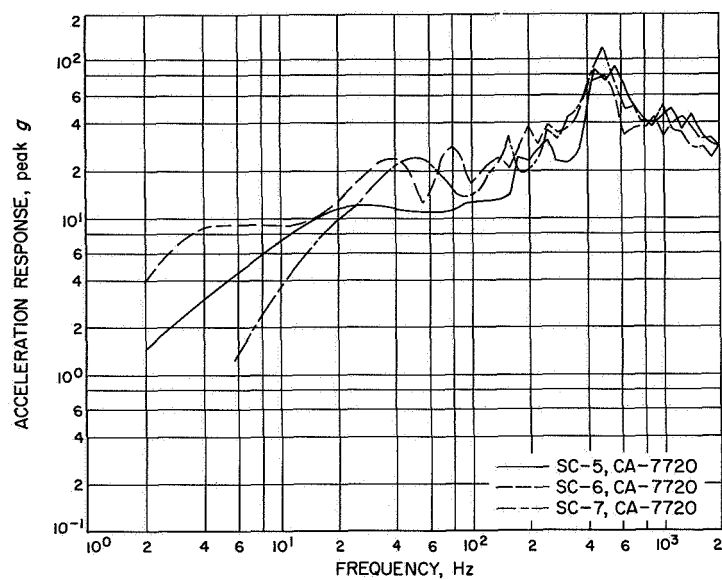


Fig. 95. Shock spectra, CA 7720, SC-5 through -7, Atlas/Centaur separation

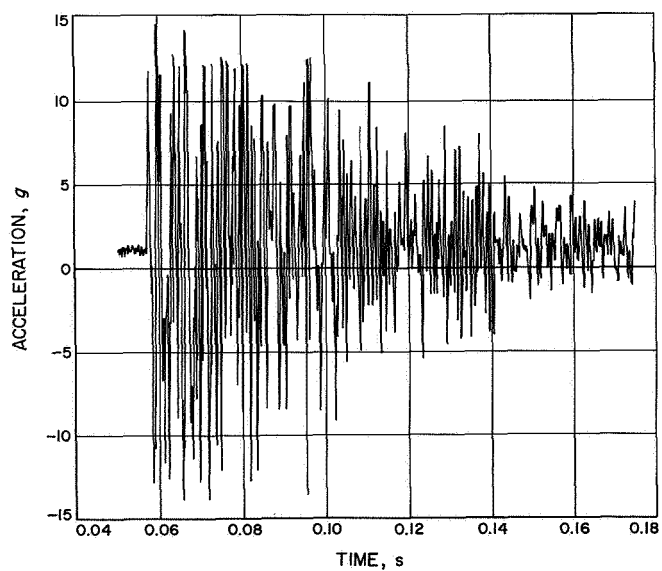


Fig. 96. Typical measured transient, CA 7730, SC-5 through -7, Atlas/Centaur separation

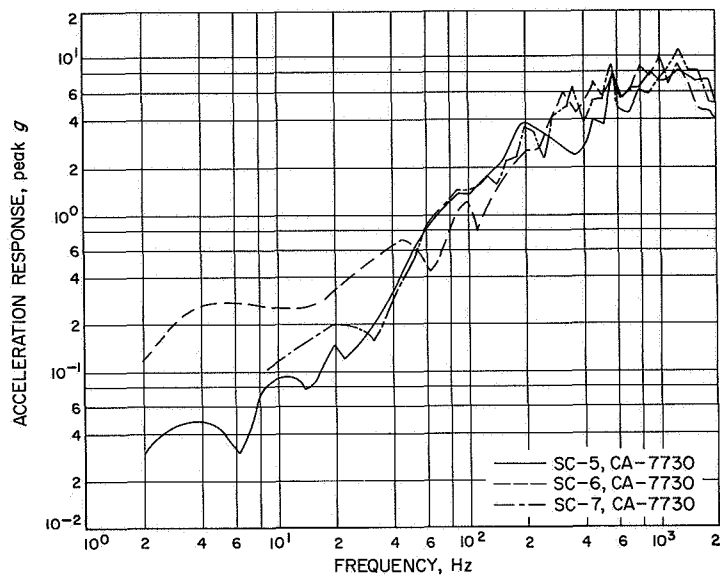


Fig. 97. Shock spectra, CA 7730, SC-5 through -7, *Atlas/Centaur* separation

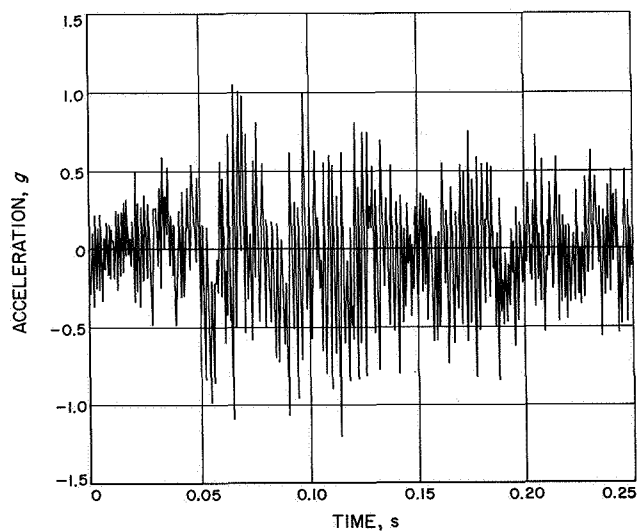


Fig. 98. Typical measured transient, CA 7720, SC-5 through -7, *Centaur* main engine cutoff

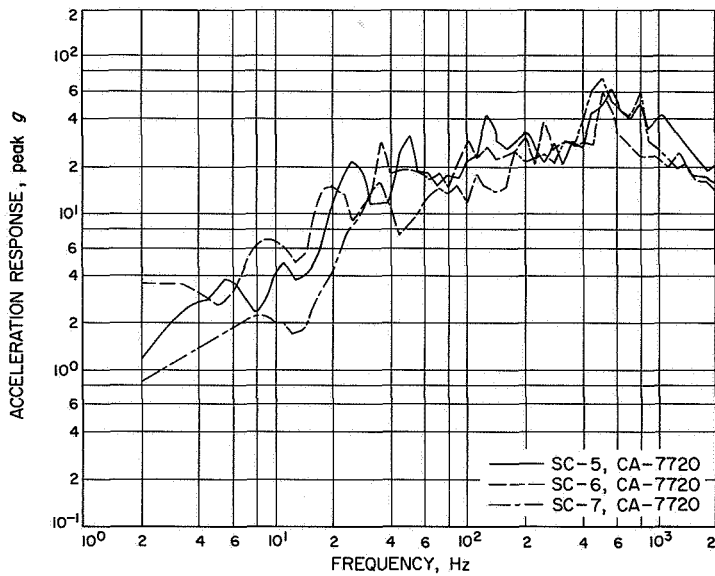


Fig. 99. Shock spectra, CA 7720, SC-5 through -7, Centaur main engine cutoff

Fig. 100. Typical measured transient, CA 7720, SC-5 through -7, Centaur main engine cutoff 2

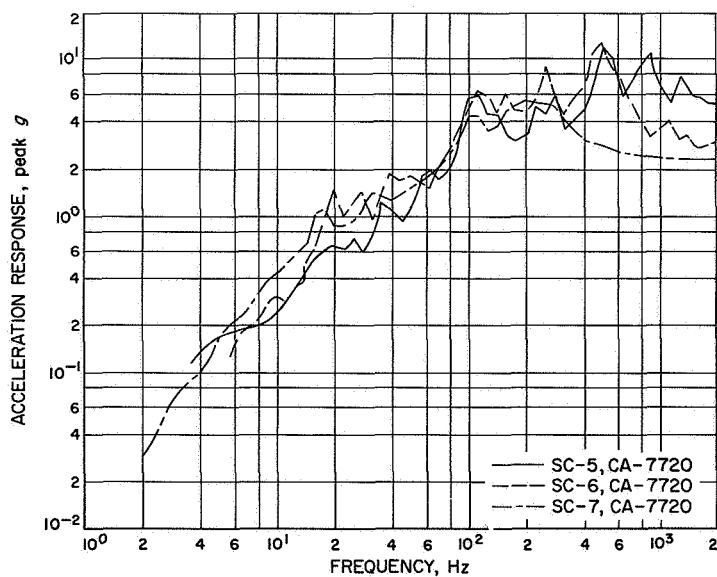
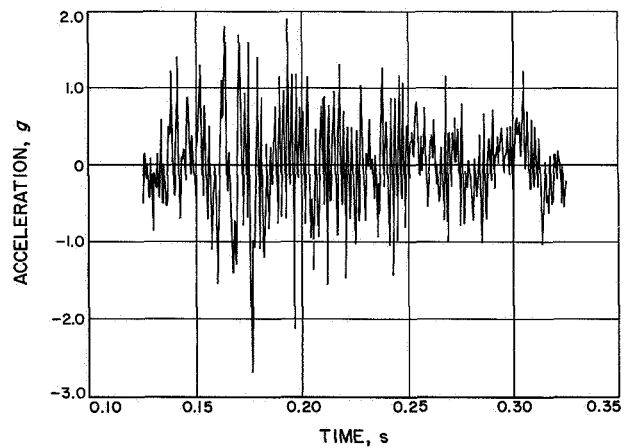


Fig. 101. Shock spectra, CA 7720, SC-5 through -7, Centaur main engine cutoff 2

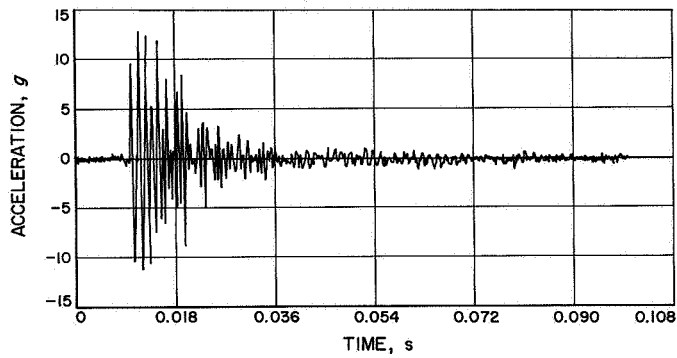


Fig. 102. Typical measured transient, CY 520, 530, or 540, SC-1 through -4, landing gear extension

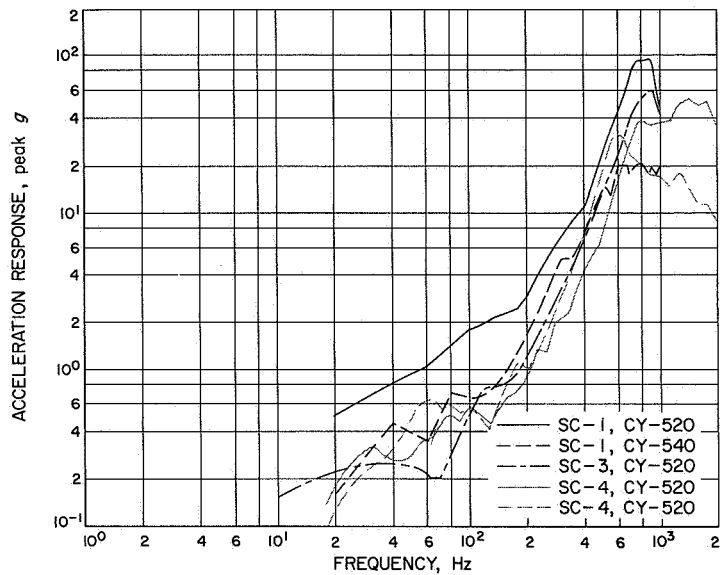


Fig. 103. Shock spectra, CY 520, 530, and 540, SC-1 through -4, landing gear extension

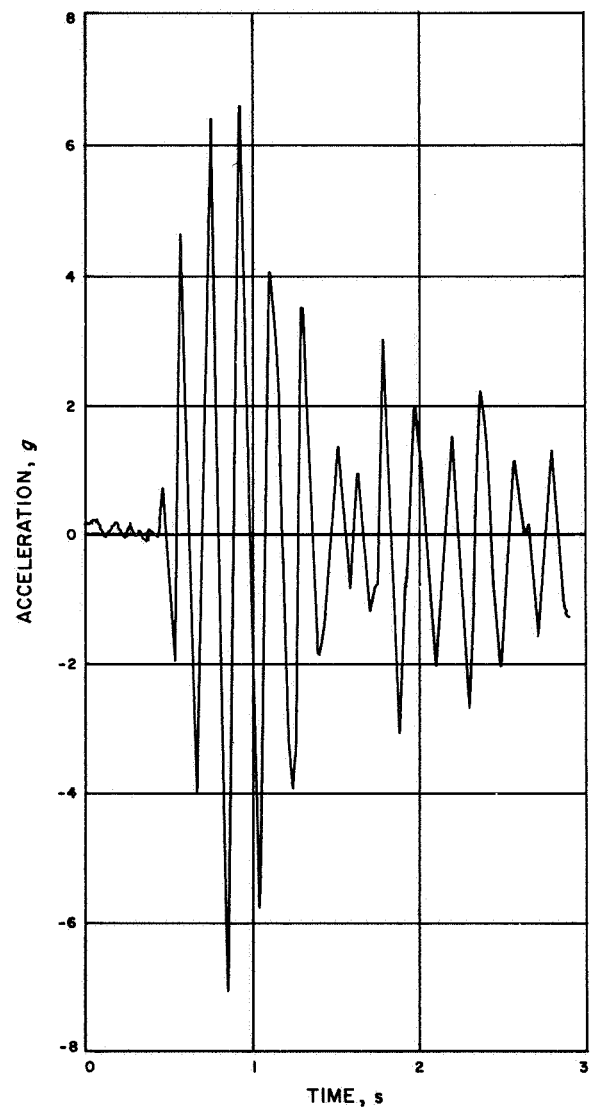


Fig. 104. Typical measured transient, CA 7720, SC-5 through -7, landing gear extension

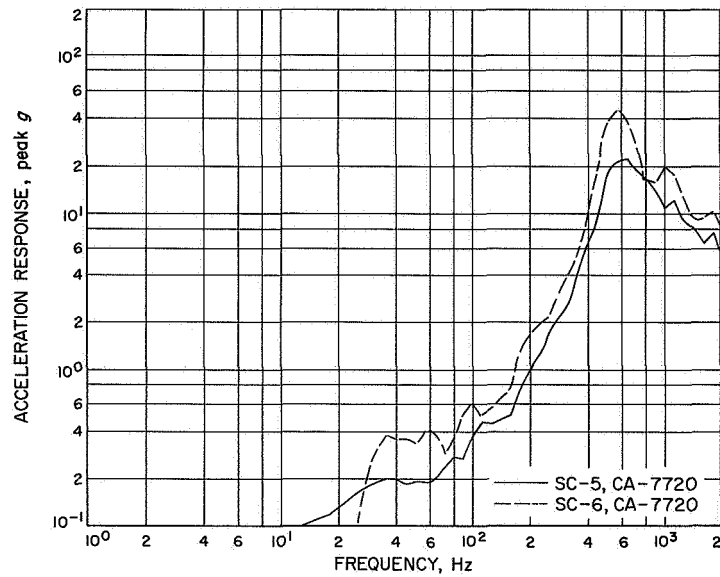


Fig. 105. Shock spectra, CA 7720, SC-5 through -7, landing gear extension

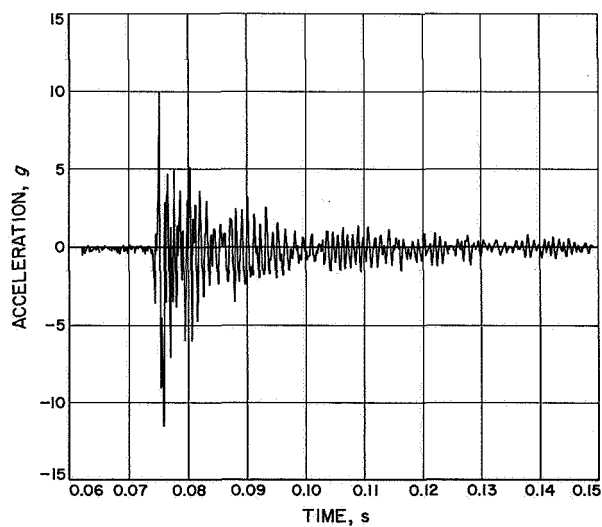


Fig. 106. Typical measured transient, CA 7730, SC-5 through -7, landing gear extension

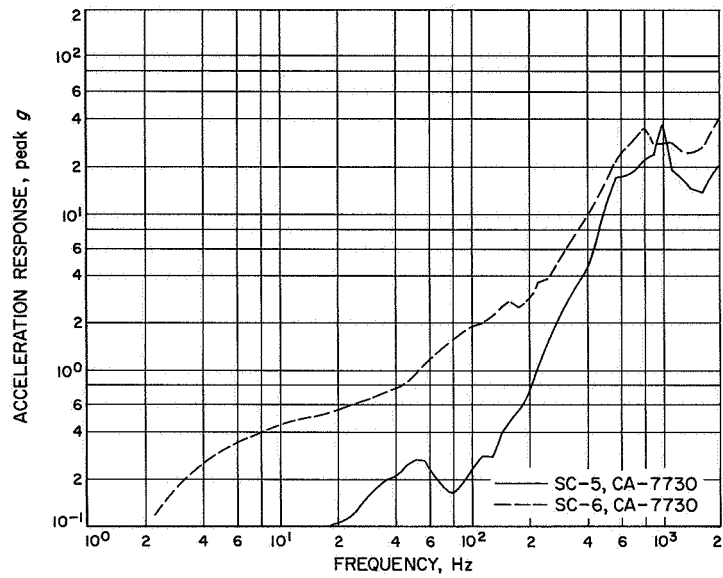


Fig. 107. Shock spectra, CA 7730, SC-5 through -7, landing gear extension

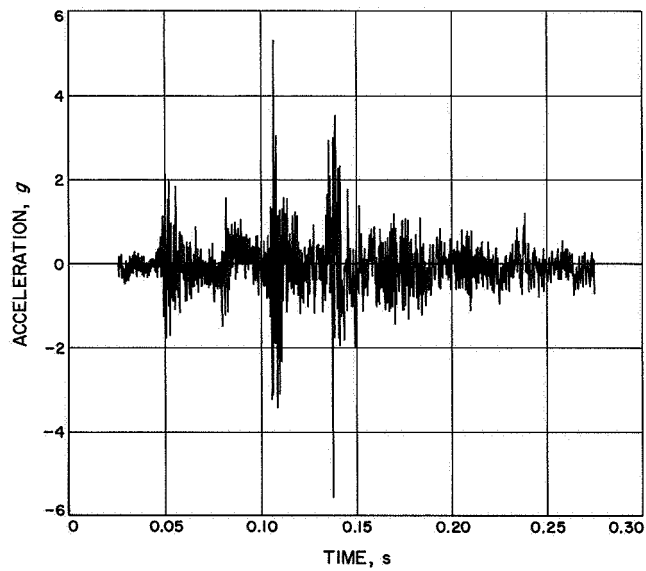
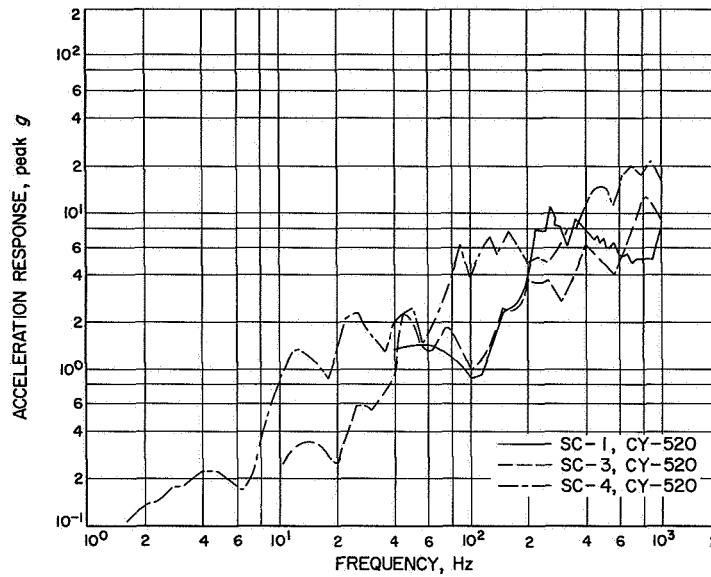
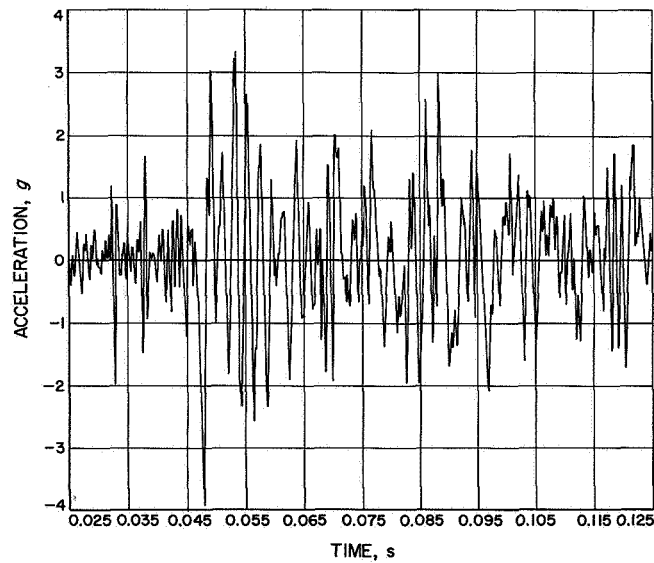


Fig. 108. Typical measured transient, CY 520, 530, or 540, SC-1 through -4, landing gear lock



**Fig. 109. Shock spectra, CY 520, 530, and 540,
SC-1 through -4, landing gear lock**



**Fig. 110. Typical measured transient, CA 7720,
SC-5 through -7, landing gear lock**

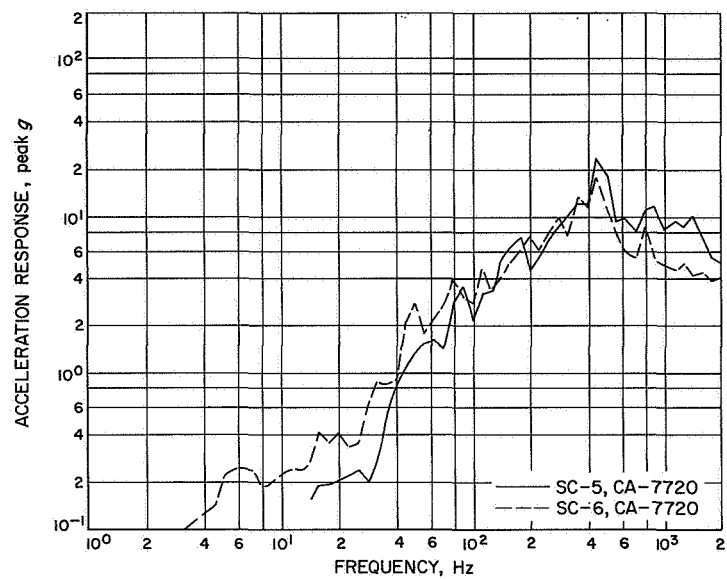


Fig. 111. Shock spectra, CA 7720, SC-5 through -7, landing gear lock

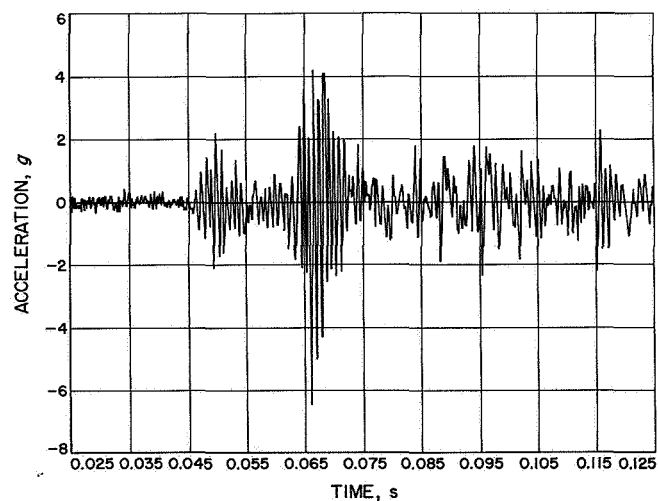


Fig. 112. Typical measured transient, CA 7730, SC-5 through -7, landing gear lock

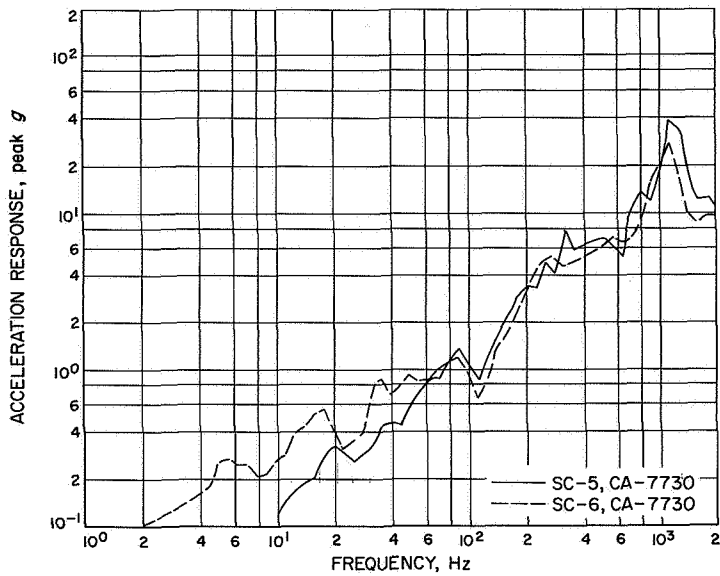


Fig. 113. Shock spectra, CA 7730, SC-5 through -7, landing gear lock

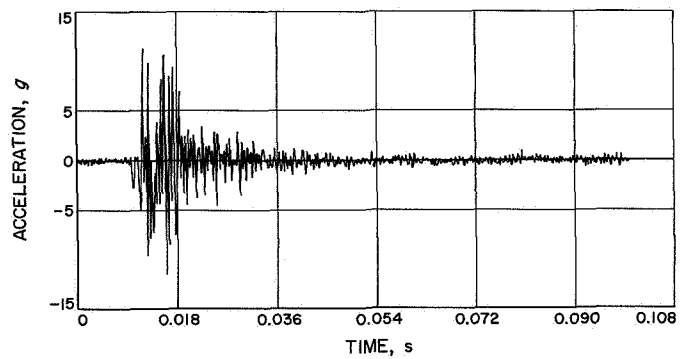


Fig. 114. Typical measured transient, CY 520, 530, or 540, SC-1 through -4, omni antenna deploy

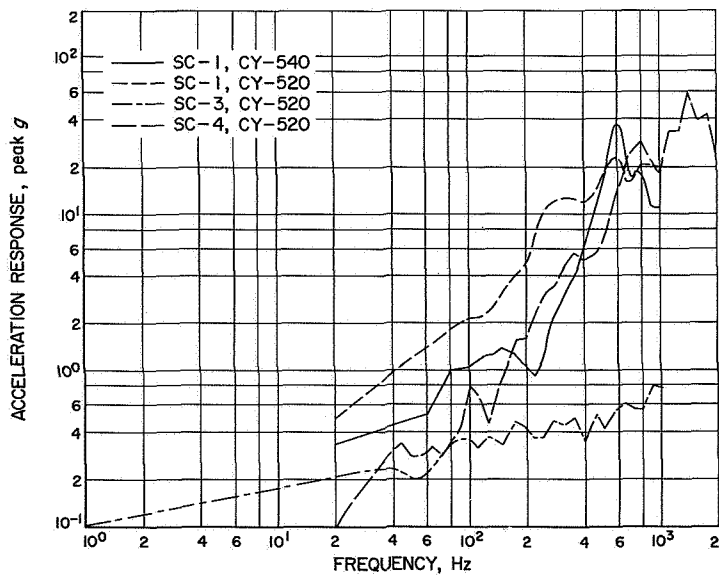


Fig. 115. Shock spectra, CY 520, 530, and 540, SC-1 through -4, omni antenna deploy

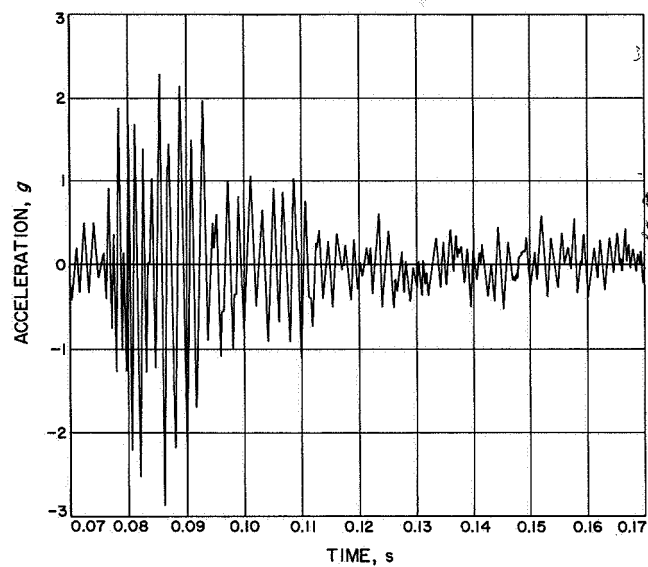


Fig. 116. Typical measured transient, CA 7720, SC-5 through -7, omni antenna deploy

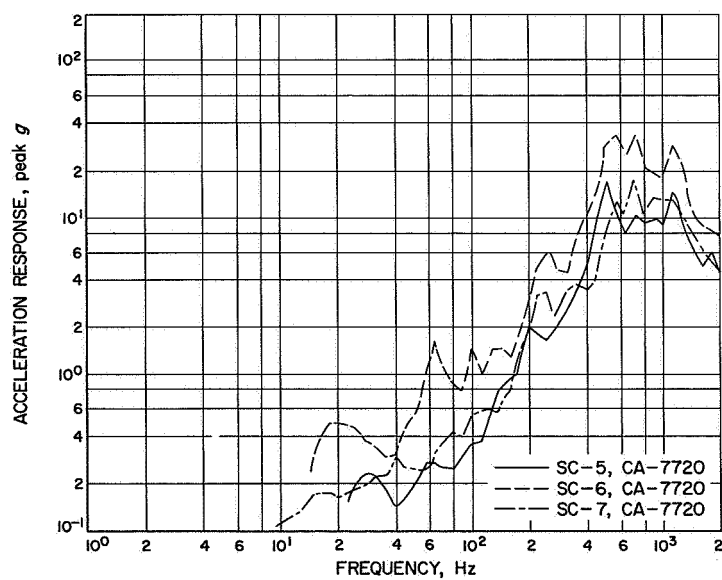
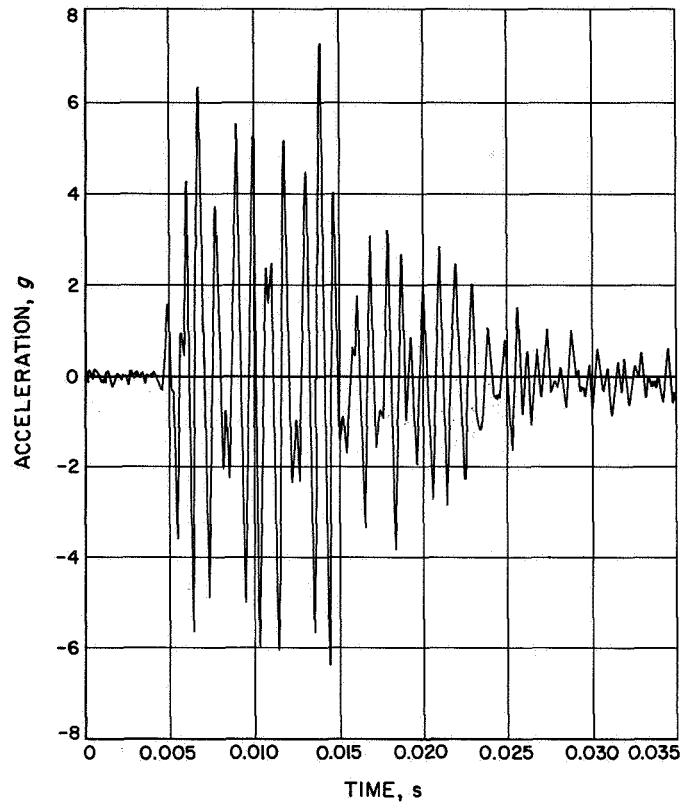
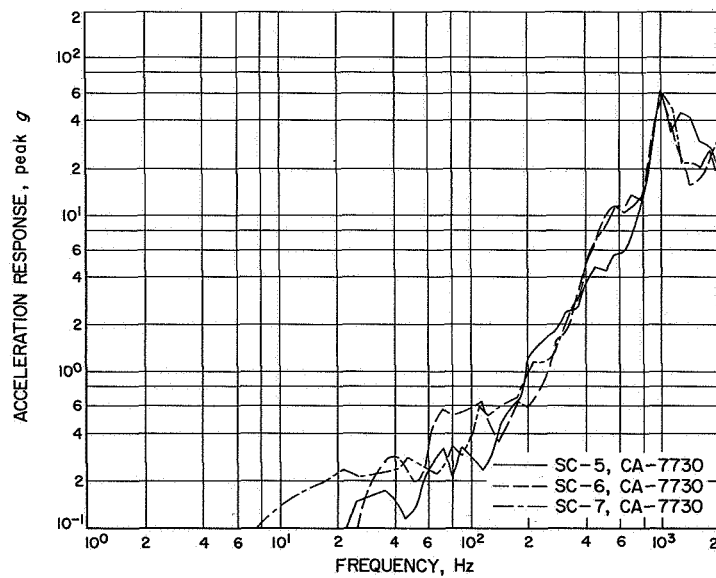


Fig. 117. Shock spectra, CA 7720, SC-5 through -7, omni antenna deploy



**Fig. 118. Typical measured transient, CA 7730,
SC-5 through -7, omni antenna deploy**



**Fig. 119. Shock spectra, CA 7730, SC-5 through -7,
omni antenna deploy**

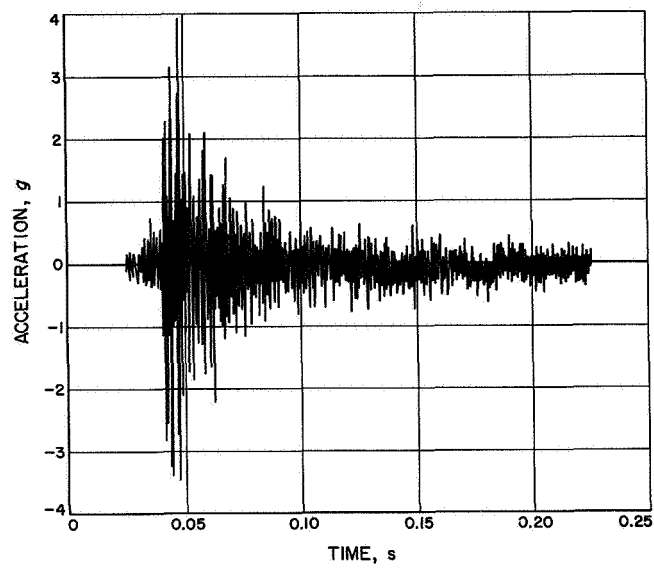


Fig. 120. Typical measured transient, CY 520, 530, or 540, SD-2 and SC-1 through -4, anomaly

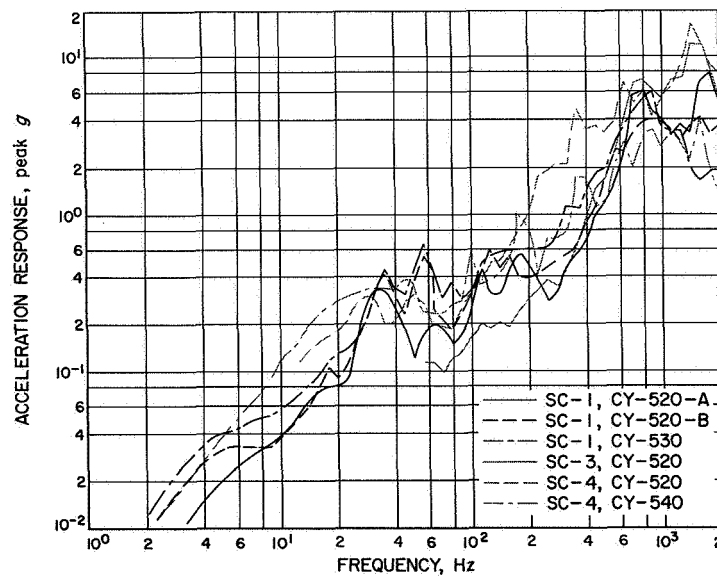
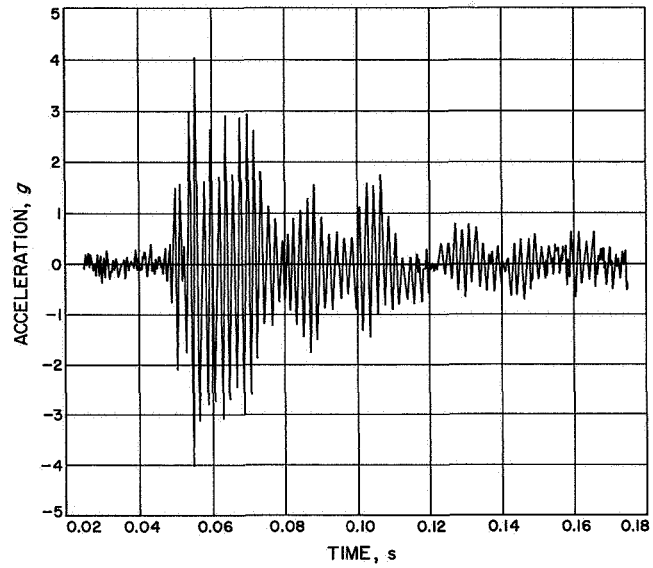
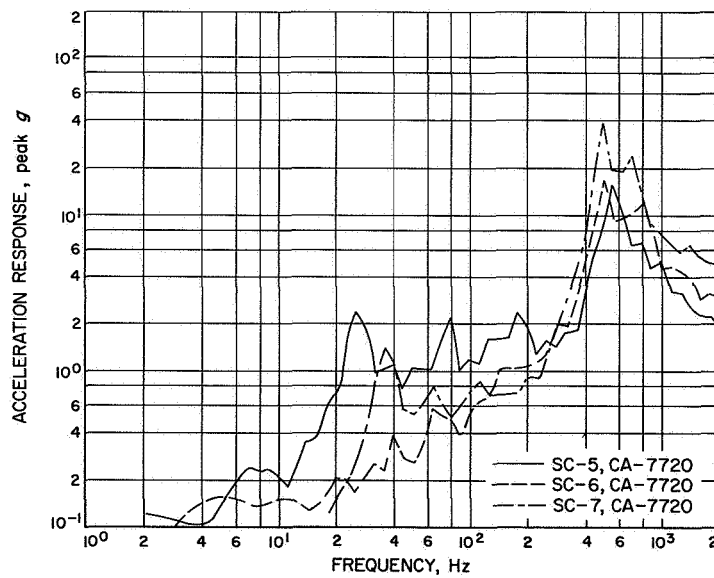


Fig. 121. Shock spectra, CY 520, 530, and 540, SD-2 and SC-1 through -4, anomaly



**Fig. 122. Typical measured transient, CA 7720,
SC-5 through -7, anomaly**



**Fig. 123. Shock spectra, CA 7720,
SC-5 through -7, anomaly**

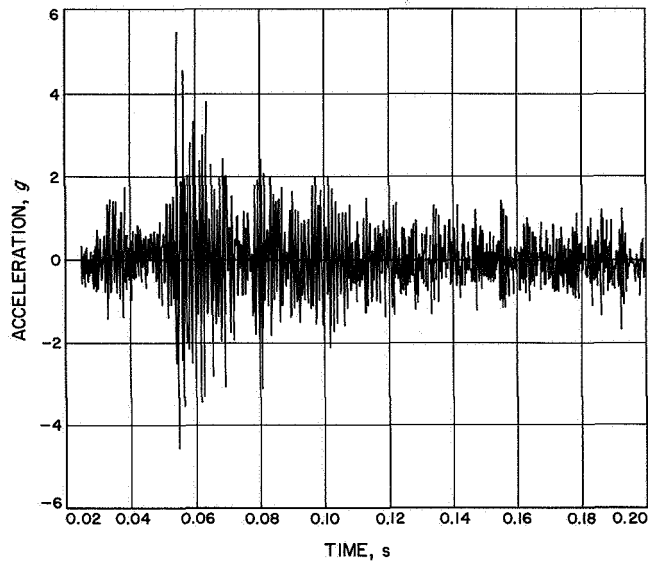


**Fig. 124. Typical measured transient, CA 7730,
SC-5 through -7, anomaly**

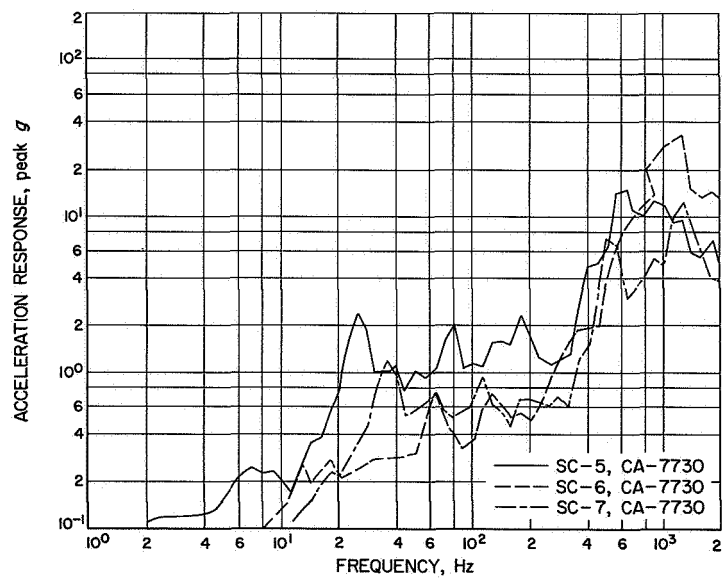


**Fig. 125. Shock spectra, CA 7730,
SC-5 through -7, anomaly**

IV. Conclusions and Recommendations

This report has presented a large amount of dynamic data collected from the launches of the *Surveyor* series of spacecraft. These data provide a basis for the definition of the *Atlas-Centaur* shock and vibration environment as observed at the spacecraft. In addition, the instrumentation and telemetry system characteristics and the data analysis limitations, as they affect the measured data, are described. A discussion of how these data were used in establishing and modifying environmental requirements on the *Surveyor* program and a comparison between this reduced flight data and the test requirements are contained in Section X of the *Surveyor* final report.¹

The dynamic models provided an excellent opportunity for the comprehensive measurement of the flight dynamic environment before the flight of an operational spacecraft. The instrumentation plan for these flights was, in general, acceptable. The only weakness in the basic plan that is apparent was the lack of high-frequency lateral axis measurements. Unfortunately, the SD-1 flight terminated shortly after liftoff and a complete, comprehensive, flight dynamic history was available from SD-2 only.

The SC-1 through -4 instrumentation plan was actually a condensation of the SD-1 and -2 plan. The two weaknesses in this plan were the lack of lateral axis measurements and the commutation of four accelerometers on one channel. The lack of lateral axis transducers was particularly important since this environment was measured only on SD-2 (except for the liftoff portion of the SD-1 flight). Had this plan been devised after the flight of the dynamic models, the lateral axis measurements would have been recommended. It is appropriate here to point out the fact that the transducers on SC-1 through -4 were originally to be used to measure the dynamic environment of the spacecraft at touchdown on the moon only. Lateral axis vibrations at the separation plane would have generally been inconsequential compared with longitudinal vibration at touchdown. Fortunately, the longitudinal axis transducers on SC-1 through -4 were placed at basically the same location as on SD-1 and -2 allowing a flight-to-flight comparison and the basis for statistical manipulation. The commutation of four accelerometers on one data channel resulted in a minimum of useful information from any one transducer. For any particular transient, either a transducer was

being read that was not at the separation plane or the commutator was switching. During the random vibration portions of the flight, the commutation resulted in a serious reduction of sample time.

An attempt was made after the SC-2 flight to incorporate a SD-1 and -2 type instrumentation plan into the SC-5 through -7 spacecraft, since no instrumentation was planned for those vehicles. A minimum of telemetry channels was available, however, and it was deemed inadvisable to add any accelerometers to the spacecraft because of the production changes required. The result was the two transducers mounted on the *Centaur* payload adapter whose main use was the identification of any anomalous dynamic environment and the investigation of flight-to-flight repeatability.

Perhaps the most important single omission in the acquisition of dynamic data from the *Surveyor* spacecraft was the lack of end-to-end calibration of the transducer systems except for the SC-5 flight, the data from which was of limited usefulness. Without such an end-to-end calibration, the accuracy of the system can only be estimated. This end-to-end calibration should include everything between the transducer and the plotted data, the result being complete gain and phase information as a function of frequency. This type of calibration technique should be designed into every environmental instrumentation system.

The type of data analysis utilized on any raw data depends on the end use of the reduced data. Additionally, the requirement of flight-to-flight comparison dictates that analysis parameters be uniform from flight-to-flight. With this in mind it is recommended that the data analysis scheme be planned early in any program with all techniques and parameters selected after a thorough review of the end use of the data.

A summary of the above discussion, which serves to reemphasize the important points is given below:

- (1) Dynamic models provide an excellent opportunity for early assessment of dynamic environments on new programs.
- (2) Complete definition of the dynamic environment at even a few locations requires more instrumentation than was generally available on the *Surveyor* program.
- (3) Provisions should be made for an end-to-end calibration of the flight instrumentation.
- (4) Time-commutated measurements should not be used for dynamic environment data.

¹*Surveyor Project Final Report. Part I. Project Description and Performance*, Technical Report 32-1265. Jet Propulsion Laboratory, Pasadena, Calif. (to be published).